A Novel Factor in Olfactory Ensheathing Cell-Astrocyte Crosstalk: Anti-Inflammatory Protein α-Crystallin B

Aybike Saglam[1,2*], Anne L. Calof[3#] and Susan Wray[1†‡]

[1]Cellular & Developmental Neurobiology Section, NINDS, NIH, Bethesda, MD

[2]Program in Neuroscience & Cognitive Science, Univ. of Maryland, College Park

[3]Dept of Anatomy & Neurobiology and the Center for Complex Biological Systems, Univ. of California, Irvine, California

Key words: astrocyte, neuroinflammation, neurotoxicity, olfactory ensheathing cells (OECs), alpha-crystallin B (CryAB), exosome, nuclear factor kappa B (NFκB)

*E-mail: asaglam@umd.edu

#Email: alcalof@uci.edu

†Corresponding author.

‡E-mail: wrays@ninds.nih.gov

Main Points:

- Astrocytes uptake OEC-secreted exosomes.
- WT OEC-exosomes, but not CryAB-null OEC-exosomes, block nuclear NFκB translocation in astrocytes.
- CryAB, and other factors secreted by OECs, suppresses multiple neurotoxicity-associated astrocyte transcripts.

Author contributions: AS and SW designed the research. AS performed the experiments. AS analyzed the data and AS, AC and SW wrote the manuscript.

Abstract

Astrocytes are key players in CNS neuroinflammation and neuroregeneration that may help or hinder recovery, depending on the context of the injury. Although pro-inflammatory factors that promote astrocyte-mediated neurotoxicity have been shown to be secreted by reactive microglia, anti-inflammatory factors that suppress astrocyte activation are not well-characterized. Olfactory ensheathing cells (OECs), glial cells that wrap axons of olfactory sensory neurons, have been shown to moderate astrocyte reactivity, creating an environment conducive to regeneration. Similarly, astrocytes cultured in medium conditioned by cultured OECs (OEC-CM) show reduced nuclear translocation of Nuclear Factor kappa-B (NFκB), a pro-inflammatory protein that induces neurotoxic reactivity in astrocytes. In this study, we screened primary and immortalized OEC lines to identify these factors and discovered that Alpha B-crystallin (CryAB), an anti-inflammatory protein, is secreted by OECs via exosomes, coordinating an intercellular immune response. Our results showed: 1) OEC exosomes block nuclear NFκB translocation in astrocytes while exosomes from *CryAB*-null OECs could not; 2) OEC exosomes could be taken up by astrocytes and 3) CryAB treatment suppressed multiple neurotoxicity-associated astrocyte transcripts. Our results indicate that OEC-secreted factors are potential agents that can ameliorate, or even reverse, the growth-inhibitory environment created by neurotoxic reactive astrocytes following CNS injuries.

1 Introduction

Damage to the central nervous system (CNS) provokes morphological and molecular changes in astrocytes, causing them to become 'reactive astrocytes' (Liddelow & Barres, 2017). These reactive cells play positive roles during CNS injury, such as confining inflammation by surrounding the damaged tissue and creating a barrier between it and uninjured tissues (Silver*, et al., 2*015). Reactive astrocytes have been traditionally characterized by increased expression of intermediate filament proteins such as GFAP (Glial Fibrillary Acidic Protein), vimentin, and nestin (summarized in Liddelow & Barres, 2017). Excessive or sustained astrocyte reactivity is characterized by activation of pro-inflammatory pathways such as the NFκB pathway (Liddelow & Barres., 2017; Wheeler 2020). This activity can be deleterious to functional recovery, since it can lead to chronic inflammation and neurotoxicity (Sofroniew, *et al.,* 2010). A better understanding of the molecular mechanisms that govern astrocyte reactivity would therefore be helpful to create environments conducive to regeneration following CNS injury.

The mammalian olfactory system shows robust neurogenesis throughout life. Data suggest that both neural niche signals and the surrounding glia, including olfactory ensheathing cells (OECs), give the olfactory mucosa this unique capability (Li, *et al.,* 2005; Roet & Verhaagen, 2014). Several groups have transplanted OECs into CNS injury sites, and observed improved axonal regeneration (Li *et al.,* 1997; Imaizumi *et al*., 2000), functional recovery (Johansson *et al*., 2005), reduced astrocytic scar tissue (Ramer *et al*., 2004), and an attenuated hostile astrocyte response (Lakatos *et al*., 2003; summarized in Roet & Verhaagen, 2014). Moreover, factors secreted by OECs have been shown to moderate astrocyte reactivity, at least insofar as their presence results in reduction of GFAP expression and nuclear translocation of NFκB (Chuah *et al.,* 2011; O'Toole *et al*., 2007). Identification of molecules secreted by OECs, which specifically affect astrocyte reactivity, should lead not only to a better understanding of the crosstalk between astrocytes and OECs; it may also reveal mechanisms that can block the metamorphosis of astrocytes into neurotoxic cells.

To identify such molecules, this study used lipopolysaccharide (LPS)-treated astrocytes, a model for neurotoxic reactive astrocytes, and assessed conditioned medium (CM) from immortalized clonal mouse OEC cell lines (Calof & Guevara, 1993). Nuclear NFκB translocation in astrocytes was measured to determine if CM from these cell lines could mimic primary OEC-CM, which blocked the LPS pro-inflammatory response in astrocytes. Two immortalized cell lines were chosen for further study: one whose CM mimicked the effect of primary OECs (positive control); and a second, whose CM did not block the LPS response in astrocytes (negative control). These two cell lines and primary OECs were challenged with LPS, and the conditioned media screened by mass spectrometry. Using this strategy, the heat-shock protein

CryAB (D'Agostino *et al.*, 2013) was identified. Subsequent experiments showed that: 1) CryAB is secreted by OECs via exosomes; 2) exogenous CryAB suppressed LPS-induced astrocyte reactivity; 3) exosomes containing CryAB are taken up by astrocytes; and 4) unlike wildtype (WT) OEC-exosomes, *CryAB*-null (*CryAB*$^{-/-}$) OEC exosomes fail to suppress LPS-induced astrocyte reactivity measured by nuclear NFκB translocation. Finally, examination of transcripts that are associated with neurotoxic-reactive astrocytes (Liddelow *et al.*, 2017) revealed that either exogenous CryAB or OEC-CM can suppress expression of several of these transcripts. Taken together, the data indicate that CryAB secreted by OECs, via exosomes, is an important factor for OEC-astrocyte crosstalk that can block astrocytes from becoming neurotoxic cells. Ultimately, mimicking appropriate astrocyte-OEC crosstalk *in vivo* may contribute to an environment conducive to regeneration following a broad range of CNS injuries.

2 Materials & Methods

2.1 Mice

All mice were maintained, and all animal handling procedures were performed according to protocols approved by the National Institutes of Health NINDS Institutional Animal Care and Use Committee. *CryAB*-null (*CryAB*$^{Del(9Hspb2\text{-}Cryab)1Wawr}$, henceforth referred to as *CryAB*$^{-/-}$) mice (Brady *et al.*, 2001) were obtained as homozygous sperm, revived by IVF using eggs from C57bl6/N mice (Jackson Laboratory), and resulting heterozygotes intercrossed to obtain obtain *CryAB*$^{-/-}$ and *CryAB*$^{+/+}$ (wildtype, WT) lines, which were used as the source for OEC primary cultures (see below). Mice were genotyped using a three-primer PCR protocol: 5'-TAGCTTAATAATCTGGGCCA-3', 5'-GGAGTTCCACAGGAAGT-ACC-3', and 5'-TGGAAGGATTGGAG-CTACGG-3' primers were used in 4:1:1 molar ratio. Amplification was performed for 40 cycles at 94^{0}C for 15 sec, 62^{0}C for 30 sec and 72^{0}C at 1 min. PCR produced a 310-bp product for the WT allele and a 600-bp product for the null allele.

2.2 Cell culture and reagents

Primary cultures of OECs were generated as described previously (Dairaghi *et al.*, 2018). Briefly, olfactory bulbs of postnatal (PN) day 0-7 mice were collected and placed in an enzyme mix: 300µg/ml hyaluronidase (Sigma, Cat# H3631, St. Louis, MO), 30U/ml dispase I (Sigma, Cat# D4818), 1.2 mg/ml collagenase type 4 (Worthington, Cat# 43E14231, Lakewood, NJ), 10U/ml DNAse I (Worthington, Cat# 54E7315); for 35 min at 37^{0}C with constant agitation (Au & Roskams, 2003). Cells were run through a 40µm cell strainer to remove non-dissociated tissue pieces and then washed with DMEM-F12 medium. Subsequently, cells were purified by the differential cell adhesion method (Nash *et al.*, 2001), which consists of three steps: 1) Cells were seeded into uncoated T75 flasks (4x10^6 viable cells/flask, VWR, Cat# 734-2788, Radnor, PA) for 18 hrs to remove fibroblasts; 2) the supernatant of the first step was seeded into another uncoated flask for up to 36 hrs to remove astrocytes; and finally 3) the supernatant of the second flask was seeded onto poly-L-lysine (Sigma, Cat# P4707)-coated flasks to grow primary OECs. Cells were cultured for up to 2 weeks and medium was changed every 2–3 days. OECs constituted more than 90% of the cells in the culture based on p75 and S100B immunostaining (data not shown). For OECs to be co-cultured with primary astrocytes, the medium was gradually changed to serum-free medium (Klenke & Taylor-Burds, 2012) supplemented with 5ng/ml HB-EGF (PeproTech, Cat# 100-47, Rocky Hill, NJ), and B27 (Thermo Fisher Scientific, Cat# A3582901) to provide a medium compatible with astrocyte culture, since serum has been shown to induce astrocyte reactivity (Foo *et al.*, 2011).

Primary astrocyte cultures were obtained by magnetic sorting as previously described (Holt *et al.*, 2019), with some modifications. Briefly, 10-20 cortices of PN day 2-4 pups were dissociated using the MACS Neural

Tissue Dissociation Kit-T (Miltenyi Biotec, Cat# 130-093-231, Auburn, CA) at 37^0C (5% CO^2, 30 min). Non-dissociated tissue was removed using a 40µm cell strainer (Fisher Scientific, Cat# 22-363-547), and the remaining cell solution was centrifuged (300g, 5 min). Next, a discontinuous density gradient, prepared using 1:1 albumin-ovomucoid solution (10mg/ml of each) (Worthington, Cat# OI; GeminiBio, Cat# 700-102P, West Sacramento, CA), was used to remove cell debris and inhibit enzyme activity. The cell pellet was resuspended in 80µl Hank's Balanced Salt Solution (HBSS) (Gibco, Cat# 14025-092) plus 20µl anti-GLAST (ACSA-1) MicroBeads (Miltenyi Biotec, Cat# 130-095-825, Auburn, CA) for up to 10^7 cells, and incubated for 10 min (4^0C). Cells were washed and incubated in 90µl HBSS plus 10µl anti-Biotin MicroBeads for another 15 min (4^0C) before running through MACS column for positive selection of astrocytes. Cells were cultured for one week and then the same procedure was followed with anti-Prominin-1 MicroBeads (Miltenyi Biotec, Cat# 130-092-564) for the negative selection of radial glia, followed by another positive selection with anti-GLAST antibody the same day, to increase the purity of astrocyte cultures. Sorted cells were cultured in T25 flasks coated with poly-L-lysine, in 5ml serum-free astrocyte culture medium (ACM, described above). In our hands, astrocytes isolated by this method and cultured in ACM were not reactive when stained with NFκB (not shown). The same method was adjusted to obtain oligodendrocyte cultures using anti-O4-MicroBeads (Miltenyi Biotec, Cat# 130-096-670). The immortalized mouse astrocyte line C8D30 (ATCC, VA, USA) was cultured in DMEM-F12 (Gibco, Cat# 10313-02, 11765-054, Long Island, NY) containing 10% Fetal Bovine Serum (FBS) (Gibco, Cat# 10438-026), plus 0.5% antibiotic-antimycotic (Gibco, Cat# 15240-062) at 37^0C in 5%CO2.

2.3 Immortalized OEmyc790 Cell Lines

Six immortalized OEC lines (OEmyc790-C7s.D, D6s.AB8, C6s.BG9, D10 and D4), derived from retrovirus-mediated transformation of primary embryonic mouse olfactory epithelium cultures derived from E15 mouse embryos (Calof & Guevara, 1993), were analyzed; two lines, OEmyc790-C7s.D (C7) and OEmyc790-C4 (C4), were used for the studies described below. Cells were plated on cell culture plates (Fisher Scientific, Cat# 130190, Waltham, MA) and cultured in DMEM-F12 as described above. Medium was changed every 3-5 days. When 60% confluent, a 1:4 dilution of trypsin was used (Gibco, Cat# 15400054) to split the cells into thirds.

2.4 Primary antibodies and recombinant proteins

The following antibodies were used: CryAB rabbit polyclonal antibody (Millipore, Cat# ABN185, Darmstadt, Germany, 1:1K for WB, 1:4K for immunofluorescence (IF); Histone mouse monoclonal antibody (Fisher Scientific, Cat# AHO1432, Waltham, MA, 1:200 for WB); NFκB rabbit polyclonal antibody (C-20, Santa Cruz, Cat# sc-372, Santa Cruz, CA, 1:650 for WB, 1:750 for IF); Sox10 goat polyclonal antibody

(N-20, Santa Cruz, Cat# sc-17342, 1:300 for IF); Alix mouse monoclonal antibody (3A9, Cell Signaling, Cat# 2171T, 1:1K for WB); GFAP chicken polyclonal antibody (Aves, 1:4K for IF); Flotillin-1 rabbit polyclonal antibody (D2V7J, Cell Signaling, Cat# 18634, 1:1K for WB); β-actin mouse monoclonal antibody (AC-74, Millipore, Cat# A2228, 1:1K for WB); Tomm20 rabbit polyclonal antibody (FL-145, Santa Cruz, Cat# sc-11415, 1:1K for WB); CD63 biotinylated antibody (Miltenyi Biotec, Cat# 130-108-922, Auburn, CA, 1:15 for IF); BLBP mouse monoclonal antibody (Abcam, Cat# ab131137, 1:2K for IF) and p75-NGFR rabbit polyclonal antibody (Millipore, Cat# AB1554, 1:5K). Recombinant chicken Anosmin1 (MyBioSource, Cat# MBS963562-COA, San Diego, CA) was used at 5nM while recombinant CryAB protein (MyBioSource, Cat# MBS964495) and recombinant myoglobin (MyBioSource, Cat# MBS142891) were used at 50ng/ml unless stated otherwise.

2.5 Mass spectrometry

Primary OECs, and immortalized C7 and C4 OEC cell lines, were established by seeding them in T75 flasks at a concentration of $8x10^5$ cells/flask in regular growth medium. To concentrate secreted proteins, the cells in each flask were rinsed and media replaced with 10ml/flask of Earle's Balanced Salt Solution (EBSS) with 5.5mM D-Glucose (Gibco, Cat# 14155-063); conditioned medium (CM) was collected after 48 hrs total of incubation. For the last 2 hrs of the 48-hr collection period, either 1µl/ml LPS (Sigma, Cat# L6529) or 5nM recombinant chicken Anosmin1 was added. CM was then collected, centrifuged to remove debris, and frozen at -80^0C. Frozen samples were freeze-dried using a lyophilizer (Novalyphe-NL150, Savant Instruments, Holbrook, NY). The pellets were reconstituted in water and bicinchoninic acid (BCA) protein assay was performed. 200µg/60ul protein per group was submitted for mass spectrometry analysis (NINDS Protein Facility, NIH). Each sample was digested with trypsin. Tandem Mass Tag (TMT) labeled samples were mixed together (TMT 126-131). The mixture was separated using hydrophilic interaction liquid chromatography (HILIC) high performance liquid chromatography (HPLC) system. Five HILIC fractions were collected from the mixed sample. One liquid chromatography-tandem mass spectrometry (LC/MS/MS) experiment was performed for each HILIC fraction, using an Orbitrap Fusion Lumos Mass Spectrometer (Thermo Fisher Scientific, Waltham, MA) coupled to a 3000 Ultimate high-pressure liquid chromatography instrument (Thermo Fisher Scientific). Proteome Discoverer 2.2 software used for database search and TMT quantification, and data were mapped against the Sprot mouse database. "Primary OEC+LPS-CM" was used as reference to calculate the ratio for LPS treated samples; "Primary OEC+5nMA1-CM" was used as reference to calculate the ratio for 5nMAnosmin1-treated samples. No normalization was performed. See Supplemental Data 1 and 2 for obtained values.

2.6 Immunoblot analysis

As a readout of reactivity, quantitative immunoblot analysis was performed on nuclear fractions of immortalized C8D30 astrocytes treated with 1µl/ml LPS or vehicle control for 2 hrs. For co-culture groups, OECs seeded on porous inserts (0.4µm Millicell Cell Culture Insert, Millipore, Cat# PICM0RG50) were placed on top of astrocytes for 24 hrs and were discarded at the end of the incubation period, so that only astrocytes were collected for subsequent protein analysis. For the CM treated groups, CM from each line was collected (after 24 hr incubation) and then added to astrocytes for 22 hrs, followed by a 2-hour LPS treatment. Astrocytes were then collected by scraping and the CNMCS Compartmental Protein Extraction Kit (BioChain Cat# K3013010 Hayward, CA) with protease/phosphatase inhibitors (PI, Cell Signaling, Cat# 5872S, Danvers, MA) was used and the nuclear fractions were isolated for each treatment condition. The fractions were run on BioRad Mini-Protean TGX Stain-Free Gels (Cat#4568084), transferred to PVDF stain-free blot (Trans-Blot Turbo Transfer Pack, Cat#1704156) via the Trans-Blot Turbo transfer system (BioRad), and blocked with 5% dry milk (BioRad, Cat #170-6404) prior to staining with NFκB antibody. Membranes were exposed to Clarity enhanced chemiluminescence (ECL) reagent (Cat. # 170–5061, Bio-Rad) for 5 min and the signal was detected using ChemiDoc MP (Cat. # 170–8280, Bio-Rad). Quantification of band intensities was calculated using Image Lab 5.0 software (Bio-Rad) and normalized by the loading control immunostained for Histone on the same sample and the same blot. Three biological replicates were used for statistical analysis.

2.7 Quantitative immunofluorescence

Fluorescent immunostaining for nuclear NFκB and cytoplasmic NFκB was quantified in immortalized C8D30 astrocytes following 2-hr treatment with 1µg/ml LPS or a cocktail of 3 cytokines: Il-1α (3ng/ml, Sigma, Cat# I3901), TNFα (30ng/ml, Cell Signaling, Cat# 8902SF) and C1q (400ng/ml, MyBioSource, Cat# MBS143105, San Diego, CA), as follows: After immunofluorescence staining for NFκB, confocal images were taken on a Zeiss LSM 800 Confocal Microscope (Carl Zeiss, Thornwood, NY). A defined area was measured in both nuclear and cytoplasmic compartments for each astrocyte, and the fluorescence intensity was quantified for each area in each cell using Imaris software. The ratio of nuclear to cytoplasmic fluorescence intensity was used as a quantitative readout of astrocyte reactivity. Median values were calculated for each biological replicate (N=3) obtained from multiple images (2-3/well) containing a total of ~100 cells/treatment (Figure 1C, cell numbers in Supplemental Table 1) or ~50 cells/treatment (Figure 2B, cell numbers in Supplemental Table 2). Values greater than one indicate that the NFκB value was higher in the nucleus compared to cytoplasm, and cells were reactive. Statistics (ANOVA) were performed and the average median value ±standard deviation (SD) per treatment plotted.

2.8 Isolation of exosomes and exosome uptake experiments

For isolation of exosomes, the protocol of Adolf and colleagues (2018) was used with slight modifications. Briefly, 24 hr prior to exosome collection, cells were washed and medium changed to exosome depleted medium (EDM) containing 10% exosome-depleted FBS (Gibco, Cat# A27208-03). CM was collected, (protease inhibitor (PI) was added immediately for immunoblotting) and samples kept at 4^0C until exosome isolation. Exosomes were isolated through three centrifugation steps: 1) CM was spun for 10 min at 2,000*g* to remove debris; 2) the resulting supernatant was centrifuged for 30 min at 10,000*g* to pellet microvesicles; and 3) this second supernatant was centrifuged for 4 hrs at 100,000*g* (Optima MAX-XP ultracentrifuge, TLA-100.3 rotor, Beckman Coulter). Following ultracentrifugation, pelleted exosomes were re-suspended in buffer (for ELISA and immunoblotting) or cell culture medium, as required. For astrocyte uptake experiments, isolated OEC-exosomes were resuspended by pipetting and added directly to the culture medium of *CryAB*$^{-/-}$ astrocytes for 4 hrs. Cultures were then fixed with 4% paraformaldehyde and stained for markers of interest. Images were taken on a stimulated emission depletion (STED) confocal microscope (Leica, Wetzlar, Germany) for the visualization of internalized exosomes in astrocytes.

2.9 CryAB Immunoprecipitation

CryAB was immunoprecipitated (IP-CryAB) from isolated OEC-exosome fractions that were lysed in RIPA buffer. Briefly, 200µl Protein A Dynabeads (30mg/ml, Invitrogen, Cat# 10001D, Carlsbad, CA) were washed 3 times in PBS+ 0.1% Tween (PBST) using a magnetic stand (Millipore, PureProteome Cat# LSKMAGS08), CryAB antibody (400µl, 1:50 (10 µg/mL) in PBST) was added to the beads, and the mixture was incubated (30 min, RT) with constant agitation. The antibody solution was removed, beads washed (3x), exosome fractions resuspended in PBS were added, and the mixture was incubated overnight (4^0C). Beads were then washed (4x) and CryAB protein eluted by addition of 60µl of 0.2M Glycine (pH 2.5); the pH of the eluate was neutralized by addition of 5µl of 1M Tris (pH 8.5). Cell culture, immunoblotting or ELISA was performed.

2.10 ELISA

CryAB concentration was measured in exosome fractions using a competitive ELISA kit (MyBioSource, Cat# MBS7239470, San Diego, CA) according to manufacturer's instructions. Isolated exosomes were sonicated and lysed in Buffer M (containing NP40) plus PI from Protein Extraction Kit (BioChain). Equivalent quantities of total exosomal protein or supernatant CM protein, determined by BCA protein assay, were brought to equivalent volumes in EDM. 100µl of samples were added to each well and measured with a microplate reader (FlexStation 3; Molecular Devices, Sunnyvale, CA). Results were analyzed with SoftMax Pro Software (Molecular Devices).

2.11 Quantitative RT-PCR (q-RT-PCR)

cDNA synthesis was performed using Superscript™ III reverse transcriptase (Invitrogen), and PCR carried out using the ViiA7 Real-Time PCR System (Applied Biosystems, Waltham, MA) in 20µl final volume, containing 10µl of SsoAdvanced Universal SYBR Green Supermix (BioRad Cat#1725271), 2µl of a primer mix with a concentration of 1µM of each primer and 1µl of cDNA and 7µl water. Samples were run in triplicate. The expression levels of genes of interest were normalized using the primers (forward; reverse) (AGTGCCAGCCTCGTCCCGTA; TGAGCCCTTCCACAATGCCA), for expression of GAPDH (see Supplemental Data 3 for obtained values). All other primer sequences are detailed in (Liddelow *et al.*, 2017; Clarke *et al.,* 2018). Data were analyzed by one-way ANOVA followed by Dunnett's multiple post hoc test.

2.12 Statistical analysis and cell counting

All statistical analyses were done using GraphPad Prism 8.00 software. The results are shown as mean ± SD. Statistical analysis was performed using one-way or two-way ANOVA, unless otherwise stated. Probability values of 0.05 ($p \leq 0.05$) were considered to indicate statistical significance. N=biological replicates, n=technical replicates.

3 Results

3.1 OECs secrete anti-inflammatory factor(s) that reduce astrocyte reactivity

Nuclear translocation of the pro-inflammatory protein NFκB was used as a readout of astrocyte reactivity evoked by bacterial endotoxin LPS (Rothhammer *et al.*, 2016), as measured by immunoblot analysis of the nuclear fraction of astrocyte lysates (Figure 1A, inset). As expected, NFκB increased in the nuclear fraction of immortalized C8D30 astrocytes treated with LPS (Figure 1A, gray bars, $p \leq 0.05$). Co-culture of astrocytes with OECs blocked nuclear translocation of NFκB in response to LPS, as previously reported (Hale *et al.*, 2011; Figure 1A, purple bars). Adding CM from untreated OEC monocultures, (OEC-CM), also decreased NFκB translocation into nuclei of astrocytes exposed to LPS (Figure 1A, red bars,), indicating that anti-inflammatory factor(s) are secreted by OECs even in the absence of a stress signal.

To facilitate identification of OEC factors of interest, the anti-inflammatory capacity of six immortalized OEC lines (Calof & Guevara, 1993) were screened. Immortalized astrocytes (C8D30) were treated with CM from the different OEC lines, treated with LPS, immunostained for NFκB (Figure 1B), and the nuclear/cytoplasmic ratio of NFκB immunostaining was determined. As shown in Figure 1C, CM from two of the immortalized OEC lines, C7 and D6, significantly reduced nuclear NFκB translocation in C8D30 astrocytes compared to LPS treatment alone (Figure 1C, red bars, $p \leq 0.05$), while D4 and C4 CM were similar to LPS alone. Original characterization of these immortalized OEC lines had been based on morphology and immunostainining with markers expressed by primary OECs (Calof & Guevara, 1993). Characterization of the re-grown lines was consistent with earlier reports, with C7 cells, for example, showing heterogeneous morphologies depending on culture conditions and density (Figure 1D): these included Schwann Cell spindle-like (majority; Figure 1Da), astrocyte-like type1 (Figure 1Db), and astrocyte-like type2 (Figure 1Dc) morphologies (Huang *et al.,* 2008). Cell lines were re-examined by immunofluorescence for expression of OEC-specific markers, such as p75, Sox10, and brain lipid-binding protein (BLBP). Both C7 and C4 cell lines were positive for these OEC markers (Figure 1E). Since C7-CM significantly suppressed nuclear NFκB translocation in astrocytes, whereas C4-CM did not (Figure1B, C), and both lines expressed the OEC markers tested, C7-CM was used as a positive control, and C4-CM as a negative control in further experiments.

3.2 OEC-secreted CryAB suppresses LPS-induced astrocyte reactivity

To identify OEC-derived molecules potentially involved in crosstalk between OECs and astrocytes, secreted proteins from primary OEC-CM, C7-CM and C4-CM were compared by mass spectrometry. Before collection of CM, LPS was added to cultures as a stress signal. Secreted proteins from LPS-treated cells were ranked based on 1) their abundance in C7-CM compared to C4-CM; 2) their abundance in C7-CM compared to primary OEC-CM; and 3) absence from C4-CM (Figure 2A). Proteins that were secreted at similar levels

by C7 cells and primary OECs (Figure 2A, horizontal dashed line), but are not likely to be present in C4-CM (Figure 2A, X axis) were determined. Based on these criteria, we identified two proteins of particular interest: the heat shock protein alpha crystallin B chain (CryAB), and the cell surface glycoprotein MUC18 (MCAM). To identify OEC secreted molecules in response to an endogenous signal from astrocytes, similar experiments were performed after treatment with Anosmin1, an extracellular binding protein secreted by mature astrocytes (Gianola *et al.,* 2009) and shown to act on OECs (Hu *et al.,* 2019). Even though the ortholog is yet to be identified for this protein in mice, we observed a robust migration of primary mouse OECs towards recombinant Anosmin-1 (personal observation). Notably, both CryAB and MCAM were identified as major secreted proteins in this screen as well (Figure 2B). CryAB was selected for further study because of its known role as an anti-inflammatory protein involved in stress responses by CNS glia (e.g., Ousman *et al*., 2007; Kuipers *et al*., 2017), and because it was the most abundant protein fitting our criteria in screens of both LPS (Fig. 2A) and Anosmin-1 (Fig. 2B) treated samples. Recombinant CryAB protein mimicked the effect of OEC-CM or C7-CM on astrocyte reactivity, as measured by suppressed nuclear translocation of NFκB, following either LPS- or cytokine-induced inflammation (Figure 2C).

3.3 Exosomes secreted by OECs contain CryAB, which moderates intercellular immune response

Since it has been shown that CryAB secretion can occur via exosomes (Sreekumar *et al*., 2010; Kore *et al*., 2014; Guo *et al*., 2019), exosomes were isolated from OECs to determine whether they were positive for CryAB and whether the CryAB secreted via OEC-exosomes had the ability to attenuate astrocyte reactivity. For these experiments, exosome fractions were isolated from culture supernatants of OECs generated from both *CryAB*$^{-/-}$ mice and WT (*CryAB*$^{+/+}$) controls. To ensure the quality of fractions used, exosomes and whole cell lysates (CL) from WT OECs were analyzed by immunoblotting for the following proteins: the structural protein, β-actin; a mitochondrial protein, Tomm20; a nuclear protein, histone H3; and the extravesicular protein Flotilin-1. The exosome fraction was devoid of β-actin, Tomm20 and histone H3, but was positive for Flotilin-1 (Figure 3A), consistent with published information for exosome fractions (Jeppesen *et al*., 2019). Competitive ELISA against CryAB confirmed the presence of CryAB in OEC exosomes. Exosomes derived from 1x10^{6} OECs contained 9.22 ± 0.2 ng CryAB, whereas CryAB protein was undetectable in CM from which exosomes were depleted (Supplemental Figure 1A). Next, exosomes from both genotypes were immunoblotted for CryAB and the endocytosis protein, Alix, which is concentrated in exosomes (Figure 3B; Jeppesen *et al*., 2019). CryAB was present in WT OECexo fractions but was absent in *CryAB*$^{-/-}$OECexo fractions; while the exosome marker Alix was present in exosome fractions from OECs of both genotypes. Finally, to assay whether CryAB present in OEC exosomes could suppress astrocyte reactivity, the exosomes were added to immortalized C8D30 astrocytes for 24 hrs, and treated with LPS for

the last 2 hours of this incubation. As shown in Figure 3C, quantitative immunoblotting demonstrated that: a) exosomes from WT OECs were able to suppress astrocyte reactivity, as measured by reduced nuclear translocation of NFκB; b) astrocytes treated with *CryAB*$^{-/-}$OECexo remained reactive; and c) the reactivity of astrocytes treated with *CryAB*$^{-/-}$OECexo was reduced by the presence of recombinant CryAB protein. Immunostaining OEC-astrocyte co-cultures for NFκB further showed strong nuclear NFκB immunostaining exhibited by astrocytes co-cultured with *CryAB*$^{-/-}$OECs (Figure 3D, lower right). whereas astrocytes co-cultured with WT OECs showed little if any nuclear NFκB immunostaining (Figure 3D, lower left). Together, these results are consistent with CryAB, secreted by OECs in exosomes being an important protein for OEC-astrocyte crosstalk, and functioning as an anti-inflammatory molecule for astrocytes.

3.4 Astrocytes internalize CryAB-containing OEC exosomes

To determine whether astrocytes take up CryAB-containing exosomes secreted by OECs, *CryAB*$^{-/-}$ astrocytes were cultured with exosome fractions from OEC cultures generated from WT mice. Uptake was visualized by immunostaining of GFAP-positive astrocytes (Figure 4, magenta); colabeled with antibodies to endosome/exosome marker CD63 (red) and CryAB (green). CryAB and CD63 colocalized in *CryAB*$^{-/-}$ astrocytes treated with exosomes for 4 hrs (Figure 4, insets). Neither untreated *CryAB*$^{-/-}$ astrocytes (Figure 4B) nor WT astrocytes (Figure 4C) showed such specific colocalization, consistent with the uptake of CryAB-containing OEC exosomes by astrocytes.

3.5 OEC secreted factors, including CryAB, reduce astrocytes' expression of genes associated with neurotoxic reactivity

To evaluate the effects of OEC-secreted CryAB on expression of "neurotoxic" genes, astrocytes were exposed to LPS alone; or WT OEC-CM, *CryAB*$^{-/-}$OEC-CM, or CryAB immunoprecipitated from isolated OEC-exosome fractions (IP-CryAB) together with LPS. mRNA from treated astrocytes was then analyzed for 12 transcripts known to be associated with neurotoxic astrocyte reactivity (Liddelow *et al.*, 2017). Q-RT-PCR analysis (Figure 5) showed that all tested transcripts were reduced in expression in the presence of WT OEC-CM, and this effect was significant for 9 of the 12 (Figure 5, second row, white arrows, $p \leq 0.05$ A vs B). In contrast, 4 of the transcripts showed increased expression when treated with *CryAB*$^{-/-}$OEC-CM (Figure 5C, black arrows). The analysis also suggests that suppression of expression of *Ggta1*, *Serping1*, *ligp1*, *Gbp2* and *Amigo2* was CryAB-dependent, for the following reasons: a) suppression of expression failed to occur with *CryAB*$^{-/-}$OEC-CM treatment, while still taking place with IP-CryAB treatment (Figure 5, C vs D); or b) expression was upregulated in the *CryAB*$^{-/-}$OEC-CM group (Figure 5, C vs A). Suppression of expression of 4 genes (*H2-T23, Srgn*, *H2D1*and *C3*) appeared to be independent of CryAB, since it still occurred in

astrocytes treated with *CryAB*$^{-/-}$OEC-CM (Figure 5, C vs A). In contrast to either OEC-CM treatments (*CryAB*$^{-/-}$or WT), a significant increase in *Fbln5* was detected in astrocytes treated with IP-CryAB (Figure 5, D vs A). These results are consistent with the finding that CryAB, secreted by OECs, functions as an anti-inflammatory agent for astrocytes. In addition, comparison of OEC-CM treatment to IP-CryAB for transcripts *Ugt1a1*, *C3* and *Fbln5* suggest that there are factors in OEC-CM, in addition to CryAB, that suppress neurotoxic astrocyte reactivity.

4. Discussion

4.1 OEC-secreted factors that moderate astrocyte reactivity

Astrocyte reactivity is a pathological response that occurs in a wide range of CNS injuries, inflammation and diseases. *In vivo* studies show that some reactive astrocytes induced by ischemia can promote neural recovery and repair (reviewed in Rossi *et al.*, 2007); in contrast, reactive astrocytes induced by bacterial endotoxins such as LPS are neurotoxic (Zamanian *et al.*, 2012). This harmful, neurotoxic astrocyte reactivity appears to be driven by pro-inflammatory cytokines secreted by activated microglia (Liddelow *et al.*, 2017). However, anti-inflammatory factors that suppress neurotoxic astrocyte reactivity are largely unknown. Olfactory system is one of the few niches in the mammalian CNS that supports neuronal regeneration (Forni *et al.*, 2013). Olfactory sensory neurons are vulnerable to damage due to their exposed location in the nasal cavity and have a remarkable capacity for regeneration (Calof *et al.*, 1996, Forni *et al.*, 2013), suggesting the presence of robust anti-inflammatory factors in the olfactory system. OECs wrap and guide axons of the olfactory sensory neurons en route to the OB, where they establish new connections. Moreover, OECs directly interact with astrocytes at the entry point into the CNS, enabling regenerating olfactory axons to make new connections (Williams *et al.,* 2004; Li *et al.*, 2005; Raisman & Li, 2007). Notably, both transplanted OECs (Lakatos *et al.*, 2003; reviewed in Roet & Verhaagen, 2014) and co-cultured OECs (Hale *et al.*, 2011) have been shown to intermingle with astrocytes and to moderate astrocyte activation.

The studies in this report investigate anti-inflammatory factors secreted by OECs participating in OEC-astrocyte crosstalk. Mass spectrometry was used to analyze proteins in CM from primary OECs and compared to the CM of immortalized OEC lines with different anti-inflammatory capacities. Two proteins were identified as potential factors that could suppress neurotoxic astrocyte reactivity: MCAM and CryAB. MCAM (also called CD146 or MUC18) is a signaling receptor that can be cleaved from the cell membrane, generating a soluble form that is associated with increased cell migration and invasion (Seftalioglu & Karakoc, 2000), and primarily has been studied in endothelial cell angiogenesis and cancer metastasis (reviewed in Dye *et al.*, 2013). Studies on Multiple Sclerosis (MS) patients showed no association between MCAM expression and disease activity (Petersen *et al.*, 2019). In contrast, CryAB treatment of MS patients was associated with a therapeutic outcome, downregulation of T cell proliferation and pro-inflammatory cytokine production (Quach *et al.*, 2013; van Noort *et al.*, 2015). In addition, CryAB has been shown to have neuroprotective and regenerative effects in neuroinflammatory animal model systems (Arac *et al.*, 2011; Ousman *et al.,* 2007; van Noort *et al.*, 2015). Moreover, there is a correlation between glial activation and increased CryAB levels in Alexander, Alzheimer's and Parkinson's diseases, as well as traumatic brain injury and stroke (reviewed in Dulle & Fort, 2016). Thus, we investigated the role of OEC-secreted CryAB in OEC- astrocyte crosstalk.

4.2 Exosomal release of CryAB

Our results show that OECs secrete CryAB via exosomes, and that these exosomes produce an intercellular anti-inflammatory effect following their uptake by astrocytes. Exosomes are small vesicles packaged inside multivesicular endosomes (MVE) and released into the extracellular matrix when MVE fuse with the plasma membrane (Jeppesen *et al.*, 2019). Subsequent uptake by a neighboring cell initiates intercellular communication. Notably, released exosomes are functional components of the extracellular matrix that can be induced by stress signals but are associated with cell-cell communication rather than apoptosis (Jeppesen *et al.*, 2019; Gupta *et al.*, 2014). Consistent with our findings, recent studies suggest that CryAB can be secreted by glia in an autocrine manner (Kore *et al.*, 2014; Guo *et al.*, 2019) and play a protective role (Ousman *et al.*, 2007). Although the downstream effects of CryAB in astrocytes that we demonstrate have yet to be fully explored, one important role of CryAB may be its interaction with transcription factors, including NFκB, to suppress inflammation by inhibition of their nuclear translocation (Shao *et al.,* 2013; Zhang *et al.,* 2015; Qiu *et al.*, 2016). However, exosome-mediated regulation of the astrocytic immune response by OECs may also be a unique interaction, as membrane composition and protein content of exosomes is cell type (Kalra *et al.*, 2012; Keerthikumar *et al.*, 2015; Kim *et al.,* 2015) and context specific (György *et al.,* 2011; Müller *et al.*, 2012). The robust anti-inflammatory response induced by OEC-secreted CryAB, shown in the present report, may also be a function of concentration, as our results indicate the concentration of CryAB in OEC exosomes to be higher than that found in astrocyte exosomes. We found that CryAB in OEC secreted exosomes was ~21% higher than that of astrocyte exosomes (Supplemental Figure 1A) and exposure to LPS increased OEC secreted CryAB concentration by ~25% (Supplemental Figure 1B), indicating OECs actively respond to stress by either secreting more exosomes or increasing CryAB concentration in exosomes, or both. In addition, exposure to Anosmin1 increased CryAB concentration by ~77% (Supplemental Figure 1C), compared to control protein recombinant myoglobin, suggesting OECs can actively respond to extracellular astrocyte signals by increasing CryAB concentrations.

4.3 CryAB, as well as other factors secreted by OECs, can suppress neurotoxic astrocyte reactivity

Stress causes denaturation of correctly folded proteins that can result in their aggregation and binding to CryAB (Muranova *et al.,* 2018) and subsequent changes in gene expression (Singh *et al.,* 2019). Our results show that OEC-secreted CryAB suppressed expression of a number of genes associated with neurotoxic astrocyte reactivity and suggest there are additional factor(s) in OEC-CM that further suppress this harmful reactivity. In fact, complement component-3 (C3) expression in IP-CryAB +LPS-treated astrocytes, although not significantly different than that observed in astrocytes treated with LPS alone, was significantly greater

than expression in astrocytes treated with either OEC-CM groups (Figure 5). C3 is an important marker for neurotoxic astrocytes, evident by knockout mice showing reduced activity in microglia and astrocytes, as well as neuron loss (Shi *et al.*, 2017). Moreover, C3 is found colocalized with astrocyte markers in regions of neurodegeneration in human post-mortem tissue (Liddelow *et al.*, 2017). Therefore, more experiments are required to identify OEC-secreted factor(s) that can suppress C3. In this regard, other proteins identified in our mass spectrometric screen, showing smaller changes, may be worthwhile to evaluate. Certainly, crosstalk mechanisms between OECs and surrounding niche cells, including astrocytes, are highly complicated (Chuah *et al.*, 2011). In addition to unidentified anti-inflammatory factors, absence or suppression of pro-inflammatory factors might also play a role in OEC-CM's effect on astrocyte reactivity. For example, our mass spectrometry screening showed higher concentration of S100A4 and S100A6 proteins in C4-CM compared to pOEC-CM or C7-CM (Figure 2, Supplemental Data-1 & 2). S100 proteins are known to modulate neuroinflammation (Donato, 2001), and as such are also candidate molecules that may contribute to the observed difference in the inflammatory reactivity of astrocytes treated with C4-CM versus pOEC-CM or C7-CM.

Recent studies have transformed our perception of astrocytes from a passive structural support network for neurons, to active effectors in the regulation of synaptic transmission, neural excitability, plasticity and recovery. In this paper, we identify OEC secreted CryAB as an anti-inflammatory factor that can moderate astrocyte reactivity, suppressing both transcription of neurotoxic classified genes and nuclear translocation of pro-inflammatory factor NFκB. Improving our understanding of the crosstalk between astrocytes and OECs may inform strategies to identify other endogenous repair mechanisms that facilitate CNS repair, and consequently impact function, in the injured nervous system.

Figure Legends

Figure 1: OEC-CM alone is sufficient to suppress LPS-induced astrocyte reactivity, an effect mimicked by a subset of immortalized OEC lines.

(A) Quantitative immunoblotting for NFκB was performed on the nuclear fraction of C8D30 astrocyte lysates (inset). All groups were compared using a one-way ANOVA (N=3). Treatment with LPS for 2 hrs significantly increased NFκB activity (* indicates $p \leq 0.05$, gray bars). The presence of OECs blocked the effect of LPS (purple bars). OEC conditioned medium (OEC-CM) alone also blocked the increase in nuclear NFκB (red bars). (B and C) CM from six immortalized OEC lines were investigated for their ability to block the effect of LPS on nuclear NFκB translocation in C8D30 astrocytes, as measured by the ratio of fluorescence intensity of nuclear to cytoplasmic NFκB. (B) Photomicrograph of images of C8D30 astrocytes cocultured with CM of immortalized cell lines. (C) Fluorescent NFκB nuclear and cytoplasmic intensities were measured and ratios plotted. Pink dashed line depicts value of astrocytes treated with primary OEC-CM +LPS and red dashed line depicts value of astrocytes +LPS. A median value was calculated from ~100 cells per field, and then a mean/group was calculated. C7-CM and D6-CM decreased NFκB nuclear translocation ($N = 3$; * $p \leq 0.05$; one-way ANOVA), while C4-CM treated groups was not significantly different than astrocytes +LPS alone ($N = 3$; * $p \leq 0.05$; one-way ANOVA). (D) Photomicrograph from line C7. Multiple morphologies were found in all the OEC cell lines: (a) Schwann Cell-like, (b) astrocyte-like type1, and (c) astrocyte-like type2. Schwann cell-like spindle cells (a) predominated in C7. (E) C7 and C4 olfactory cell lines share multiple markers with OECs including BLBP (magenta), Sox10 (green) and P75 (red). Scale bars represent 25 and 20μm.

Figure 2: OEC-secreted anti-inflammatory protein CryAB and recombinant CryAB is sufficient to suppress astrocyte reactivity measured by NFκB.

(A, B) Comparison of factors secreted from C7 line, C4 line and primary OECs (pOECs), analyzed by mass spectrometry. Proteins detected in CM following LPS treatment (A) or Anosmin1 treatment (B) were ranked by their relative abundance indicated by color code (heat map, inset). Relative abundance of detected proteins in C7-CM compared to pOEC-CM is graphed on the Y axes, and relative absence of the same proteins from C4-CM (1-P(C4-CM) = probability of not being found in C4-CM) is graphed on the X axes. Proteins of similar abundance in CMs from C7 cells and pOECs (horizontal red-dashed lines), and not likely to be present in C4-CM (Y axes) were identified. Alpha crystallin B chain (CryAB) had the highest C7/C4 expression ratio and was equally abundant in CM from C7 cells and pOECs. (C) Recombinant CryAB alone suppressed the inflammatory response, quantified as the ratio of nuclear to cytoplasmic NFκB (Y axis) in astrocytes exposed to either LPS or a cocktail of the cytokines Il-1α, TNFα and C1q for 2 hrs. Group values were obtained from

triplicate wells in which a median value was calculated from ~50 cells per field. N = 3; (*p ≤ 0.05; **p ≤ 0.01; ****p ≤ 0.0001;) two-way ANOVA.

Figure 3: CryAB, secreted by primary OECs into exosomes, suppresses inflammatory response in an astrocyte cell line.

(A) Immunoblot of exosome (Exo, left) and whole cell lysate (CL, right) fractions from WT primary OECs were screened for β-actin, Tomm20, histone H3, and Flotilin-1. The exosome fraction from WT exosomes was devoid of cellular β-actin, Tomm20 and histone H3, but contained the extravesicular protein Flotilin-1. (B) Immunoblots for CryAB and the exosome marker Alix were performed on exosome fractions made from *CryAB*$^{-/-}$ and WT (*CryAB*$^{+/+}$) OEC cultures. CryAB was absent in exosome fractions from *CryAB*$^{-/-}$ OEC culture medium, whereas the exosome marker Alix was present. (C) C8D30 astrocytes were treated for 24 hours with exosomes isolated from WT or *CryAB*$^{-/-}$ OECs. Astrocytes were exposed to 1μg/ml LPS for the last 2 hrs of exosome treatment. Nuclear fractions of astrocytes were analyzed via quantitative immunoblotting for NFκB and Histone H3. Inset shows a representative immunoblot and graph shows mean ± SD of NFκB/histone ratio. All conditions were compared to astrocyte alone group (Control, N = 3; p ≤ 0.05; one-way ANOVA). Treatment of astrocytes with WT OEC-exosomes (exo) + LPS, blocked nuclear NFκB translocation. In contrast, *CryAB*$^{-/-}$OEC-exosomes failed to suppress nuclear NFκB translocation. Recombinant CryAB (50ng/ml) added to *CryAB*$^{-/-}$OEC-exosomes was sufficient to attenuate NFκB translocation induced by LPS, with levels comparable to WT OEC-exo +LPS. (D) C8D30 astrocytes treated with LPS for 2 hrs (top right: "+ LPS") showed stronger immunostaining for NFκB in the nucleus (magenta) compared to untreated controls (top left). Astrocytes co-cultured with *CryAB*$^{-/-}$ OECs (Sox 10-positive cells with blue nuclei) had increased levels of NFκB immunostaining in the nucleus (bottom right: "+*CryAB*$^{-/-}$OECs +LPS") compared to astrocytes co-cultured with WT OECs (bottom left: "+OECs +LPS"). Scale bar represents 40μm.

Figure 4: CryAB in OEC exosomes is internalized by astrocytes.

(A) OEC exosomes from WT mice were co-cultured with primary astrocytes from CryAB KO mice. (B) Untreated astrocytes from CryAB KO. (C) Untreated astrocytes from WT mice. All groups were stained for CD63 (endosomes; red), CryAB (green), GFAP (magenta) and Dapi (blue). Uptake of OEC secreted CryAB (green) is detected in CryAB$^{-/-}$ astrocytes and is often associated with endosomes (red) (A, arrows, top arrow area shown in inset, arrowhead points to CryAB positive endosome). No CryAB staining (green) is detected in untreated astrocytes from CryAB KO (B, inset). CryAB (green) is present in untreated astrocytes from WT

mice but rarely associated with endosomes (C, inset, arrowhead). Scale bar represents 5μm in low mag and 1μm in insets.

Figure 5: OEC-CM suppresses multiple transcripts associated with neurotoxic astrocyte reactivity in LPS-treated astrocytes.

Heat map illustrating results of Q-RT-PCR (Supplemental Data 3) to detect neurotoxic astrocyte transcripts in primary astrocytes treated with LPS (A); LPS plus WT OEC-CM (B); LPS plus *CryAB*$^{-/-}$OEC-CM (C); or IP-CryAB for 24 hrs (D). Compared to LPS, OEC-CM (B) significantly suppressed 9 transcripts, whereas *CryAB*$^{-/-}$OEC-CM (C) significantly suppressed 4. (D) IP-CryAB suppressed 6 of the 9 transcripts suppressed by OEC-CM. In addition, *CryAB*$^{-/-}$OEC-CM+LPS caused a significant increase in 4 transcripts, while IP-CryAB caused a significant increase in one. Finally, one transcript, C3, was significantly suppressed by both OEC-CM treatments (*CryAB*$^{-/-}$ or WT) but was elevated by IP-CryAB treatment. Q-RT-PCR experiments were analyzed by one-way ANOVA followed by Dunnett's multiple post hoc test (n= 3; arrows $p \leq 0.05$).

Acknowledgements

We thank Dr. S. Kawauchi for help transferring OEmyc790 cell lines; Dr. Y. Li and the NINDS Protein/Peptide Sequencing Facility for mass spectrometry analysis; Dr. L. Dong and the NEI transgenic mouse core for providing cryopreserved sperm from *CryAB*$^{-/-}$ mice; Dr. J. Pickel and the NIMH transgenic mouse core facility for rejuvenation of mice; Dr. V. Schram and the NINDS Light Imaging Facility for use of the confocal scanning and STED microscopy. We also thank the Amara Lab, Sibley Lab and Friedman Lab for the use equipment. Dr. Y. Shan, Dr. J. Chen and Dr. S. Inagaki for technical assistance. We are grateful to Drs E. Quinlan, S. Constantin, H. Cho, N. Whittington, P. Yuen, J. Street and M. Barzik for providing helpful advice.

This work was supported by the Intramural Research Program of the National Institutes of Health, National Institute of Neurological Disorders and Stroke (ZIA NS002824-28). The authors declare that there are no potential conflicts of interest.

References

Adolf, A., Rohrbeck, A., Münster-Wandowski, A., Johansson, M., Kuhn, H. G., Kopp, M. A., … Höltje, M. (2019). Release of astroglial vimentin by extracellular vesicles: Modulation of binding and internalization of C3 transferase in astrocytes and neurons. Glia, 67(4), 703–717. https://doi.org/10.1002/glia.23566

Arac, A., Brownell, S. E., Rothbard, J. B., Chen, C., Ko, R. M., Pereira, M. P., … Steinberg, G. K. (2011). Systemic augmentation of alpha B-crystallin provides therapeutic benefit twelve hours post-stroke onset via immune modulation. Proceedings of the National Academy of Sciences. https://doi.org/10.1073/pnas.1107368108

Au, E., & Roskams, A. J. (2003). Olfactory ensheathing cells of the lamina propria in vivo and in vitro. GLIA, 41(3), 224–236. https://doi.org/10.1002/glia.10160

Brady, J. P., Garland, D. L., Green, D. E., Tamm, E. R., Giblin, F. J., & Wawrousek, E. F. (2001). B-Crystallin in Lens Development and Muscle Integrity: A Gene Knockout Approach. Investigative Ophthalmology & Visual Science (Vol. 42).

Calof, A. L., & Guevara, J. L. (1993). Cell lines derived from retrovirus-mediated oncogene transduction into olfactory epithelium cultures. Methods in Neurosciences, 3, 222–231. https://doi.org/10.1006/ncmn.1993.1057

Calof, A. L., Hagiwara, N., Holcomb, J. D., Mumm, J. S., & Shou, J. (1996). Neurogenesis and cell death in olfactory epithelium. Journal of Neurobiology, 30(1), 67–81. https://doi.org/10.1002/(SICI)1097-4695(199605)30:1<67::AID-NEU7>3.0.CO;2-E

Chuah, M. I., Hale, D. M., & West, A. K. (2011). Interaction of olfactory ensheathing cells with other cell types in vitro and after transplantation: Glial scars and inflammation. Experimental Neurology. https://doi.org/10.1016/j.expneurol.2010.08.012

Clarke, L. E., Liddelow, S. A., Chakraborty, C., Münch, A. E., Heiman, M., & Barres, B. A. (2018). Normal aging induces A1-like astrocyte reactivity. Proceedings of the National Academy of Sciences of the United States of America, 115(8), E1896–E1905. https://doi.org/10.1073/pnas.1800165115

D'Agostino, M., Lemma, V., Chesi, G., Stornaiuolo, M., Serio, M. C., D'Ambrosio, C., … Bonatti, S. (2013). The cytosolic chaperone α-crystallin B rescues folding and compartmentalization of misfolded multispan transmembrane proteins. Journal of Cell Science, 126(18), 4160–4172. https://doi.org/10.1242/jcs.125443

Dairaghi, L., Flannery, E., Giacobini, P., Saglam, A., Saadi, H., Constantin, S., … Wray, S. (2018). Reelin can modulate migration of olfactory ensheathing cells and gonadotropin releasing hormone neurons via the canonical pathway. Frontiers in Cellular Neuroscience. https://doi.org/10.3389/fncel.2018.00228

Donato, R. (2001). S100: a multigenic family of calcium-modulated proteins of the EF-hand type with intracellular and extracellular functional roles. The International Journal of Biochemistry & Cell Biology (Vol. 33). Retrieved from www.elsevier.com/locate/ijbcb*

Dulle, J. E., & Fort, P. E. (2016). Crystallins and neuroinflammation: The glial side of the story. Biochimica et Biophysica Acta - General Subjects, 1860(1), 278–286. https://doi.org/10.1016/j.bbagen.2015.05.023

Dye, D. E., Medic, S., Ziman, M., & Coombe, D. R. (2013). Melanoma biomolecules: Independently identified but functionally intertwined. Frontiers in Oncology. https://doi.org/10.3389/fonc.2013.00252

Foo, L. C., Allen, N. J., Bushong, E. A., Ventura, P. B., Chung, W. S., Zhou, L., … Barres, B. A. (2011). Development of a method for the purification and culture of rodent astrocytes. Neuron. https://doi.org/10.1016/j.neuron.2011.07.022

Forni, P. E., Bharti, K., Flannery, E. M., Shimogori, T., & Wray, S. (2013). The indirect role of fibroblast growth factor-8 in defining neurogenic niches of the olfactory/GnRH systems. Journal of Neuroscience, 33(50), 19620–19634. https://doi.org/10.1523/JNEUROSCI.3238-13.2013

Gianola, S., de Castro, F., & Rossi, F. (2009). Anosmin-1 stimulates outgrowth and branching of developing Purkinje axons. Neuroscience, 158(2), 570–584. https://doi.org/10.1016/j.neuroscience.2008.10.022

Guo, Y. shun, Liang, P. Zhou, Lu, S. Zhao, Chen, R., Yin, Y. Qing, & Zhou, J. Wei. (2019). Extracellular αB-crystallin modulates the inflammatory responses. Biochemical and Biophysical Research Communications, 508(1), 282–288. https://doi.org/10.1016/j.bbrc.2018.11.024

Gupta, A., & Pulliam, L. (2014). Exosomes as mediators of neuroinflammation. Journal of Neuroinflammation, 11, 1–10. https://doi.org/10.1186/1742-2094-11-68

György, B., Szabó, T. G., Pásztói, M., Pál, Z., Misják, P., Aradi, B., … Buzás, E. I. (2011). Membrane vesicles, current state-of-the-art: Emerging role of extracellular vesicles. Cellular and Molecular Life Sciences. https://doi.org/10.1007/s00018-011-0689-3

Hale, D. M., Ray, S., Leung, J. Y., Holloway, A. F., Chung, R. S., West, A. K., & Chuah, M. I. (2011). Olfactory

ensheathing cells moderate nuclear factor kappaB translocation in astrocytes. Molecular and Cellular Neuroscience. https://doi.org/10.1016/j.mcn.2010.09.004

Holt, L. M., Stoyanof, S. T., & Olsen, M. L. (2019). Magnetic Cell Sorting for In Vivo and In Vitro Astrocyte, Neuron, and Microglia Analysis. Current Protocols in Neuroscience. https://doi.org/10.1002/cpns.71

Hu, Y., Butts, T., Poopalasundaram, S., Graham, A., & Bouloux, P. M. (2019). Extracellular matrix protein anosmin-1 modulates olfactory ensheathing cell maturation in chick olfactory bulb development. European Journal of Neuroscience, 50(9), 3472–3486. https://doi.org/10.1111/ejn.14483

Huang, Z. H., Wang, Y., Cao, L., Su, Z. Da, Zhu, Y. L., Chen, Y. Z., … He, C. (2008). Migratory properties of cultured olfactory ensheathing cells by single-cell migration assay. Cell Research. https://doi.org/10.1038/cr.2008.38

Imaizumi, T., Lankford, K. L., Burton, W. V., Fodor, W. L., & Kocsis, J. D. (2000). Xenotransplantation of transgenic pig olfactory ensheathing cells promotes axonal regeneration in rat spinal cord. Nature Biotechnology. https://doi.org/10.1038/79432

Jeppesen, D. K., Fenix, A. M., Franklin, J. L., Higginbotham, J. N., Zhang, Q., Zimmerman, L. J., … Coffey, R. J. (2019). Reassessment of Exosome Composition. Cell, 177(2), 428-445.e18. https://doi.org/10.1016/j.cell.2019.02.029

Johansson, S., Lee, I. H., Olson, L., & Spenger, C. (2005). Olfactory ensheathing glial co-grafts improve functional recovery in rats with 6-OHDA lesions. Brain. https://doi.org/10.1093/brain/awh644

Kalra, H., Simpson, R. J., Ji, H., Aikawa, E., Altevogt, P., Askenase, P., … Mathivanan, S. (2012). Vesiclepedia: A Compendium for Extracellular Vesicles with Continuous Community Annotation. PLoS Biology. https://doi.org/10.1371/journal.pbio.1001450

Keerthikumar, S., Chisanga, D., Ariyaratne, D., Al Saffar, H., Anand, S., Zhao, K., … Mathivanan, S. (2016). ExoCarta: A Web-Based Compendium of Exosomal Cargo. Journal of Molecular Biology. https://doi.org/10.1016/j.jmb.2015.09.019

Kim, D. K., Lee, J., Kim, S. R., Choi, D. S., Yoon, Y. J., Kim, J. H., … Gho, Y. S. (2015). EVpedia: A community web portal for extracellular vesicles research. Bioinformatics. https://doi.org/10.1093/bioinformatics/btu741

Klenke, U., & Taylor-Burds, C. (2012). Culturing embryonic nasal explants for developmental and physiological study. Current Protocols in Neuroscience.

https://doi.org/10.1002/0471142301.ns0325s59

Kore, R. A., & Abraham, E. C. (2014). Inflammatory cytokines, interleukin-1 beta and tumor necrosis factor-alpha, upregulated in glioblastoma multiforme, raise the levels of CRYAB in exosomes secreted by U373 glioma cells. Biochemical and Biophysical Research Communications. https://doi.org/10.1016/j.bbrc.2014.09.068

Kuipers, H. F., Yoon, J., Van Horssen, J., Han, M. H., Bollyky, P. L., Palmer, T. D., & Steinman, L. (2017). Phosphorylation of αB-crystallin supports reactive astrogliosis in demyelination. Proceedings of the National Academy of Sciences of the United States of America, 114(9), E1745–E1754. https://doi.org/10.1073/pnas.1621314114

Lakatos, A., Barnett, S. C., & Franklin, R. J. M. (2003). Olfactory ensheathing cells induce less host astrocyte response and chondroitin sulphate proteoglycan expression than Schwann cells following transplantation into adult CNS white matter. Experimental Neurology. https://doi.org/10.1016/S0014-4886(03)00270-X

Li, Y., Field, P. M., & Raisman, G. (2005). Olfactory ensheathing cells and olfactory nerve fibroblasts maintain continuous open channels for regrowth of olfactory nerve fibres. GLIA, 52(3), 245–251. https://doi.org/10.1002/glia.20241

Li, Y., Field, P. M., & Raisman, G. (1997). Repair of adult rat corticospinal tract by transplants of olfactory ensheathing cells. Science, 277(5334), 2000–2002. https://doi.org/10.1126/science.277.5334.2000

Liddelow, S. A., & Barres, B. A. (2017). Reactive Astrocytes: Production, Function, and Therapeutic Potential. Immunity, 46(6), 957–967. https://doi.org/10.1016/j.immuni.2017.06.006

Liddelow, S. A., Guttenplan, K. A., Clarke, L. E., Bennett, F. C., Bohlen, C. J., Schirmer, L., … Barres, B. A. (2017). Neurotoxic reactive astrocytes are induced by activated microglia. Nature, 541(7638), 481–487. https://doi.org/10.1038/nature21029

Müller, G. (2012). Microvesicles/exosomes as potential novel biomarkers of metabolic diseases. Diabetes, Metabolic Syndrome and Obesity: Targets and Therapy. https://doi.org/10.2147/dmso.s32923

Muranova, L. K., Sudnitsyna, M. V., & Gusev, N. B. (2018). αB-Crystallin Phosphorylation: Advances and Problems. Biochemistry (Moscow). https://doi.org/10.1134/S000629791810005X

Nash, H. H., Borke, R. C., & Anders, J. J. (2001). New Method of Purification for Establishing Primary Cultures of Ensheathing Cells from the Adult Olfactory Bulb. GLIA (Vol. 34).

https://doi.org/10.1002/glia.1043

O'Toole, D. A., West, A. K., & Chuah, M. I. (2007). Effect of olfactory ensheathing cells on reactive astrocytes in vitro. Cellular and Molecular Life Sciences. https://doi.org/10.1007/s00018-007-7106-y

Ousman, S. S., Tomooka, B. H., Van Noort, J. M., Wawrousek, E. F., O'Conner, K., Hafler, D. A., … Steinman, L. (2007). Protective and therapeutic role for αB-crystallin in autoimmune demyelination. Nature. https://doi.org/10.1038/nature05935

Petersen, E. R., Ammitzbøll, C., Søndergaard, H. B., Oturai, A. B., Sørensen, P. S., Nilsson, A. C., … Sellebjerg, F. (2019). Expression of melanoma cell adhesion molecule-1 (MCAM-1) in natalizumab-treated multiple sclerosis. Journal of Neuroimmunology, 337. https://doi.org/10.1016/j.jneuroim.2019.577085

Qiu, J., Yan, Z., Tao, K., Li, Y., Li, Y., Li, J., … Chen, H. (2016). Sinomenine activates astrocytic dopamine D2 receptors and alleviates neuroinflammatory injury via the CRYAB/STAT3 pathway after ischemic stroke in mice. Journal of Neuroinflammation, 13(1). https://doi.org/10.1186/s12974-016-0739-8

Quach, Q. L., Metz, L. M., Thomas, J. C., Rothbard, J. B., Steinman, L., & Ousman, S. S. (2013). CRYAB modulates the activation of CD4+ T cells from relapsing-remitting multiple sclerosis patients. Multiple Sclerosis Journal, 19(14), 1867–1877. https://doi.org/10.1177/1352458513489853

Raisman, G., & Li, Y. (2007). Repair of neural pathways by olfactory ensheathing cells. Nature Reviews Neuroscience, 8(April), 313. https://doi.org/10.1038/nrn2099

Ramer, L. M., Au, E., Richter, M. W., Liu, J., Tetzlaff, W., & Roskams, A. J. (2004). Peripheral Olfactory Ensheathing Cells Reduce Scar and Cavity Formation and Promote Regeneration after Spinal Cord Injury. Journal of Comparative Neurology. https://doi.org/10.1002/cne.20049

Roet, K. C. D., & Verhaagen, J. (2014). Understanding the neural repair-promoting properties of olfactory ensheathing cells. Experimental Neurology. Academic Press Inc. https://doi.org/10.1016/j.expneurol.2014.05.007

Rossi, D. J., Brady, J. D., & Mohr, C. (2007, November). Astrocyte metabolism and signaling during brain ischemia. Nature Neuroscience. https://doi.org/10.1038/nn2004

Rothhammer, V., Mascanfroni, I. D., Bunse, L., Takenaka, M. C., Kenison, J. E., Mayo, L., … Quintana, F. J. (2016). Type I interferons and microbial metabolites of tryptophan modulate astrocyte activity and central nervous system inflammation via the aryl hydrocarbon receptor. Nature Medicine, 22(6), 586–

597. https://doi.org/10.1038/nm.4106

Seftalioglu, A., & Karakoc, L. (2000). Expression of CD146 adhesion molecules (MUC18 or MCAM) in the thymic microenvironment. acta histochem (Vol. 102). https://doi.org/10.1078/0065-1281-00544.

Shao, W., Zhang, S. Z., Tang, M., Zhang, X. H., Zhou, Z., Yin, Y. Q., … Zhou, J. W. (2013). Suppression of neuroinflammation by astrocytic dopamine D2 receptors via αb-crystallin. Nature, 494(7435), 90–94. https://doi.org/10.1038/nature11748

Shi, Q., Chowdhury, S., Ma, R., Le, K. X., Hong, S., Caldarone, B. J., … Lemere, C. A. (2017). Complement C3 deficiency protects against neurodegeneration in aged plaque-rich APP/PS1 mice. Science Translational Medicine. https://doi.org/10.1126/scitranslmed.aaf6295

Silver, J., Schwab, M. E., & Popovich, P. G. (2015). Central nervous system regenerative failure: Role of oligodendrocytes, astrocytes, and microglia. Cold Spring Harbor Perspectives in Biology, 7(3). https://doi.org/10.1101/cshperspect.a020602

Singh, J. P., Kumar, R. R., Goswami, S., Rai, G. K., Sakhare, A., Kumar, S., … Praveen, S. (2019). A putative heat-responsive transcription factor (TaHD97) and its targets in wheat (Triticum aestivum) providing thermotolerance. Indian Journal of Biotechnology. http://nopr.niscair.res.in/handle/123456789/53098

Sofroniew, M. V., & Vinters, H. V. (2010, January). Astrocytes: Biology and pathology. Acta Neuropathologica. https://doi.org/10.1007/s00401-009-0619-8

Sreekumar, P. G., Kannan, R., Kitamura, M., Spee, C., Barron, E., Ryan, S. J., & Hinton, D. R. (2010). αB crystallin is apically secreted within exosomes by polarized human retinal pigment epithelium and provides neuroprotection to adjacent cells. PLoS ONE, 5(10). https://doi.org/10.1371/journal.pone.0012578

van Noort, J. M., Bsibsi, M., Nacken, P. J., Verbeek, R., & Venneker, E. H. G. (2015). Therapeutic intervention in multiple sclerosis with alpha B-crystallin: A randomized controlled phase IIa trial. PLoS ONE, 10(11). https://doi.org/10.1371/journal.pone.0143366

Wheeler, M. A., Clark, I. C., Tjon, E. C., Li, Z., Zandee, S. E. J., Couturier, C. P., … Quintana, F. J. (2020). MAFG-driven astrocytes promote CNS inflammation. Nature, 578(7796), 593–599. https://doi.org/10.1038/s41586-020-1999-0

Williams, S. K., Franklin, R. J. M., & Barnett, S. C. (2004). Response of Olfactory Ensheathing Cells to the

Degeneration and Regeneration of the Peripheral Olfactory System and the Involvement of the Neuregulins. Journal of Comparative Neurology, 470(1), 50–62. https://doi.org/10.1002/cne.11045

Zamanian, J. L., Xu, L., Foo, L. C., Nouri, N., Zhou, L., Giffard, R. G., & Barres, B. A. (2012). Genomic Analysis of Reactive Astrogliosis. Journal of Neuroscience. https://doi.org/10.1523/JNEUROSCI.6221-11.2012

Zhang, Y., Chen, Y., Wu, J., Manaenko, A., Yang, P., Tang, J., … Zhang, J. H. (2015). Activation of Dopamine D2 Receptor Suppresses Neuroinflammation Through αb-Crystalline by Inhibition of NF-κB Nuclear Translocation in Experimental ICH Mice Model. Stroke, 46(9), 2637–2646. https://doi.org/10.1161/STROKEAHA.115.009792

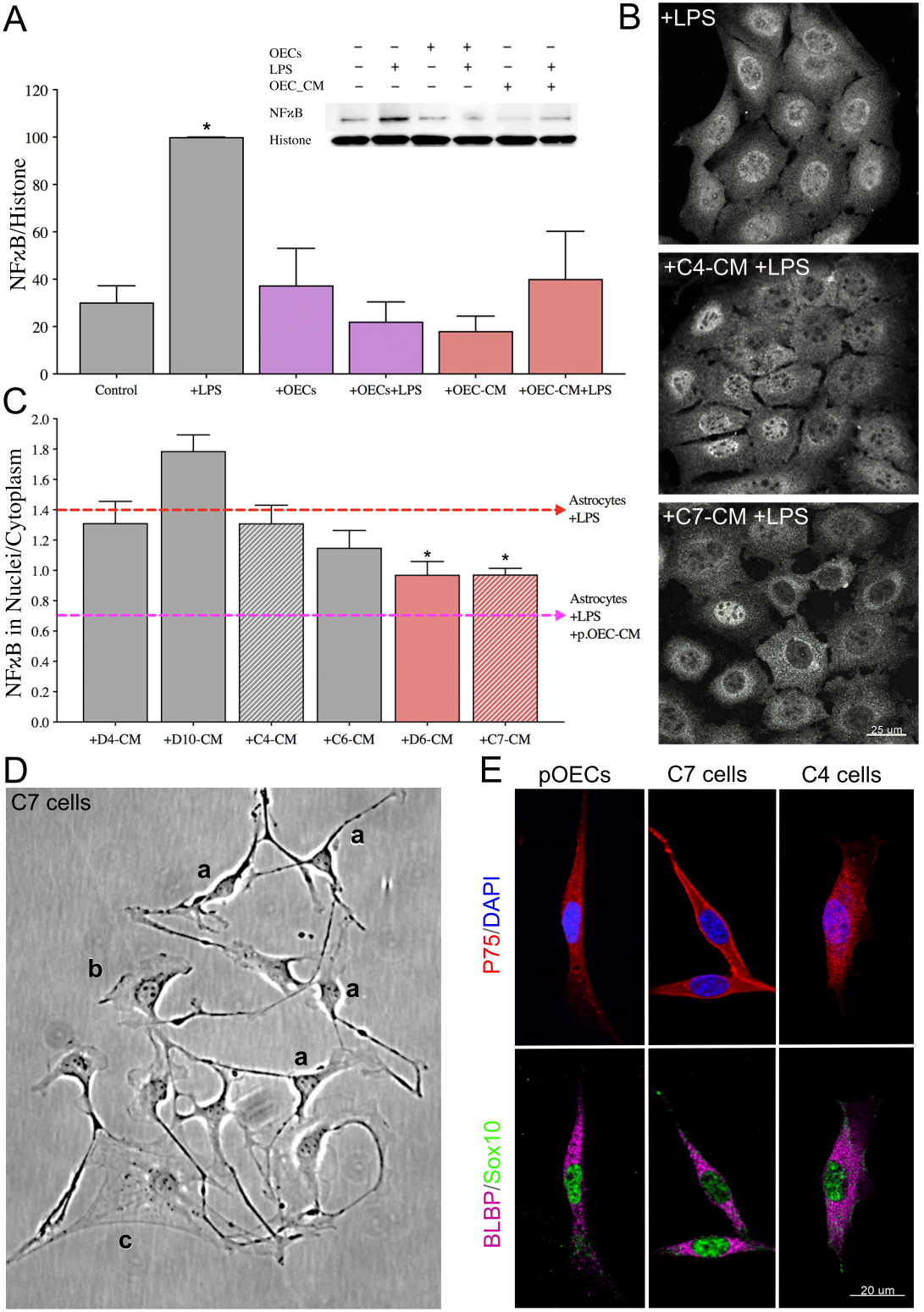
A
OECs
LPS
OEC_CM
NFκB
Histone
NFκB/Histone
120
100
80
60
40
20
0
*
Control
+LPS
+OECs
+OECs+LPS
+OEC-CM
+OEC-CM+LPS
B
+LPS
+C4-CM +LPS
+C7-CM +LPS
25 um
C
NFκB in Nuclei/Cytoplasm
2.0
1.8
1.6
1.4
1.2
1.0
0.8
0.6
0.4
0.2
0.0
Astrocytes +LPS
Astrocytes +LPS +p.OEC-CM
+D4-CM
+D10-CM
+C4-CM
+C6-CM
+D6-CM
+C7-CM
D
C7 cells
a
b
c
E
pOECs
C7 cells
C4 cells
P75/DAPI
BLBP/Sox10
20 um

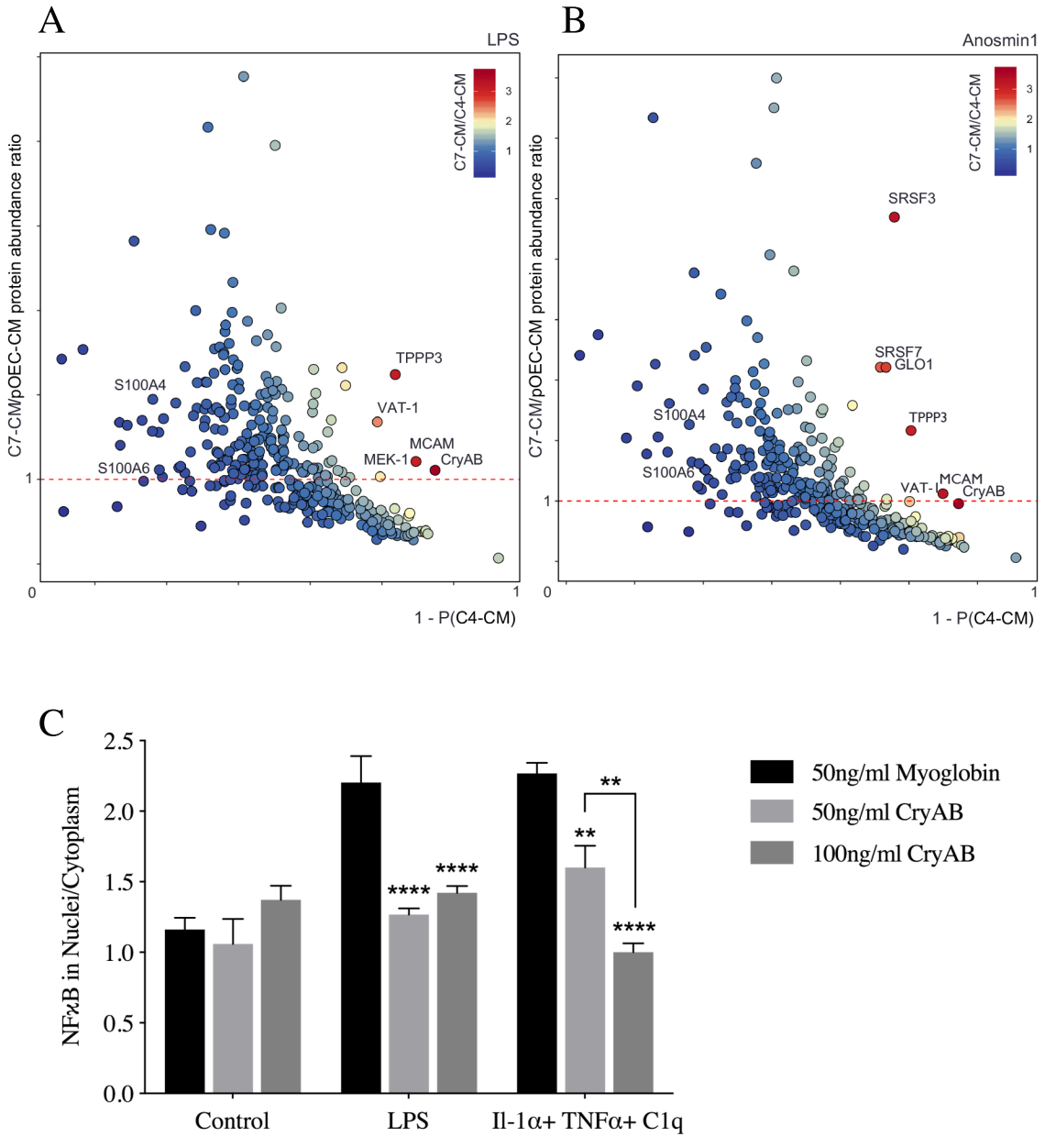
A
LPS
C7-CM/C4-CM
3
2
1
C7-CM/pOEC-CM protein abundance ratio
TPPP3
S100A4
VAT-1
MCAM
MEK-1
CryAB
S100A6
1
0
1
1 - P(C4-CM)
B
Anosmin1
C7-CM/C4-CM
3
2
1
C7-CM/pOEC-CM protein abundance ratio
SRSF3
SRSF7
GLO1
S100A4
TPPP3
S100A6
VAT-1
MCAM
CryAB
1
0
1
1 - P(C4-CM)
C
NFκB in Nuclei/Cytoplasm
2.5
2.0
1.5
1.0
0.5
0.0
****
****
**
**
****
Control
LPS
Il-1α+ TNFα+ C1q
50ng/ml Myoglobin
50ng/ml CryAB
100ng/ml CryAB

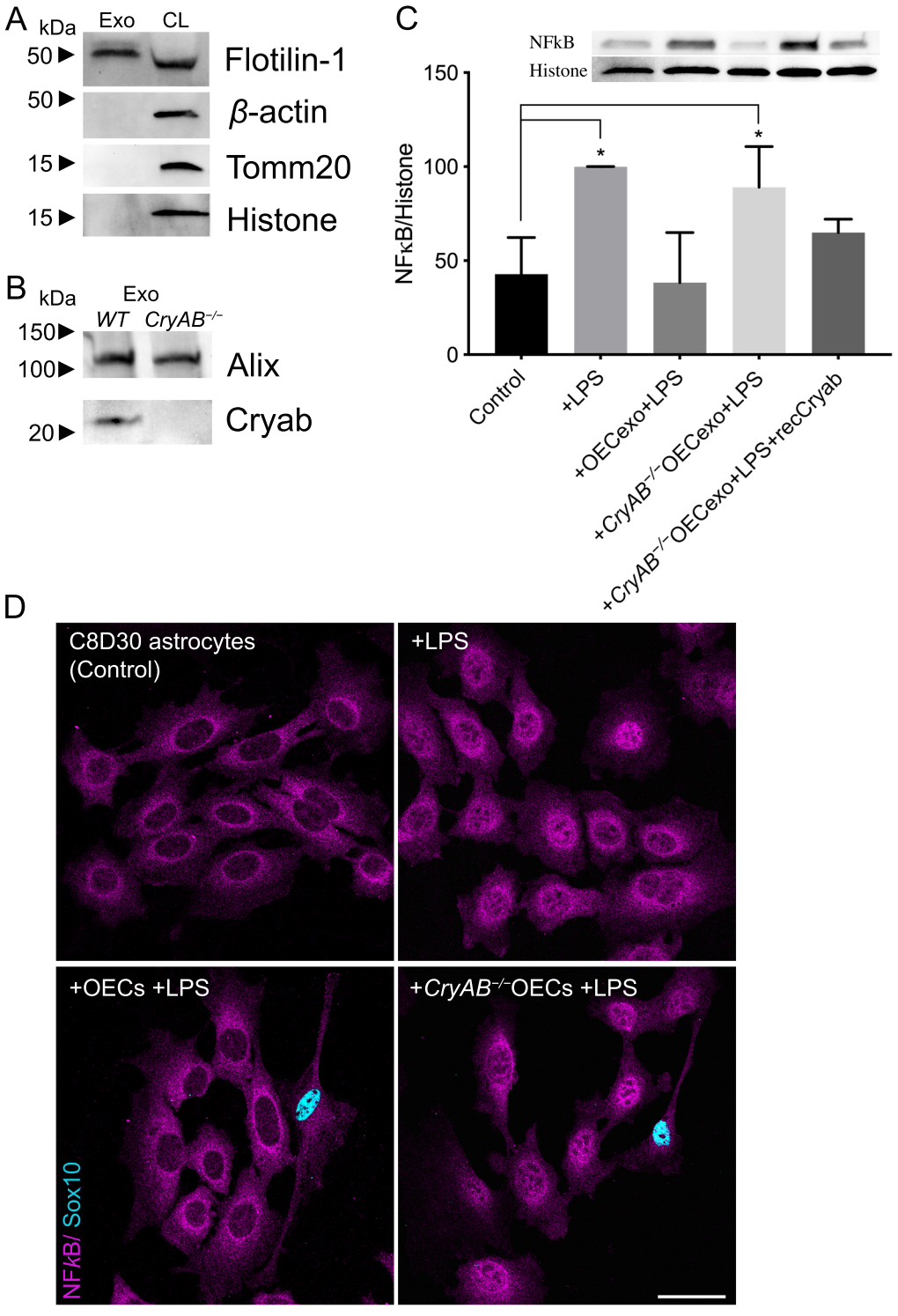
A
kDa
Exo
CL
50
Flotilin-1
50
β-actin
15
Tomm20
15
Histone
B
kDa
Exo
WT
CryAB−/−
150
100
Alix
20
Cryab
C
NFkB
Histone
NFκB/Histone
150
100
50
0
*
*
Control
+LPS
+OECexo+LPS
+CryAB−/−OECexo+LPS
+CryAB−/−OECexo+LPS+recCryab
D
C8D30 astrocytes
(Control)
+LPS
+OECs +LPS
+CryAB−/−OECs +LPS
NFkB/ Sox10

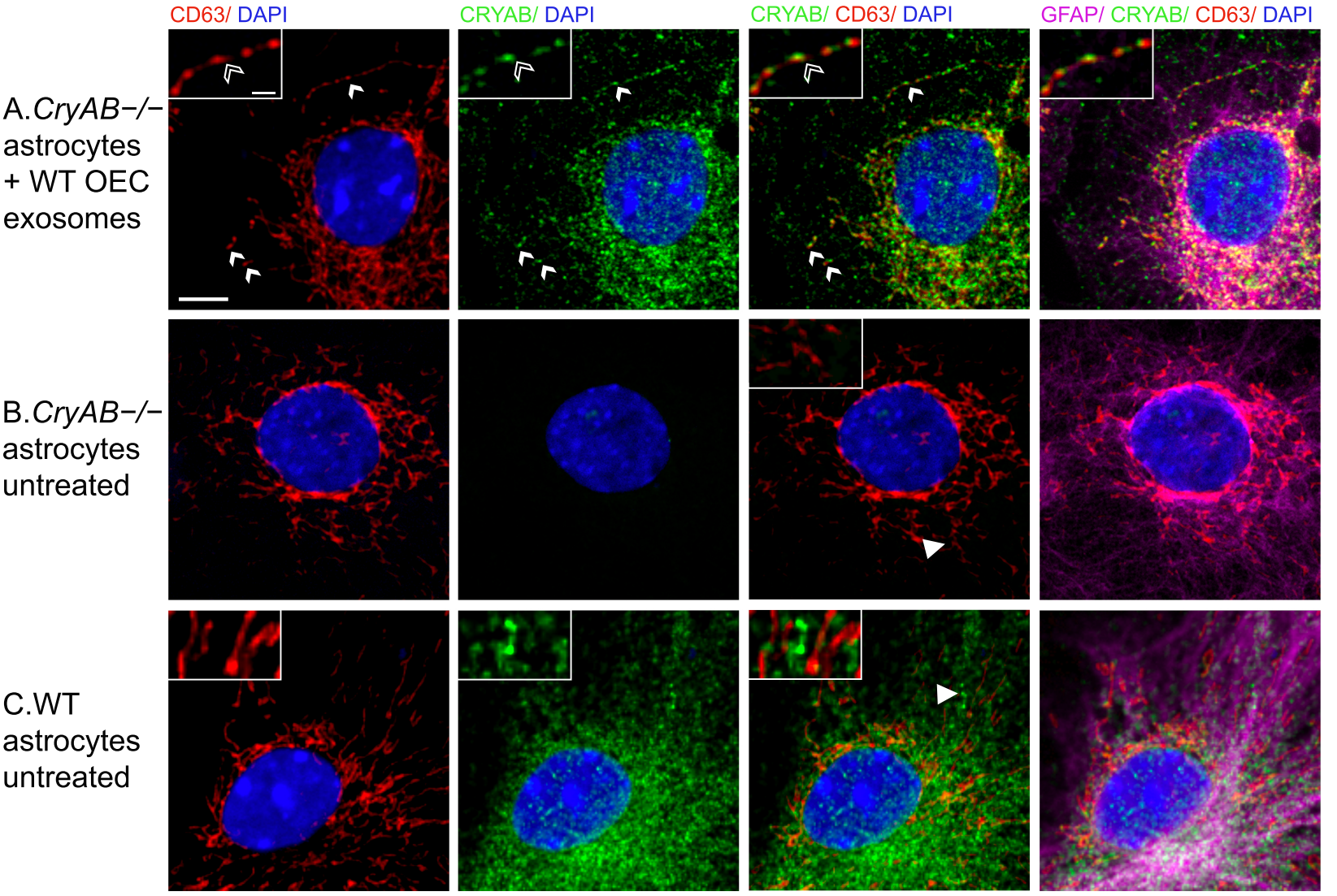
CD63/ DAPI
CRYAB/ DAPI
CRYAB/ CD63/ DAPI
GFAP/ CRYAB/ CD63/ DAPI
A.*CryAB−/−* astrocytes + WT OEC exosomes
B.*CryAB−/−* astrocytes untreated
C.WT astrocytes untreated

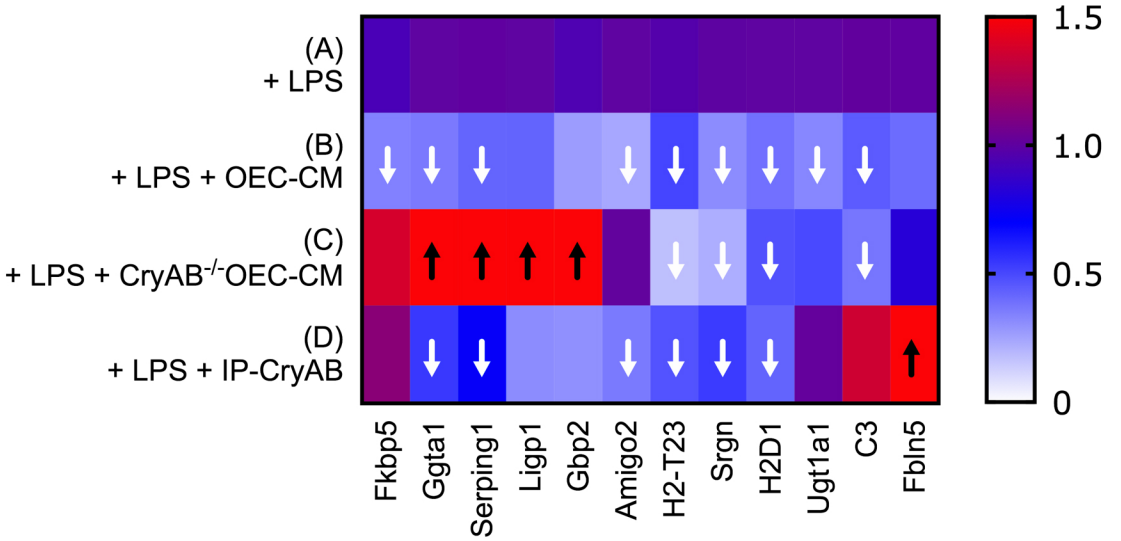
(A)
+ LPS
(B)
+ LPS + OEC-CM
(C)
+ LPS + CryAB-/-OEC-CM
(D)
+ LPS + IP-CryAB
Fkbp5
Ggta1
Serping1
Ligp1
Gbp2
Amigo2
H2-T23
Srgn
H2D1
Ugt1a1
C3
Fbln5
1.5
1.0
0.5
0

Supplementary Figure 1: Competitive ELISA against CryAB was used to examine exosomes. (A) Exosomes (exo) derived from $1x10^6$ OECs were determined to have 9.22 ± 0.2 ng CryAB. CryAB in OEC secreted exosomes was not significantly different than the concentration in oligodendrocyte exosomes but %21.1 higher than that of astrocyte exosomes. (B) Exposure to LPS increased OEC secreted CryAB concentration by 25.17% (C). Although OECs' exposure to LPS or astrocytic signals were not necessary for the suppressive effect of OECs on NFκB translocation in C8D30 astrocytes, whether the CryAB secretion would be facilitated by external signals was investigated by stimulating with LPS or Anosmin1. Exposure to Anosmin-1 increased CryAB concentration by 77.17%, compared to control protein recombinant myoglobin.

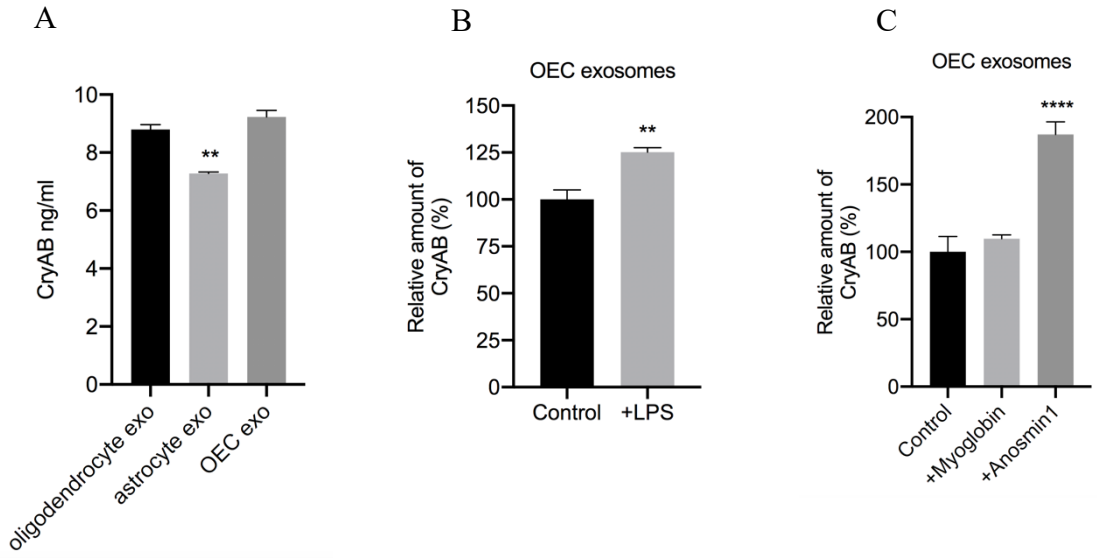

SUPPLEMENTARY ONLINE MATERIAL

SUPLLEMENTARY TABLE 1

+D4-CM	+D10-CM	+C4-CM	+C6-CM	+D6-CM	+C7-CM	+pOECs	LPS control
102	74	81	83	113	127	79	123
129	78	67	64	126	77	84	100
92	107	74	69	131	80	95	88

SUPLLEMENTARY TABLE 2

	Medium	50ng/ml Cryab	100ng/ml Cryab
Medium	50 55 44	52 28 43	43 36 51
LPS	53 52 56	50 25 40	47 53 54
Il-1α+ TNFα+ C1q	52 41 49	46 29 59	59 65 61

Median values were calculated for each biological replicate obtained from multiple images containing around 100 cells for Figure 1C and 50 cells for Figure 2B.

SUPPLEMENTARY ONLINE MATERIAL

SUPLLEMENTARY TABLE 3

Sample		dCt	dCt	dCt	mean	SD	SEM	ddCT	2^(-ddCT)	2^-(ddCT-SEM)	2^-(ddCT+SEM)
LPS	Fkbp5	7.831	7.461	8.015	7.769	0.282	0.163	0.000	1.000	1.120	0.893
	Ggta1	6.781	6.949	7.044	6.925	0.134	0.077	0.000	1.000	1.055	0.948
	Serping1	4.895	4.539	4.655	4.697	0.181	0.105	0.000	1.000	1.075	0.930
	Ligp1	7.240	7.012	7.063	7.105	0.120	0.069	0.000	1.000	1.049	0.953
	Gbp2	1.580	1.415	1.755	1.583	0.170	0.098	0.000	1.000	1.070	0.934
	Amigo2	9.793	9.748	9.844	9.795	0.048	0.028	0.000	1.000	1.019	0.981
	H2-T23	3.418	3.566	3.830	3.605	0.209	0.120	0.000	1.000	1.087	0.920
	Srgn	5.651	5.635	5.730	5.672	0.051	0.030	0.000	1.000	1.021	0.980
	H2D1	-4.439	-4.486	-4.382	-4.436	0.052	0.030	0.000	1.000	1.021	0.979
	Ugt1a1	7.087	7.195	7.317	7.200	0.115	0.066	0.000	1.000	1.047	0.955
	C3	6.603	6.681	7.080	6.788	0.256	0.148	0.000	1.000	1.108	0.903
	Fbln5	11.742	11.483	11.806	11.677	0.171	0.099	0.000	1.000	1.071	0.934
LPS +OEC-CM	Fkbp5	9.217	9.269	9.114	9.200	0.079	0.046	1.431	0.371	0.383	0.359
	Ggta1	8.041	8.182	9.227	8.484	0.648	0.374	1.559	0.339	0.440	0.262
	Serping1	5.899	5.969	5.964	5.944	0.039	0.022	1.248	0.421	0.428	0.415
	Ligp1	8.242	8.474	8.401	8.372	0.119	0.069	1.267	0.416	0.436	0.396
	Gbp2	3.030	3.230	4.131	3.463	0.587	0.339	1.880	0.272	0.344	0.215
	Amigo2	11.367	11.378	14.133	12.293	1.594	0.920	2.498	0.177	0.335	0.094
	H2-T23	4.164	4.506	4.531	4.400	0.205	0.119	0.796	0.576	0.625	0.531
	Srgn	7.426	7.711	7.011	7.383	0.352	0.203	1.711	0.306	0.352	0.265
	H2D1	-3.297	-3.152	-2.696	-3.048	0.314	0.181	1.387	0.382	0.433	0.337
	Ugt1a1	8.151	9.198	9.449	8.932	0.688	0.397	1.733	0.301	0.396	0.228
	C3	8.288	7.970	7.645	7.968	0.322	0.186	1.179	0.442	0.502	0.388
	Fbln5	13.173	12.940	12.920	13.011	0.141	0.081	1.334	0.397	0.420	0.375
LPS +CryABKO OEC-CM	Fkbp5	7.034	7.021	7.562	7.205	0.309	0.178	-0.563	1.478	1.672	1.306
	Ggta1	4.680	4.735	4.673	4.696	0.034	0.020	-2.229	4.687	4.752	4.623
	Serping1	2.442	2.555	2.483	2.493	0.057	0.033	-2.203	4.605	4.711	4.501
	Ligp1	5.831	6.017	5.579	5.809	0.220	0.127	-1.296	2.455	2.681	2.248
	Gbp2	0.146	1.509	0.293	0.650	0.748	0.432	-0.933	1.910	2.576	1.416
	Amigo2	9.983	9.845	9.550	9.793	0.221	0.128	-0.002	1.002	1.094	0.917
	H2-T23	7.413	5.966	5.216	6.198	1.117	0.645	2.594	0.166	0.259	0.106
	Srgn	6.305	7.722	8.020	7.349	0.916	0.529	1.677	0.313	0.451	0.217
	H2D1	-3.402	-3.416	-3.233	-3.351	0.102	0.059	1.085	0.471	0.491	0.452
	Ugt1a1	7.791	8.941	8.113	8.282	0.593	0.342	1.082	0.472	0.599	0.373
	C3	8.070	7.776	9.057	8.301	0.671	0.387	1.513	0.350	0.458	0.268
	Fbln5	11.586	12.106	12.276	11.989	0.359	0.207	0.313	0.805	0.930	0.697
LPS +IP-CryAB	Fkbp5	7.057	7.839	7.602	7.499	0.401	0.232	-0.269	1.205	1.415	1.026
	Ggta1	7.713	7.937	7.758	7.803	0.119	0.069	0.878	0.544	0.571	0.519
	Serping1	5.114	5.172	5.249	5.178	0.068	0.039	0.482	0.716	0.736	0.697
	Ligp1	8.687	8.955	8.787	8.810	0.135	0.078	1.704	0.307	0.324	0.291
	Gbp2	3.079	3.347	3.246	3.224	0.135	0.078	1.641	0.321	0.338	0.304
	Amigo2	10.597	11.388	12.252	11.412	0.828	0.478	1.617	0.326	0.454	0.234
	H2-T23	4.391	5.143	4.150	4.561	0.518	0.299	0.957	0.515	0.634	0.419
	Srgn	6.580	6.512	6.626	6.573	0.057	0.033	0.901	0.536	0.548	0.524
	H2D1	-3.032	-3.279	-3.256	-3.189	0.136	0.079	1.247	0.421	0.445	0.399
	Ugt1a1	8.277	6.647	7.045	7.323	0.850	0.490	0.123	0.918	1.290	0.654
	C3	6.097	6.949	6.158	6.401	0.476	0.275	-0.387	1.308	1.582	1.081
	Fbln5	10.750	10.186	10.053	10.329	0.370	0.214	-1.347	2.544	2.950	2.194

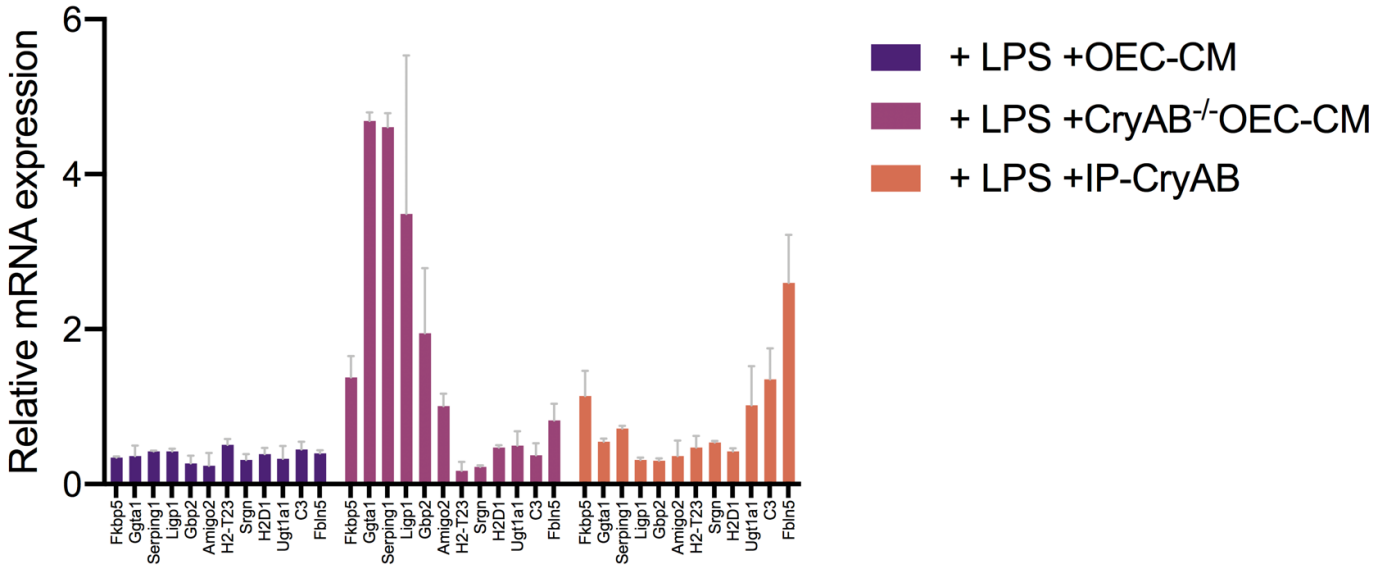

Checked	Protein FDI	Master	Accession	Description	Exp. q-valu	Sum PEP Sc	Coverage ['	# Peptides	# PSMs	# Unique Pe	# Protein G	# AAs	MW [kDa]	calc. pI	Score Sequ	# Peptides	Abundance Ratio: (F1, 127) / (F1, 126)	Abundance Ratio: (F1, 128) / (F1, 126)
FALSE	High	Master Pro	Q9QXS1-1	plectin [OS=Mus musculus]	0	168.56	11	45	87	45	1	4691	533.9	5.96	306.49	45	1.331	1.372
FALSE	High	Master Pro	P58252	Elongation factor 2 [OS=Mus musculus]	0	99.744	21	16	66	16	1	858	95.3	6.83	247.29	16	2.312	2.225
FALSE	High	Master Pro	P11276	fibronectin [OS=Mus musculus]	0	97.128	11	20	50	20	1	2477	272.4	5.59	188.54	20	0.751	1.223
FALSE	High	Master Pro	P52480	Pyruvate kinase PKM [OS=Mus musculus]	0	86.418	35	14	45	2	1	531	57.8	7.47	180.9	14	2.065	1.576
FALSE	High	Master Pro	P63017	Heat shock cognate 71 kDa protein [OS=Mus musculus]	0	75.674	21	13	55	10	1	646	70.8	5.52	210.48	13	2.161	1.679
FALSE	High	Master Pro	P09411	phosphoglycerate kinase 1 [OS=Mus musculus]	0	68.779	34	13	46	13	1	417	44.5	7.9	157.04	13	2.997	3.399
FALSE	High	Master Pro	P60710	Actin, cytoplasmic 1 [OS=Mus musculus]	0	68.401	39	12	43	5	1	375	41.7	5.48	164.18	12	1.401	0.982
FALSE	High	Master Pro	Q8BTM8	Filamin-A [OS=Mus musculus]	0	68.209	8	19	44	15	1	2647	281	6.04	160.39	19	1.054	1.234
FALSE	High	Master Pro	P17182	alpha-enolase [OS=Mus musculus]	0	63.905	33	11	43	11	1	434	47.1	6.8	172.55	11	1.866	1.746
FALSE	High	Master Pro	P20152	Vimentin [OS=Mus musculus]	0	58.757	28	13	49	13	1	466	53.7	5.12	176.17	13	2.473	2.522
FALSE	High	Master Pro	P52480-2	Isoform M1 of Pyruvate kinase PKM [OS=Mus musculus]	0	58.552	29	13	38	1	1	531	57.9	7.14	136.08	13	0.975	0.662
FALSE	High	Master Pro	P10107	annexin A1 [OS=Mus musculus]	0	57.805	29	10	28	10	1	346	38.7	7.37	107.18	10	1.885	2.007
FALSE	High	Master Pro	P26041	Moesin [OS=Mus musculus]	0	56.362	28	15	40	10	1	577	67.7	6.6	131.47	15	1.622	2.126
FALSE	High	Master Pro	P57780	Alpha-actinin-4 [OS=Mus musculus]	0	48.178	14	12	35	3	1	912	104.9	5.41	113.6	12	0.91	1.157
FALSE	High	Master Pro	P05064	fructose-bisphosphate aldolase A [OS=Mus musculus]	0	48.053	29	10	30	9	1	364	39.3	8.09	104.94	10	1.38	1.306
FALSE	High	Master Pro	P11087-1	Collagen alpha-1(I) chain [OS=Mus musculus]	0	46.912	11	14	28	13	1	1453	137.9	5.85	97.19	14	0.758	0.605
FALSE	High	Master Pro	P10126	Elongation factor 1-alpha 1 [OS=Mus musculus]	0	45.662	21	9	28	9	1	462	50.1	9.01	109.97	9	1.811	1.718
FALSE	High	Master Pro	Q64727	Vinculin [OS=Mus musculus]	0	45.505	11	10	15	10	1	1066	116.6	6	54.03	10	0.493	0.651
FALSE	High	Master Pro	P01027-1	Complement C3 [OS=Mus musculus]	0	45.355	5	8	28	8	1	1663	186.4	6.73	112.15	8	0.38	0.343
FALSE	High	Master Pro	Q07235	Glia-derived nexin [OS=Mus musculus]	0	44.736	24	9	21	9	1	397	44.2	9.85	77.39	9	0.994	0.976
FALSE	High	Master Pro	P26039	Talin-1 [OS=Mus musculus]	0	43.551	6	12	23	12	1	2541	269.7	6.18	67.37	12	0.703	0.772
FALSE	High	Master Pro	Q7TPR4	Alpha-actinin-1 [OS=Mus musculus]	0	43.441	12	10	29	1	1	892	103	5.38	94.42	10	0.634	0.702
FALSE	High	Master Pro	Q8VDD5	Myosin-9 [OS=Mus musculus]	0	41.956	6	11	22	9	1	1960	226.2	5.66	73.14	11	0.999	1.395
FALSE	High	Master Pro	Q61171	Peroxiredoxin-2 [OS=Mus musculus]	0	41.525	32	6	21	6	1	198	21.8	5.41	86.85	6	1.852	1.598
FALSE	High	Master Pro	P18760	Cofilin-1 [OS=Mus musculus]	0	41.122	54	7	24	7	1	166	18.5	8.09	106.74	7	2.546	2.713
FALSE	High	Master Pro	Q80X90	Filamin-B [OS=Mus musculus]	0	39.005	4	9	21	5	1	2602	277.7	5.71	75.34	9	0.701	0.478
FALSE	High	Master Pro	Q61598	Rab GDP dissociation inhibitor beta [OS=Mus musculus]	0	38.652	25	8	18	6	1	445	50.5	6.25	68.74	8	2.052	1.658
FALSE	High	Master Pro	Q61703	Inter-alpha-trypsin inhibitor heavy chain H2 [OS=Mus musculus]	0	38.479	8	9	22	9	1	946	105.9	7.27	78.85	9	0.394	0.225
FALSE	High	Master Pro	P05213	Tubulin alpha-1B chain [OS=Mus musculus]	0	36.125	19	7	15	7	1	451	50.1	5.06	70.82	7	1.049	0.792
FALSE	High	Master Pro	P63101	14-3-3 protein zeta/delta [OS=Mus musculus]	0	35.393	38	8	23	5	1	245	27.8	4.79	85.23	8	1.697	2.176
FALSE	High	Master Pro	P62962	profilin-1 [OS=Mus musculus]	0	34.186	45	5	28	5	1	140	14.9	8.28	114.32	5	1.463	1.254
FALSE	High	Master Pro	O88569	heterogeneous nuclear ribonucleoproteins A2/B1 [OS=Mus musculus]	0	33.745	16	7	18	5	1	353	37.4	8.95	65.38	7	2.067	2.037
FALSE	High	Master Pro	Q60847	Collagen alpha-1(XII) chain [OS=Mus musculus]	0	33.473	3	10	14	10	1	3120	340	5.64	46.12	10	0.671	0.87
FALSE	High	Master Pro	P09405	Nucleolin [OS=Mus musculus]	0	32.325	14	11	28	11	1	707	76.7	4.75	88.5	11	1.405	3.119
FALSE	High	Master Pro	P15532	Nucleoside diphosphate kinase A [OS=Mus musculus]	0	32.292	53	6	26	3	1	152	17.2	7.37	90.28	6	2.567	2.648
FALSE	High	Master Pro	P62737	Actin, aortic smooth muscle [OS=Mus musculus]	0	31.81	24	8	25	1	1	377	42	5.39	77.32	8	0.833	0.66
FALSE	High	Master Pro	Q9JMH6-1	Thioredoxin reductase 1, cytoplasmic [OS=Mus musculus]	0	31.631	11	5	11	5	1	613	67	7.44	52.36	5	1.4	1.075
FALSE	High	Master Pro	Q9WVA4	Transgelin-2 [OS=Mus musculus]	0	31.513	42	8	21	8	1	199	22.4	8.24	69.09	8	1.451	1.489
FALSE	High	Master Pro	Q64433	10 kDa heat shock protein, mitochondrial [OS=Mus musculus]	0	31.398	68	8	18	8	1	102	11	8.35	67.39	8	2.538	5.685
FALSE	High	Master Pro	P27773	Protein disulfide-isomerase A3 [OS=Mus musculus]	0	30.8	19	10	19	10	1	505	56.6	6.21	62.51	10	1.699	1.355
FALSE	High	Master Pro	P06745	glucose-6-phosphate isomerase [OS=Mus musculus]	0	30.442	16	7	14	7	1	558	62.7	8.13	44.29	7	1.2	0.829
FALSE	High	Master Pro	Q01768	nucleoside diphosphate kinase b [OS=Mus musculus]	0	29.932	53	6	19	3	1	152	17.4	7.5	75.76	6	1.732	1.971
FALSE	High	Master Pro	P35441	thrombospondin-1 [OS=Mus musculus]	0	29.845	8	9	17	9	1	1170	129.6	4.96	60.03	9	0.575	0.564
FALSE	High	Master Pro	P25444	40S ribosomal protein S2 [OS=Mus musculus]	0	28.66	18	5	22	5	1	293	31.2	10.24	79.24	5	2.005	1.756
FALSE	High	Master Pro	Q05793	Basement membrane-specific heparan sulfate proteoglycan core protein [OS=Mus musculus]	0	28.565	3	9	15	9	1	3707	398	6.32	38.48	9	0.492	0.587
FALSE	High	Master Pro	Q62009	Periostin [OS=Mus musculus]	0	27.848	8	6	16	6	1	838	93.1	7.53	59.25	6	0.433	0.404
FALSE	High	Master Pro	Q9JKF1	Ras GTPase-activating-like protein IQGAP1 [OS=Mus musculus]	0	27.598	5	6	7	6	1	1657	188.6	6.48	29.32	6	1.163	0.945
FALSE	High	Master Pro	P07356	Annexin A2 [OS=Mus musculus]	0	27.585	28	9	16	9	1	339	38.7	7.69	50.66	9	1.561	0.974
FALSE	High	Master Pro	P06151	L-lactate dehydrogenase A chain [OS=Mus musculus]	0	27.541	16	5	16	5	1	332	36.5	7.74	60.26	5	1.078	1.878
FALSE	High	Master Pro	P48678-1	Prelamin-A/C [OS=Mus musculus]	0	27.457	11	8	22	8	1	665	74.2	6.98	77.17	8	1.542	1.613
FALSE	High	Master Pro	P61979-2	Isoform 2 of Heterogeneous nuclear ribonucleoprotein K [OS=Mus musculus]	0	27.04	16	5	13	5	1	464	51	5.33	53.94	5	1.777	1.908
FALSE	High	Master Pro	P17225	Polypyrimidine tract-binding protein 1 [OS=Mus musculus]	0	26.803	10	4	11	4	1	527	56.4	8.34	52.51	4	1.796	2.077
FALSE	High	Master Pro	Q61704	Inter-alpha-trypsin inhibitor heavy chain H3 [OS=Mus musculus]	0	26.569	4	4	14	4	1	889	99.3	6.05	60.83	4	0.377	0.256
FALSE	High	Master Pro	P99029	Peroxiredoxin-5, mitochondrial [OS=Mus musculus]	0	26.55	24	4	17	4	1	210	21.9	8.85	61.02	4	1.674	3.481
FALSE	High	Master Pro	Q01853	Transitional endoplasmic reticulum ATPase [OS=Mus musculus]	0	26.494	9	7	12	7	1	806	89.3	5.26	42.11	7	1.07	1.418
FALSE	High	Master Pro	Q99020	Heterogeneous nuclear ribonucleoprotein A/B [OS=Mus musculus]	0	26.267	25	6	15	5	1	285	30.8	7.91	50.92	6	2.641	2.183
FALSE	High	Master Pro	O88844	Isocitrate dehydrogenase [NADP] cytoplasmic [OS=Mus musculus]	0	26.07	21	8	14	7	1	414	46.6	7.17	50.2	8	0.924	1.508
FALSE	High	Master Pro	O08709	Peroxiredoxin-6 [OS=Mus musculus]	0	25.626	28	5	24	5	1	224	24.9	6.01	86.32	5	1.157	1.995
FALSE	High	Master Pro	P35700	peroxiredoxin-1 [OS=Mus musculus]	0	25.532	34	7	21	5	1	199	22.2	8.12	77.24	7	1.456	1.349
FALSE	High	Master Pro	P63038-1	60 kDa heat shock protein, mitochondrial [OS=Mus musculus]	0	25.225	14	6	10	6	1	573	60.9	6.18	42.24	6	1.325	2.034
FALSE	High	Master Pro	P97298	Pigment epithelium-derived factor [OS=Mus musculus]	0	25.151	15	5	10	5	1	417	46.2	6.98	44.23	5	0.357	0.311
FALSE	High	Master Pro	P14152	Malate dehydrogenase, cytoplasmic [OS=Mus musculus]	0	24.795	19	7	16	7	1	334	36.5	6.58	56.85	7	2.57	1.902
FALSE	High	Master Pro	Q9D8N0	elongation factor 1-gamma [OS=Mus musculus]	0	24.487	15	6	11	6	1	437	50	6.74	36.57	6	1.045	1.258
FALSE	High	Master Pro	Q61207	Prosaposin [OS=Mus musculus]	0	24.46	11	6	19	6	1	557	61.4	5.19	61.01	6	3.028	2.079
FALSE	High	Master Pro	Q9DBJ1	Phosphoglycerate mutase 1 [OS=Mus musculus]	0	24.19	24	4	19	4	1	254	28.8	7.18	72.08	4	1.827	2.185
FALSE	High	Master Pro	P16546	Spectrin alpha chain, non-erythrocytic 1 [OS=Mus musculus]	0	24.188	3	5	6	5	1	2472	284.4	5.33	24.36	5	1.107	0.746
FALSE	High	Master Pro	P49312-1	Heterogeneous nuclear ribonucleoprotein A1 [OS=Mus musculus]	0	24.171	13	5	15	3	1	320	34.2	9.23	53.78	5	1.478	1.48
FALSE	High	Master Pro	P62259	14-3-3 protein epsilon [OS=Mus musculus]	0	23.394	26	6	15	3	1	255	29.2	4.74	51.55	6	1.24	1.444
FALSE	High	Master Pro	P32261	Antithrombin-III [OS=Mus musculus]	0	23.178	16	9	23	9	1	465	52	6.46	68.54	9	0.289	0.337
FALSE	High	Master Pro	Q9CQV8-1	14-3-3 protein beta/alpha [OS=Mus musculus]	0	22.817	26	6	17	2	1	246	28.1	4.83	61.24	6	1.187	1.618
FALSE	High	Master Pro	P16627	Heat shock 70 kDa protein 1-like [OS=Mus musculus]	0	22.668	8	4	13	1	1	641	70.6	6.24	53.95	4	0.637	0.413
FALSE	High	Master Pro	Q60864	stress-induced-phosphoprotein 1 [OS=Mus musculus]	0	21.795	11	6	11	6	1	543	62.5	6.8	43.05	6	1.17	1.682
FALSE	High	Master Pro	P17751	Triosephosphate isomerase [OS=Mus musculus]	0	21.404	17	5	19	5	1	299	32.2	5.74	69.32	5	1.642	3.293
FALSE	High	Master Pro	Q93092	Transaldolase [OS=Mus musculus]	0	21.211	19	7	17	7	1	337	37.4	7.03	50.1	7	2.02	1.247
FALSE	High	Master Pro	Q9DCD0	6-phosphogluconate dehydrogenase, decarboxylating [OS=Mus musculus]	0	21.116	12	6	11	6	1	483	53.2	7.23	37.76	6	0.537	0.399
FALSE	High	Master Pro	P08249	Malate dehydrogenase, mitochondrial [OS=Mus musculus]	0	20.256	18	4	6	4	1	338	35.6	8.68	25.22	4	1.832	2.29
FALSE	High	Master Pro	P00493	Hypoxanthine-guanine phosphoribosyltransferase [OS=Mus musculus]	0	20.247	21	4	10	4	1	218	24.6	6.68	32.59	4	1.394	1.623
FALSE	High	Master Pro	P61982	14-3-3 protein gamma [OS=Mus musculus]	0	20.049	21	6	20	2	1	247	28.3	4.89	72.38	6	2.153	2.539
FALSE	High	Master Pro	P62082	40S ribosomal protein S7 [OS=Mus musculus]	0	20.021	30	5	11	5	1	194	22.1	10.1	39.33	5	2.975	2.748
FALSE	High	Master Pro	P29341	Polyadenylate-binding protein 1 [OS=Mus musculus]	0	19.758	6	5	9	5	1	636	70.6	9.5	30.36	5	0.569	0.643
FALSE	High	Master Pro	P20029	78 kDa glucose-regulated protein [OS=Mus musculus]	0	19.584	5	3	10	1	1	655	72.4	5.16	44.78	3	0.432	0.287
FALSE	High	Master Pro	P50396	Rab GDP dissociation inhibitor alpha [OS=Mus musculus]	0	19.466	13	5	8	3	1	447	50.5	5.08	27.29	5	2.008	1.61
FALSE	High	Master Pro	Q9Z204	Heterogeneous nuclear ribonucleoproteins C1/C2 [OS=Mus musculus]	0	19.302	15	4	8	4	1	313	34.4	5.05	35.37	4	1.225	1.61
FALSE	High	Master Pro	P13020-1	Gelsolin [OS=Mus musculus]	0	18.991	13	9	23	9	1	780	85.9	6.18	65.04	9	0.493	0.373
FALSE	High	Master Pro	Q60668-1	heterogeneous nuclear ribonucleoprotein D0 [OS=Mus musculus]	0	18.914	12	4	7	3	1	355	38.3	7.81	23.83	4	3.332	2.981
FALSE	High	Master Pro	Q61553	Fascin [OS=Mus musculus]	0	18.859	10	4	14	4	1	493	54.5	6.89	56.49	4	1.698	3.093
FALSE	High	Master Pro	P17710-1	Hexokinase-1 [OS=Mus musculus]	0	18.788	7	7	10	7	1	974	108.2	6.8	31.7	7	0.991	1.238
FALSE	High	Master Pro	Q6GQT1	Alpha-2-macroglobulin-P [OS=Mus musculus]	0	18.785	2	3	22	2	1	1474	164.2	6.61	73.42	3	0.386	0.237

FALSE	High	Master Pro	P62908	40S ribosomal protein S3 [OS=Mus musculus]	0	18.757	23	6	14	6	1	243	26.7	9.66	45.78	6	1.871	1.848
FALSE	High	Master Pro	P10649	Glutathione S-transferase Mu 1 [OS=Mus musculus]	0	18.605	23	5	16	2	1	218	26	7.94	57.61	5	1.719	2.766
FALSE	High	Master Pro	P99024	tubulin beta-5 chain [OS=Mus musculus]	0	18.548	20	7	12	7	1	444	49.6	4.89	38.22	7	0.71	0.511
FALSE	High	Master Pro	P24527	leukotriene A-4 hydrolase [OS=Mus musculus]	0	18.241	6	4	10	4	1	611	69	6.42	36.68	4	1.515	1.274
FALSE	High	Master Pro	Q04857	Collagen alpha-1(VI) chain [OS=Mus musculus]	0	17.902	5	4	11	4	1	1025	108.4	5.36	37.8	4	0.619	0.707
FALSE	High	Master Pro	P18242	Cathepsin D [OS=Mus musculus]	0	17.858	17	5	9	5	1	410	44.9	7.15	33.76	5	1.364	1.209
FALSE	High	Master Pro	Q99K51	Plastin-3 [OS=Mus musculus]	0	17.561	9	5	10	3	1	630	70.7	5.62	36.31	5	0.731	0.728
FALSE	High	Master Pro	Q9CZD3	Glycine--tRNA ligase [OS=Mus musculus]	0	17.534	8	5	12	5	1	729	81.8	6.65	33.51	5	1.895	1.217
FALSE	High	Master Pro	P68254-1	14-3-3 protein theta [OS=Mus musculus]	0	17.51	21	5	15	1	1	245	27.8	4.78	53.21	5	2.146	2.651
FALSE	High	Master Pro	Q00493	Carboxypeptidase E [OS=Mus musculus]	0	17.46	9	3	9	3	1	476	53.2	5.19	37.97	3	1.002	0.783
FALSE	High	Master Pro	P15116	Cadherin-2 [OS=Mus musculus]	0	17.422	6	4	7	4	1	906	99.7	4.78	26.23	4	0.691	0.552
FALSE	High	Master Pro	P43277	Histone H1.3 [OS=Mus musculus]	0	17.402	14	4	8	3	1	221	22.1	11.03	29.78	4	1.326	1.757
FALSE	High	Master Pro	Q91ZX7	prolow-density lipoprotein receptor-related protein 1 [OS=Mus musculus]	0	16.975	1	5	8	5	1	4545	504.4	5.36	19.79	5	0.576	0.452
FALSE	High	Master Pro	Q6P1B1	xaa-Pro aminopeptidase 1 [OS=Mus musculus]	0	16.921	8	3	6	3	1	623	69.5	5.54	23.46	3	1.166	1.1
FALSE	High	Master Pro	P17742	peptidyl-prolyl cis-trans isomerase A [OS=Mus musculus]	0	16.884	28	5	34	5	1	164	18	7.9	110.96	5	2.352	2.24
FALSE	High	Master Pro	Q9CPU0	lactoylglutathione lyase [OS=Mus musculus]	0	16.871	23	6	18	6	1	184	20.8	5.47	59.73	6	2.321	1.14
FALSE	High	Master Pro	P62827	GTP-binding nuclear protein RAN [OS=Mus musculus]	0	16.869	20	3	5	3	1	216	24.4	7.49	19.06	3	1.51	1.159
FALSE	High	Master Pro	P19324	Serpin H1 [OS=Mus musculus]	0	16.823	12	5	9	5	1	417	46.5	8.82	31.93	5	1.223	0.821
FALSE	High	Master Pro	Q8BG05	Heterogeneous nuclear ribonucleoprotein A3 [OS=Mus musculus]	0	16.653	6	3	9	1	1	379	39.6	9.01	33.45	3	1.106	1.122
FALSE	High	Master Pro	P68510	14-3-3 protein eta [OS=Mus musculus]	0	16.587	17	5	17	1	1	246	28.2	4.89	59.37	5	1.596	1.977
FALSE	High	Master Pro	P26043	radixin [OS=Mus musculus]	0	16.521	11	7	13	2	1	583	68.5	6.2	43.24	7	1.308	1.728
FALSE	High	Master Pro	P51885	Lumican [OS=Mus musculus]	0	16.356	17	5	13	5	1	338	38.2	6.43	47.21	5	0.336	0.262
FALSE	High	Master Pro	P57776-3	Isoform 3 of Elongation factor 1-delta [OS=Mus musculus]	0	16.32	4	2	7	2	1	660	72.9	6.43	29.37	2	0.805	1.258
FALSE	High	Master Pro	P39061-3	Collagen alpha-1(XVIII) chain [OS=Mus musculus]	0	16.292	3	6	15	6	1	1774	182.1	5.62	46.76	6	1.009	1.343
FALSE	High	Master Pro	P30412	peptidyl-prolyl cis-trans isomerase C [OS=Mus musculus]	0	16.284	17	3	7	3	1	212	22.8	7.5	21.67	3	0.755	0.836
FALSE	High	Master Pro	P15626	Glutathione S-transferase Mu 2 [OS=Mus musculus]	0	16.26	23	4	9	1	1	218	25.7	7.39	33.94	4	0.601	0.308
FALSE	High	Master Pro	P80315	T-complex protein 1 subunit delta [OS=Mus musculus]	0	16.246	10	3	4	3	1	539	58	8.02	15.57	3	0.764	0.58
FALSE	High	Master Pro	P14206	40S ribosomal protein SA [OS=Mus musculus]	0	16.091	17	5	6	5	1	295	32.8	4.87	22.24	5	1.486	1.365
FALSE	High	Master Pro	Q61316	Heat shock 70 kDa protein 4 [OS=Mus musculus]	0	16.089	4	3	8	3	1	841	94.1	5.24	31.23	3	1.189	1.333
FALSE	High	Master Pro	Q91VM5	RNA binding motif protein, X-linked-like-1 [OS=Mus musculus]	0	16.048	10	4	9	4	1	388	42.1	9.99	31.49	4	1.978	1.474
FALSE	High	Master Pro	Q922R8	Protein disulfide-isomerase A6 [OS=Mus musculus]	0	15.839	7	2	4	2	1	440	48.1	5.14	13.45	2	0.714	0.51
FALSE	High	Master Pro	Q60605	Myosin light polypeptide 6 [OS=Mus musculus]	0	15.68	25	3	8	3	1	151	16.9	4.65	26.86	3	1.285	1.397
FALSE	High	Master Pro	P10639	thioredoxin [OS=Mus musculus]	0	15.323	21	2	9	2	1	105	11.7	4.92	44.43	2	1.223	1.124
FALSE	High	Master Pro	P16045	Galectin-1 [OS=Mus musculus]	0	15.04	30	4	11	4	1	135	14.9	5.49	35.77	4	2.121	2.149
FALSE	High	Master Pro	Q9CR57	60S ribosomal protein L14 [OS=Mus musculus]	0	14.814	12	2	5	2	1	217	23.5	11.02	23.51	2	1.134	1.084
FALSE	High	Master Pro	Q6ZWN5	40S ribosomal protein S9 [OS=Mus musculus]	0	14.652	23	5	9	5	1	194	22.6	10.65	29.22	5	2.748	2.697
FALSE	High	Master Pro	P06801	NADP-dependent malic enzyme [OS=Mus musculus]	0	14.516	10	4	6	4	1	572	63.9	7.44	15.73	4	0.462	0.432
FALSE	High	Master Pro	P33434-1	72 kDa type IV collagenase [OS=Mus musculus]	0	14.437	9	6	8	6	1	662	74.1	5.53	24.84	6	0.805	0.85
FALSE	High	Master Pro	Q9D0F9	Phosphoglucomutase-1 [OS=Mus musculus]	0	14.399	10	5	8	5	1	562	61.4	6.57	26.94	5	0.738	0.683
FALSE	High	Master Pro	P48036	annexin A5 [OS=Mus musculus]	0	14.367	14	4	9	4	1	319	35.7	4.96	29.55	4	2.303	1.384
FALSE	High	Master Pro	P68040	Receptor of activated protein C kinase 1 [OS=Mus musculus]	0	14.207	14	5	12	5	1	317	35.1	7.69	35.75	5	1.943	2.045
FALSE	High	Master Pro	O70251	Elongation factor 1-beta [OS=Mus musculus]	0	13.931	17	4	13	4	1	225	24.7	4.69	39.29	4	1.569	2.781
FALSE	High	Master Pro	Q9JII6	alcohol dehydrogenase [NADP(+)] [OS=Mus musculus]	0	13.906	14	4	7	4	1	325	36.6	7.39	24.78	4	1.087	0.94
FALSE	High	Master Pro	P26040	Ezrin [OS=Mus musculus]	0	13.824	10	6	12	1	1	586	69.4	6.1	38.8	6	0.752	0.789
FALSE	High	Master Pro	Q3TCN2	Putative phospholipase B-like 2 [OS=Mus musculus]	0	13.818	5	3	9	3	1	594	66.2	6.13	34.86	3	1.041	1.183
FALSE	High	Master Pro	P07724	Serum albumin [OS=Mus musculus]	0	13.806	4	2	118	2	1	608	68.6	6.07	412.31	2	0.357	0.214
FALSE	High	Master Pro	P62301	40S ribosomal protein S13 [OS=Mus musculus]	0	13.77	29	4	8	4	1	151	17.2	10.54	27.15	4	1.52	1.45
FALSE	High	Master Pro	P21460	Cystatin-C [OS=Mus musculus]	0	13.737	25	4	7	4	1	140	15.5	9	24.31	4	1.125	1.317
FALSE	High	Master Pro	P62855	40S ribosomal protein S26 [OS=Mus musculus]	0	13.687	21	2	6	2	1	115	13	11	24.23	2	2.022	1.712
FALSE	High	Master Pro	P40142	Transketolase [OS=Mus musculus]	0	13.564	5	3	10	3	1	623	67.6	7.5	35.43	3	0.869	0.578
FALSE	High	Master Pro	P47754	F-actin-capping protein subunit alpha-2 [OS=Mus musculus]	0	13.559	15	3	6	2	1	286	32.9	5.85	20.59	3	0.796	0.822
FALSE	High	Master Pro	P70168	Importin subunit beta-1 [OS=Mus musculus]	0	13.449	3	2	7	2	1	876	97.1	4.78	30.55	2	1.055	1.349
FALSE	High	Master Pro	P14869	60S acidic ribosomal protein P0 [OS=Mus musculus]	0	13.334	11	3	5	3	1	317	34.2	6.25	16.44	3	0.92	0.791
FALSE	High	Master Pro	Q9R0P5	Destrin [OS=Mus musculus]	0	13.148	25	3	9	3	1	165	18.5	7.97	26.96	3	0.687	0.5
FALSE	High	Master Pro	Q9Z1N5	spliceosome RNA helicase DDX39B [OS=Mus musculus]	0	13.105	9	4	8	4	1	428	49	5.67	23.6	4	0.617	0.612
FALSE	High	Master Pro	Q99PT1	rho GDP-dissociation inhibitor 1 [OS=Mus musculus]	0	13.101	11	2	8	2	1	204	23.4	5.2	26.74	2	0.905	0.824
FALSE	High	Master Pro	P62204	Calmodulin [OS=Mus musculus]	0	13.02	27	4	7	4	1	149	16.8	4.22	24.8	4	2.151	2.518
FALSE	High	Master Pro	Q9CPV4-1	Glyoxalase domain-containing protein 4 [OS=Mus musculus]	0	12.993	12	3	4	3	1	298	33.3	5.47	16.06	3	0.735	0.792
FALSE	High	Master Pro	P09103	Protein disulfide-isomerase [OS=Mus musculus]	0	12.894	9	5	9	5	1	509	57	4.88	30.54	5	1.583	1.883
FALSE	High	Master Pro	Q91ZJ5-1	UTP--glucose-1-phosphate uridylyltransferase [OS=Mus musculus]	0	12.811	9	4	9	4	1	508	56.9	7.61	27.8	4	1.621	1.512
FALSE	High	Master Pro	Q8R2Y2-1	Cell surface glycoprotein MUC18 [OS=Mus musculus]	0	12.719	5	3	6	3	1	648	71.5	5.83	23.08	3	1.212	0.399
FALSE	High	Master Pro	Q8K4Z3	NAD(P)H-hydrate epimerase [OS=Mus musculus]	0	12.695	13	3	8	3	1	282	31	7.69	24.84	3	0.898	0.991
FALSE	High	Master Pro	P63242	Eukaryotic translation initiation factor 5A-1 [OS=Mus musculus]	0	12.453	33	4	14	4	1	154	16.8	5.24	33.44	4	2.139	2.091
FALSE	High	Master Pro	Q99KI0	Aconitate hydratase, mitochondrial [OS=Mus musculus]	0	12.34	5	4	8	4	1	780	85.4	7.93	28.5	4	0.88	1.72
FALSE	High	Master Pro	Q9Z2X1-1	Heterogeneous nuclear ribonucleoprotein F [OS=Mus musculus]	0	12.083	8	2	3	1	1	415	45.7	5.49	10.03	2	1.905	2.76
FALSE	High	Master Pro	Q920E5	Farnesyl pyrophosphate synthase [OS=Mus musculus]	0	12.059	8	2	4	2	1	353	40.6	5.66	14.02	2	0.989	1.437
FALSE	High	Master Pro	Q9CWJ9	bifunctional purine biosynthesis protein purH [OS=Mus musculus]	0	12.046	7	3	5	3	1	592	64.2	6.76	18.24	3	0.738	0.914
FALSE	High	Master Pro	P50580	proliferation-associated protein 2G4 [OS=Mus musculus]	0	11.912	8	3	7	3	1	394	43.7	6.86	26.93	3	2.148	1.753
FALSE	High	Master Pro	Q64674	spermidine synthase [OS=Mus musculus]	0	11.838	10	3	7	3	1	302	34	5.5	23.99	3	0.927	0.891
FALSE	High	Master Pro	Q8CGC7	Bifunctional glutamate/proline--tRNA ligase [OS=Mus musculus]	0	11.544	4	5	6	5	1	1512	170	7.66	12.79	5	1.238	1.456
FALSE	High	Master Pro	Q9CQ65	S-methyl-5'-thioadenosine phosphorylase [OS=Mus musculus]	0	11.511	23	4	5	4	1	283	31	7.14	11.8	4	0.668	0.542
FALSE	High	Master Pro	P61205	ADP-ribosylation factor 3 [OS=Mus musculus]	0	11.503	17	2	8	2	1	181	20.6	7.43	34.14	2	1.72	1.483
FALSE	High	Master Pro	P45376	aldose reductase [OS=Mus musculus]	0	11.226	11	4	9	4	1	316	35.7	7.18	31.34	4	1.103	1.078
FALSE	High	Master Pro	P22777	Plasminogen activator inhibitor 1 [OS=Mus musculus]	0	11.226	10	3	5	3	1	402	45.1	6.64	18	3	0.533	0.531
FALSE	High	Master Pro	Q8VEK3	Heterogeneous nuclear ribonucleoprotein U [OS=Mus musculus]	0	11.19	4	3	5	3	1	800	87.9	6.24	17	3	0.981	1.74
FALSE	High	Master Pro	Q9WUM4	coronin-1C [OS=Mus musculus]	0	11.189	7	3	5	3	1	474	53.1	7.08	17.93	3	1.136	0.895
FALSE	High	Master Pro	Q99K85	phosphoserine aminotransferase [OS=Mus musculus]	0	11.14	15	4	4	4	1	370	40.4	8.03	11.19	4	0.627	0.612
FALSE	High	Master Pro	Q9Z175	Lysyl oxidase homolog 3 [OS=Mus musculus]	0	10.979	6	4	5	4	1	754	83.7	7.01	19.05	4	0.517	0.976
FALSE	High	Master Pro	Q00612	Glucose-6-phosphate 1-dehydrogenase X [OS=Mus musculus]	0	10.86	5	2	4	2	1	515	59.2	6.49	14.96	2	1.796	1.18
FALSE	High	Master Pro	P62900	60S ribosomal protein L31 [OS=Mus musculus]	0	10.816	18	2	7	2	1	125	14.5	10.54	25.37	2	1.842	2.398
FALSE	High	Master Pro	Q7TQI3	Ubiquitin thioesterase otub1 [OS=Mus musculus]	0	10.756	12	3	6	3	1	271	31.3	4.94	22.35	3	0.927	1.213
FALSE	High	Master Pro	Q6ZQ38	cullin-associated nedd8-dissociated protein 1 [OS=Mus musculus]	0	10.753	3	3	4	3	1	1230	136.2	5.78	12.17	3	1.15	1.401
FALSE	High	Master Pro	Q68FD5	Clathrin heavy chain 1 [OS=Mus musculus]	0	10.646	3	5	8	5	1	1675	191.4	5.69	21.14	5	0.72	1.096
FALSE	High	Master Pro	Q9D1A2	cytosolic non-specific dipeptidase [OS=Mus musculus]	0	10.569	13	4	7	4	1	475	52.7	5.66	26.48	4	0.58	0.39
FALSE	High	Master Pro	Q99KC8	von Willebrand factor A domain-containing protein 5A [OS=Mus musculus]	0	10.519	4	3	7	3	1	793	87.1	6.58	26.04	3	1.893	2.316
FALSE	High	Master Pro	P54728	UV excision repair protein RAD23 homolog B [OS=Mus musculus]	0	10.414	8	4	7	4	1	416	43.5	4.83	24.51	4	1.12	1.363
FALSE	High	Master Pro	Q5XJY5	Coatomer subunit delta [OS=Mus musculus]	0	10.296	4	2	7	2	1	511	57.2	6.21	24.81	2	1.424	1.5
FALSE	High	Master Pro	P24369	peptidyl-prolyl cis-trans isomerase B [OS=Mus musculus]	0	10.239	16	4	9	4	1	216	23.7	9.55	31.27	4	2.494	2.531
FALSE	High	Master Pro	P60843	Eukaryotic initiation factor 4A-I [OS=Mus musculus]	0	10.122	7	4	5	1	1	406	46.1	5.48	15.41	4	0.657	0.813

FALSE	High	Master Pro	P99027	60S acidic ribosomal protein P2 [OS=Mus musculus]	0	9.854	27	2	4	2	1	115	11.6	4.54	11.68	2	1.117	1.127
FALSE	High	Master Pro	Q61990	Poly(rC)-binding protein 2 [OS=Mus musculus]	0	9.798	6	2	6	1	1	362	38.2	6.79	18.49	2	1.85	2.154
FALSE	High	Master Pro	P61089	ubiquitin-conjugating enzyme E2 N [OS=Mus musculus]	0	9.783	16	2	10	2	1	152	17.1	6.57	35.43	2	1.41	1.599
FALSE	High	Master Pro	P19096	Fatty acid synthase [OS=Mus musculus]	0	9.593	1	4	6	4	1	2504	272.3	6.58	18.91	4	1.323	1.255
FALSE	High	Master Pro	Q9D8E6	60S ribosomal protein L4 [OS=Mus musculus]	0	9.585	6	2	2	2	1	419	47.1	11	10.19	2	0.758	0.986
FALSE	High	Master Pro	Q61035	Histidine--tRNA ligase, cytoplasmic [OS=Mus musculus]	0	9.571	4	2	7	2	1	509	57.4	6	22.62	2	1.035	0.776
FALSE	High	Master Pro	Q99KK7	dipeptidyl peptidase 3 [OS=Mus musculus]	0	9.569	7	3	3	3	1	738	82.8	5.38	10.65	3	0.592	0.473
FALSE	High	Master Pro	Q61581	Insulin-like growth factor-binding protein 7 [OS=Mus musculus]	0	9.498	7	2	6	2	1	281	29	8.31	23.92	2	0.332	0.269
FALSE	High	Master Pro	O35737	Heterogeneous nuclear ribonucleoprotein H [OS=Mus musculus]	0	9.332	8	2	2	1	1	449	49.2	6.3	7.46	2	0.691	0.624
FALSE	High	Master Pro	P05202	Aspartate aminotransferase, mitochondrial [OS=Mus musculus]	0	9.294	7	3	7	3	1	430	47.4	9	17.06	3	0.775	0.642
FALSE	High	Master Pro	P10630-2	Isoform 2 of Eukaryotic initiation factor 4A-II [OS=Mus musculus]	0	9.235	7	4	4	1	1	408	46.5	5.48	11.24	4	1.17	1.471
FALSE	High	Master Pro	P97855	Ras GTPase-activating protein-binding protein 1 [OS=Mus musculus]	0	9.162	6	2	5	2	1	465	51.8	5.59	17.32	2	0.804	0.736
FALSE	High	Master Pro	P62983	Ubiquitin-40S ribosomal protein S27a [OS=Mus musculus]	0	9.095	22	3	7	3	1	156	17.9	9.64	27.96	3	1.412	1.921
FALSE	High	Master Pro	Q9D819	Inorganic pyrophosphatase [OS=Mus musculus]	0	9.062	9	3	7	3	1	289	32.6	5.6	23.87	3	1.227	1.584
FALSE	High	Master Pro	Q11011	puromycin-sensitive aminopeptidase [OS=Mus musculus]	0	9.056	4	4	6	4	1	920	103.3	5.9	21.17	4	1.105	1.452
FALSE	High	Master Pro	Q60854	serpin B6 [OS=Mus musculus]	0	9.048	9	2	4	2	1	378	42.6	5.74	12.46	2	0.837	0.681
FALSE	High	Master Pro	P62821	Ras-related protein Rab-1A [OS=Mus musculus]	0	9.041	13	2	5	2	1	205	22.7	6.21	19.57	2	0.692	0.757
FALSE	High	Master Pro	P46638	Ras-related protein Rab-11B [OS=Mus musculus]	0	9.024	15	3	6	3	1	218	24.5	5.94	19.06	3	0.916	0.816
FALSE	High	Master Pro	P70296	phosphatidylethanolamine-binding protein 1 [OS=Mus musculus]	0	8.967	17	3	3	3	1	187	20.8	5.4	11.23	3	1.38	1.511
FALSE	High	Master Pro	Q9CRB6	Tubulin polymerization-promoting protein family member 3 [OS=Mus musculus]	0	8.868	13	2	4	2	1	176	19	9.11	13.15	2	2.241	0.719
FALSE	High	Master Pro	P62852	40S ribosomal protein S25 [OS=Mus musculus]	0	8.532	22	3	5	3	1	125	13.7	10.11	18.92	3	1.645	1.633
FALSE	High	Master Pro	Q3UGR5-1	haloacid dehalogenase-like hydrolase domain-containing protein 2 [OS=Mus musculus]	0	8.527	8	2	4	2	1	259	28.7	6.05	16.04	2	1.021	0.82
FALSE	High	Master Pro	P14131	40S ribosomal protein S16 [OS=Mus musculus]	0	8.493	12	2	8	2	1	146	16.4	10.21	30.49	2	1.851	1.696
FALSE	High	Master Pro	Q3U1J4	DNA damage-binding protein 1 [OS=Mus musculus]	0	8.469	3	4	8	4	1	1140	126.8	5.26	24.14	4	0.972	1.423
FALSE	High	Master Pro	Q9CQ60	6-phosphogluconolactonase [OS=Mus musculus]	0	8.288	9	2	5	2	1	257	27.2	5.85	18.63	2	2.871	2.446
FALSE	High	Master Pro	Q91W90	Thioredoxin domain-containing protein 5 [OS=Mus musculus]	0	8.009	8	3	4	3	1	417	46.4	5.78	13.01	3	1.138	1.635
FALSE	High	Master Pro	Q06138	Calcium-binding protein 39 [OS=Mus musculus]	0	7.962	10	4	6	4	1	341	39.8	6.89	16.14	4	0.92	0.926
FALSE	High	Master Pro	P17918	proliferating cell nuclear antigen [OS=Mus musculus]	0	7.956	11	2	5	2	1	261	28.8	4.77	15.79	2	1.807	1.525
FALSE	High	Master Pro	Q9Z247	Peptidyl-prolyl cis-trans isomerase FKBP9 [OS=Mus musculus]	0	7.892	7	2	2	2	1	570	63	5.21	7.38	2	0.621	0.545
FALSE	High	Master Pro	P68037	Ubiquitin-conjugating enzyme E2 L3 [OS=Mus musculus]	0	7.8	16	2	4	2	1	154	17.9	8.51	8.33	2	0.846	0.709
FALSE	High	Master Pro	Q9Z1Q9	Valine--tRNA ligase [OS=Mus musculus]	0	7.799	2	3	6	3	1	1263	140.1	7.77	17.11	3	1.121	0.894
FALSE	High	Master Pro	Q69ZN7-1	Myoferlin [OS=Mus musculus]	0	7.695	1	2	2	2	1	2048	233.2	6.16	8.14	2	1.141	2.001
FALSE	High	Master Pro	O08807	Peroxiredoxin-4 [OS=Mus musculus]	0	7.598	11	3	5	1	1	274	31	7.15	17.49	3	1.585	1.331
FALSE	High	Master Pro	Q61033-1	Lamina-associated polypeptide 2, isoforms alpha/zeta [OS=Mus musculus]	0	7.57	4	2	2	2	1	693	75.1	8.05	5.93	2	0.459	0.384
FALSE	High	Master Pro	P01029	Complement C4-B [OS=Mus musculus]	0	7.52	1	3	4	3	1	1738	192.8	7.53	13.95	3	0.347	0.335
FALSE	High	Master Pro	Q9R0Y5-2	Isoform 2 of Adenylate kinase isoenzyme 1 [OS=Mus musculus]	0	7.49	12	2	3	2	1	210	23.1	5.83	8.51	2	0.725	0.639
FALSE	High	Master Pro	Q6IRU2	Tropomyosin alpha-4 chain [OS=Mus musculus]	0	7.454	10	3	6	3	1	248	28.5	4.68	18.25	3	0.813	0.797
FALSE	High	Master Pro	Q61233	Plastin-2 [OS=Mus musculus]	0	7.425	4	3	7	1	1	627	70.1	5.33	23.79	3	0.531	0.399
FALSE	High	Master Pro	Q9WU78-3	Isoform 3 of Programmed cell death 6-interacting protein [OS=Mus musculus]	0	7.314	2	2	3	2	1	874	96.7	6.52	9.98	2	0.708	0.82
FALSE	High	Master Pro	Q9D154	Leukocyte elastase inhibitor A [OS=Mus musculus]	0	7.229	7	2	2	2	1	379	42.5	6.21	7.32	2	0.449	1.195
FALSE	High	Master Pro	P37804	transgelin [OS=Mus musculus]	0	7.226	15	3	3	3	1	201	22.6	8.81	7.7	3	0.069	0.042
FALSE	High	Master Pro	Q8BFR4	N-acetylglucosamine-6-sulfatase [OS=Mus musculus]	0	7.22	6	3	4	3	1	544	61.1	8.24	8.77	3	0.672	0.843
FALSE	High	Master Pro	P07214	Sparc [OS=Mus musculus]	0	7.21	8	2	5	2	1	302	34.4	4.86	16.88	2	0.654	0.369
FALSE	High	Master Pro	P63280	SUMO-conjugating enzyme ubc9 [OS=Mus musculus]	0	7.13	14	2	3	2	1	158	18	8.66	12.26	2	2.71	2.081
FALSE	High	Master Pro	P63001	Ras-related C3 botulinum toxin substrate 1 [OS=Mus musculus]	0	7.119	12	3	3	3	1	192	21.4	8.5	11.91	3	0.973	0.752
FALSE	High	Master Pro	P23927	Alpha-crystallin B chain [OS=Mus musculus]	0	7.045	11	2	3	2	1	175	20.1	7.33	10.11	2	1.109	0.304
FALSE	High	Master Pro	Q9CQE8	UPF0568 protein C14orf166 homolog [OS=Mus musculus]	0	7.036	10	2	2	2	1	244	28.1	6.89	6.02	2	1.203	1.093
FALSE	High	Master Pro	A6X935-1	inter alpha-trypsin inhibitor, heavy chain 4 [OS=Mus musculus]	0	6.946	2	2	9	2	1	942	104.6	6.4	31.46	2	0.378	0.225
FALSE	High	Master Pro	Q8R081	Heterogeneous nuclear ribonucleoprotein L [OS=Mus musculus]	0	6.868	4	2	4	2	1	586	63.9	8.1	10.56	2	2.828	2.747
FALSE	High	Master Pro	Q61398	Procollagen C-endopeptidase enhancer 1 [OS=Mus musculus]	0	6.851	5	2	4	2	1	468	50.1	8.41	11.68	2	0.854	0.819
FALSE	High	Master Pro	P60335	Poly(RC)-binding protein 1 [OS=Mus musculus]	0	6.781	6	2	6	1	1	356	37.5	7.09	17.36	2	2.256	2.497
FALSE	High	Master Pro	P61961	Ubiquitin-fold modifier 1 [OS=Mus musculus]	0	6.766	51	2	3	2	1	85	9.1	9.31	12.5	2	0.65	0.493
FALSE	High	Master Pro	O08997	Copper transport protein ATOX1 [OS=Mus musculus]	0	6.727	32	2	6	2	1	68	7.3	6.51	20.4	2	1.118	1.261
FALSE	High	Master Pro	P62897	Cytochrome c, somatic [OS=Mus musculus]	0	6.677	18	2	7	2	1	105	11.6	9.58	25.33	2	3.914	3.55
FALSE	High	Master Pro	P63323	40S ribosomal protein S12 [OS=Mus musculus]	0	6.624	20	3	6	3	1	132	14.5	7.24	17.84	3	1.202	1.133
FALSE	High	Master Pro	P62849-1	40S ribosomal protein S24 [OS=Mus musculus]	0	6.611	26	3	3	3	1	133	15.4	10.78	8.44	3	1.136	0.87
FALSE	High	Master Pro	Q9D0I9	arginine--tRNA ligase, cytoplasmic [OS=Mus musculus]	0	6.535	5	2	2	2	1	660	75.6	7.55	8.25	2	1.266	1.346
FALSE	High	Master Pro	O08553	Dihydropyrimidinase-related protein 2 [OS=Mus musculus]	0	6.508	3	2	7	2	1	572	62.2	6.38	22.03	2	0.768	0.763
FALSE	High	Master Pro	O08638-1	Myosin-11 [OS=Mus musculus]	0	6.482	2	3	5	1	1	1972	226.9	5.45	12.47	3		
FALSE	High	Master Pro	P16858	glyceraldehyde-3-phosphate dehydrogenase [OS=Mus musculus]	0	6.331	9	2	3	2	1	333	35.8	8.25	8.7	2	0.933	1.195
FALSE	High	Master Pro	Q9Z2T6	Keratin, type II cuticular Hb5 [OS=Mus musculus]	0	6.276	4	2	3	2	1	507	55.7	6.42	7.99	2	0.621	2.927
FALSE	High	Master Pro	Q8R3Q6	coiled-coil domain-containing protein 58 [OS=Mus musculus]	0	6.224	18	2	2	2	1	144	16.7	8.16	6.04	2	0.551	0.418
FALSE	High	Master Pro	P45377	Aldose reductase-related protein 2 [OS=Mus musculus]	0	6.216	9	2	3	2	1	316	36.1	6.37	4.82	2	0.899	1.015
FALSE	High	Master Pro	P61161	Actin-related protein 2 [OS=Mus musculus]	0	6.214	8	2	3	2	1	394	44.7	6.74	6.24	2	0.284	0.238
FALSE	High	Master Pro	Q9CR16	peptidyl-prolyl cis-trans isomerase D [OS=Mus musculus]	0	6.203	5	2	4	2	1	370	40.7	7.43	15.15	2	1.754	2.372
FALSE	High	Master Pro	P02088	Hemoglobin subunit beta-1 [OS=Mus musculus]	0	6.18	13	2	9	2	1	147	15.8	7.65	27.25	2	0.385	0.344
FALSE	High	Master Pro	Q9CPY7-1	cytosol aminopeptidase [OS=Mus musculus]	0	6.163	5	3	7	3	1	519	56.1	7.72	19.81	3	1.172	1.257
FALSE	High	Master Pro	Q9Z1Q5	chloride intracellular channel protein 1 [OS=Mus musculus]	0	6.118	11	2	3	2	1	241	27	5.17	10.34	2	1.603	1.461
FALSE	High	Master Pro	P47199	Quinone oxidoreductase [OS=Mus musculus]	0	6.103	8	2	3	2	1	331	35.2	8.07	11.15	2	1.357	1.276
FALSE	High	Master Pro	Q02053	Ubiquitin-like modifier-activating enzyme 1 [OS=Mus musculus]	0	6.1	3	2	2	2	1	1058	117.7	5.66	7.77	2	0.466	0.347
FALSE	High	Master Pro	O88207	Collagen alpha-1(V) chain [OS=Mus musculus]	0	6.038	2	2	5	2	1	1838	183.6	4.98	17.42	2	1.114	2.202
FALSE	High	Master Pro	O88342	WD repeat-containing protein 1 [OS=Mus musculus]	0	6.036	4	3	7	3	1	606	66.4	6.6	22.73	3	1.704	1.59
FALSE	High	Master Pro	Q8R1F1	Niban-like protein 1 [OS=Mus musculus]	0	6.028	3	2	3	2	1	749	84.8	5.94	8.06	2	1.374	0.998
FALSE	High	Master Pro	P62264	40S ribosomal protein S14 [OS=Mus musculus]	0	5.995	14	2	3	2	1	151	16.3	10.05	11.37	2	1.974	1.667
FALSE	High	Master Pro	Q9C230-1	obg-like ATPase 1 [OS=Mus musculus]	0	5.98	7	2	2	2	1	396	44.7	7.81	6.85	2	0.892	0.706
FALSE	High	Master Pro	Q03958	Prefoldin subunit 6 [OS=Mus musculus]	0	5.974	17	2	3	2	1	127	14.4	8.88	9.59	2	1	1.211
FALSE	High	Master Pro	P26369	Splicing factor U2AF 65 kDa subunit [OS=Mus musculus]	0	5.961	4	2	4	2	1	475	53.5	9.09	14.78	2	2.608	2.539
FALSE	High	Master Pro	P97371	Proteasome activator complex subunit 1 [OS=Mus musculus]	0	5.938	8	2	3	2	1	249	28.7	5.97	10.2	2	0.678	2.214
FALSE	High	Master Pro	Q64437	Alcohol dehydrogenase class 4 mu/sigma chain [OS=Mus musculus]	0	5.851	8	2	4	2	1	374	39.9	7.85	13	2	3.821	5.786
FALSE	High	Master Pro	Q9CWS0	N(G),N(G)-dimethylarginine dimethylaminohydrolase 1 [OS=Mus musculus]	0	5.848	6	2	3	2	1	285	31.4	5.97	11.03	2	0.525	0.419
FALSE	High	Master Pro	Q8CIE6	coatomer subunit alpha [OS=Mus musculus]	0	5.812	2	2	3	2	1	1224	138.3	7.65	12.04	2	1.156	1.267
FALSE	High	Master Pro	Q921M3-1	Splicing factor 3B subunit 3 [OS=Mus musculus]	0	5.773	2	2	2	2	1	1217	135.5	5.26	5.56	2	0.709	0.603
FALSE	High	Master Pro	P97351	40S ribosomal protein S3a [OS=Mus musculus]	0	5.703	9	3	8	3	1	264	29.9	9.73	23.16	3	1.087	0.926
FALSE	High	Master Pro	P47738	Aldehyde dehydrogenase, mitochondrial [OS=Mus musculus]	0	5.643	4	2	3	2	1	519	56.5	7.62	9.63	2	1.029	2.077
FALSE	High	Master Pro	Q99KJ8	dynactin subunit 2 [OS=Mus musculus]	0	5.634	8	2	2	2	1	402	44.1	5.26	7.39	2	0.614	0.44
FALSE	High	Master Pro	Q8VIJ6	splicing factor, proline- and glutamine-rich [OS=Mus musculus]	0	5.552	4	3	3	3	1	699	75.4	9.44	9.35	3	1.328	1.182
FALSE	High	Master Pro	Q9JM76	Actin-related protein 2/3 complex subunit 3 [OS=Mus musculus]	0	5.524	13	2	4	2	1	178	20.5	8.59	9.7	2	1.426	1.346
FALSE	High	Master Pro	Q8BVI4	dihydropteridine reductase [OS=Mus musculus]	0	5.51	7	2	3	2	1	241	25.6	7.81	8.85	2	1.253	1.6
FALSE	High	Master Pro	Q05186	Reticulocalbin-1 [OS=Mus musculus]	0	5.494	6	2	2	2	1	325	38.1	4.84	5.93	2	0.392	0.322

FALSE	High	Master Pro	P05201	Aspartate aminotransferase, cytoplasmic [OS=Mus musculus]	0	5.486	6	3	5	3	1	413	46.2	7.14	11.76	3	1.025	0.657
FALSE	High	Master Pro	P09671	Superoxide dismutase [Mn], mitochondrial [OS=Mus musculus]	0	5.448	10	2	3	2	1	222	24.6	8.62	9.29	2	0.898	0.696
FALSE	High	Master Pro	P42208	septin-2 [OS=Mus musculus]	0	5.404	6	2	2	2	1	361	41.5	6.55	5.51	2	0.617	0.576
FALSE	High	Master Pro	P31938	Dual specificity mitogen-activated protein kinase kinase 1 [OS=Mus musculus]	0	5.36	6	2	2	2	1	393	43.4	6.7	5.94	2	1.032	0.516
FALSE	High	Master Pro	O35887	Calumenin [OS=Mus musculus]	0	5.351	8	2	3	2	1	315	37	4.67	8.15	2	1.364	1.281
FALSE	High	Master Pro	P42932	T-complex protein 1 subunit theta [OS=Mus musculus]	0	5.332	3	2	4	2	1	548	59.5	5.62	9.65	2	0.499	0.407
FALSE	High	Master Pro	P11499	Heat shock protein HSP 90-beta [OS=Mus musculus]	0	5.307	4	3	3	2	1	724	83.2	5.03	8.92	3	1.118	1.357
FALSE	High	Master Pro	Q91Y97	fructose-bisphosphate aldolase B [OS=Mus musculus]	0	5.282	5	2	5	1	1	364	39.5	8.27	14.43	2	0.568	0.305
FALSE	High	Master Pro	P47753	F-actin-capping protein subunit alpha-1 [OS=Mus musculus]	0	5.197	9	2	4	1	1	286	32.9	5.55	14.49	2	0.624	0.621
FALSE	High	Master Pro	P21107	Tropomyosin alpha-3 chain [OS=Mus musculus]	0	5.146	6	2	3	2	1	285	33	4.72	9.99	2	0.861	1.617
FALSE	High	Master Pro	P32067	Lupus La protein homolog [OS=Mus musculus]	0	4.95	5	2	2	2	1	415	47.7	9.77	7.66	2	1.811	2.083
FALSE	High	Master Pro	P07091	Protein S100-A4 [OS=Mus musculus]	0	4.943	16	2	7	2	1	101	11.7	5.31	22.41	2	1.947	3.182
FALSE	High	Master Pro	Q08879	Fibulin-1 [OS=Mus musculus]	0	4.941	3	2	3	2	1	705	78	5.16	11.06	2	0.336	0.291
FALSE	High	Master Pro	Q9Z2W0	Aspartyl aminopeptidase [OS=Mus musculus]	0	4.937	4	2	3	2	1	473	52.2	7.25	10.29	2	0.924	1.457
FALSE	High	Master Pro	Q9DAR7	M7GpppX diphosphatase [OS=Mus musculus]	0	4.873	11	2	3	2	1	338	39	6.48	8	2	0.753	0.586
FALSE	High	Master Pro	P54822	adenylosuccinate lyase [OS=Mus musculus]	0	4.838	4	2	4	2	1	484	54.8	7.27	10.43	2	1.505	1.277
FALSE	High	Master Pro	Q11136	xaa-Pro dipeptidase [OS=Mus musculus]	0	4.828	3	2	3	2	1	493	55	5.78	5.95	2	0.743	0.509
FALSE	High	Master Pro	O55142	60S ribosomal protein L35a [OS=Mus musculus]	0	4.82	21	3	5	3	1	110	12.5	10.89	12.11	3	0.921	1.11
FALSE	High	Master Pro	Q62465	Synaptic vesicle membrane protein VAT-1 homolog [OS=Mus musculus]	0	4.804	4	2	4	2	1	406	43.1	6.37	13.27	2	1.68	0.697
FALSE	High	Master Pro	P14069	protein S100-A6 [OS=Mus musculus]	0	4.78	37	2	2	2	1	89	10	5.48	6.5	2	0.98	2.251
FALSE	High	Master Pro	Q61838	Pregnancy zone protein [OS=Mus musculus]	0	4.778	1	2	5	1	1	1495	165.7	6.68	14.14	2	0.36	0.258
FALSE	High	Master Pro	P50247	Adenosylhomocysteinase [OS=Mus musculus]	0	4.702	4	2	2	2	1	432	47.7	6.54	5.72	2	1.129	0.97
FALSE	High	Master Pro	Q9CQI3	glia maturation factor beta [OS=Mus musculus]	0	4.696	11	2	4	2	1	142	16.7	5.16	13.19	2	0.577	0.515
FALSE	High	Master Pro	P56399	Ubiquitin carboxyl-terminal hydrolase 5 [OS=Mus musculus]	0	4.628	3	2	4	2	1	858	95.8	5.01	9.79	2	0.585	0.626
FALSE	High	Master Pro	Q9CQM5	Thioredoxin domain-containing protein 17 [OS=Mus musculus]	0	4.483	15	2	5	2	1	123	14	4.77	17.41	2	2.3	2.375
FALSE	High	Master Pro	Q91WQ3	Tyrosine--tRNA ligase, cytoplasmic [OS=Mus musculus]	0	4.448	3	2	2	2	1	528	59.1	7.01	4.88	2	0.84	0.818
FALSE	High	Master Pro	Q8BFS6-1	Serine/threonine-protein phosphatase CPPED1 [OS=Mus musculus]	0	4.405	8	2	3	2	1	312	35.2	5.34	9.26	2	1.261	1.185
FALSE	High	Master Pro	Q9CXW3	Calcyclin-binding protein [OS=Mus musculus]	0	4.389	7	2	3	2	1	229	26.5	7.87	10.06	2	2.425	6.254
FALSE	High	Master Pro	P08071	Lactotransferrin [OS=Mus musculus]	0	4.378	3	2	3	1	1	707	77.8	8.53	9.98	2	0.454	0.339
FALSE	High	Master Pro	P07901	Heat shock protein HSP 90-alpha [OS=Mus musculus]	0	4.32	2	2	3	1	1	733	84.7	5.01	8.48	2	1.457	1.55
FALSE	High	Master Pro	Q6NZB0	DnaJ homolog subfamily C member 8 [OS=Mus musculus]	0	4.275	7	2	2	2	1	253	29.8	9.06	3	2	0.673	0.495
FALSE	High	Master Pro	P01942	Hemoglobin subunit alpha [OS=Mus musculus]	0	4.184	6	2	5	2	1	142	15.1	8.22	14.58	2	0.363	0.299
FALSE	High	Master Pro	P62245	40S ribosomal protein S15a [OS=Mus musculus]	0	4.152	13	2	4	2	1	130	14.8	10.13	10.56	2	2.417	2.345
FALSE	High	Master Pro	P17426	AP-2 complex subunit alpha-1 [OS=Mus musculus]	0	4.13	3	2	3	2	1	977	107.6	7.03	8.39	2	0.885	0.778
FALSE	High	Master Pro	Q9Z1X4-3	Isoform 3 of Interleukin enhancer-binding factor 3 [OS=Mus musculus]	0	4.129	3	2	2	2	1	911	97.7	8.95	3.68	2	0.971	0.792
FALSE	High	Master Pro	Q76M23	serine/threonine-protein phosphatase 2A 65 kDa regulatory subunit A alpha isoform [OS=Mus musculus]	0	4.12	4	2	3	2	1	589	65.3	5.11	9.16	2	1.186	1.043
FALSE	High	Master Pro	P43276	Histone H1.5 [OS=Mus musculus]	0	4.098	9	2	5	1	1	223	22.6	10.92	15.33	2	1.066	1.198
FALSE	High	Master Pro	Q8BML9	glutamine--tRNA ligase [OS=Mus musculus]	0	4.034	3	2	4	2	1	775	87.6	7.31	10.28	2	0.907	1.001
FALSE	High	Master Pro	Q3UEB3-1	poly(U)-binding-splicing factor PUF60 [OS=Mus musculus]	0	4.011	3	2	3	2	1	564	60.2	5.29	8.93	2	0.783	0.849
FALSE	High	Master Pro	P50608	Fibromodulin [OS=Mus musculus]	0	4.001	6	2	4	2	1	376	43	6.04	10.3	2	0.508	0.354
FALSE	High	Master Pro	Q9CZX8	40S ribosomal protein S19 [OS=Mus musculus]	0	3.987	13	2	4	2	1	145	16.1	10.4	10.04	2	5.167	4.895
FALSE	High	Master Pro	P47941	Crk-like protein [OS=Mus musculus]	0	3.928	7	2	2	2	1	303	33.8	6.74	5.61	2	0.705	0.629
FALSE	High	Master Pro	P59999	Actin-related protein 2/3 complex subunit 4 [OS=Mus musculus]	0	3.926	13	2	3	2	1	168	19.7	8.43	8.66	2	1.139	1.26
FALSE	High	Master Pro	P14824	annexin A6 [OS=Mus musculus]	0	3.83	3	2	2	2	1	673	75.8	5.5	5.81	2	0.603	0.424
FALSE	High	Master Pro	Q9WV32	Actin-related protein 2/3 complex subunit 1B [OS=Mus musculus]	0	3.611	5	2	2	2	1	372	41	8.35	6.22	2	1.107	1.303
FALSE	High	Master Pro	Q9JII5	DAZ-associated protein 1 [OS=Mus musculus]	0	3.576	8	2	2	2	1	406	43.2	8.56	2.07	2	0.521	0.328
FALSE	High	Master Pro	P70349	Histidine triad nucleotide-binding protein 1 [OS=Mus musculus]	0	3.554	27	2	2	2	1	126	13.8	6.87	2.26	2	1.087	0.717
FALSE	High	Master Pro	Q8C1A5	thimet oligopeptidase [OS=Mus musculus]	0	3.359	2	2	4	2	1	687	78	6.06	11.25	2	1.16	1.6
FALSE	High	Master Pro	Q91WJ8-2	Isoform 2 of Far upstream element-binding protein 1 [OS=Mus musculus]	0	3.356	2	2	5	1	1	672	70.8	7.69	16.77	2	2.219	1.823
FALSE	High	Master Pro	P80318	T-complex protein 1 subunit gamma [OS=Mus musculus]	0	3.334	3	2	3	2	1	545	60.6	6.7	8.04	2	0.825	0.681
FALSE	High	Master Pro	Q9CQC6	Basic leucine zipper and W2 domain-containing protein 1 [OS=Mus musculus]	0	3.263	3	2	2	2	1	419	48	5.92	6.12	2	1.556	2.671
FALSE	High	Master Pro	P62751	60S ribosomal protein L23a [OS=Mus musculus]	0	3.243	10	2	5	2	1	156	17.7	10.45	13.08	2	1.115	1.309
FALSE	High	Master Pro	P84104-1	Serine/arginine-rich splicing factor 3 [OS=Mus musculus]	0	3.225	14	2	3	1	1	164	19.3	11.65	5.11	2	5.768	4.378
FALSE	High	Master Pro	Q60972	Histone-binding protein RBBP4 [OS=Mus musculus]	0	3.076	4	2	3	2	1	425	47.6	4.89	8.79	2	1.298	1.359
FALSE	High	Master Pro	Q9EQH3	Vacuolar protein sorting-associated protein 35 [OS=Mus musculus]	0	3.073	3	2	3	2	1	796	91.7	5.44	4.9	2	1.885	1.739
FALSE	High	Master Pro	Q3U0V1	Far upstream element-binding protein 2 [OS=Mus musculus]	0	3.027	3	2	5	1	1	748	76.7	7.33	15.81	2	1.274	1.379
FALSE	High	Master Pro	Q9CPW4	Actin-related protein 2/3 complex subunit 5 [OS=Mus musculus]	0	2.966	13	2	3	2	1	151	16.3	5.67	6.39	2	0.954	0.932
FALSE	High	Master Pro	P63005-1	Platelet-activating factor acetylhydrolase IB subunit alpha [OS=Mus musculus]	0	2.924	3	2	4	2	1	410	46.6	7.37	11.2	2	1.47	1.459
FALSE	High	Master Pro	P35979	60S ribosomal protein L12 [OS=Mus musculus]	0	2.886	10	2	5	2	1	165	17.8	9.42	13.54	2	1.179	1.071
FALSE	High	Master Pro	Q8VCT3	aminopeptidase B [OS=Mus musculus]	0	2.847	2	2	4	2	1	650	72.4	5.35	9.59	2	0.702	1.228
FALSE	High	Master Pro	Q8BL97-1	serine/arginine-rich splicing factor 7 [OS=Mus musculus]	0	2.767	9	2	3	1	1	267	30.8	11.9	4.16	2	2.112	1.042
FALSE	High	Master Pro	P63163	small nuclear ribonucleoprotein-associated protein N [OS=Mus musculus]	0	2.765	6	2	2	2	1	240	24.6	11.19	5.7	2	3.958	3.871
FALSE	High	Master Pro	Q91VW3	SH3 domain-binding glutamic acid-rich-like protein 3 [OS=Mus musculus]	0	2.717	18	2	4	2	1	93	10.5	5.14	9.44	2	1.33	1.638
FALSE	High	Master Pro	Q8CJG0	Protein argonaute-2 [OS=Mus musculus]	0	2.703	3	2	2	2	1	860	97.2	9.19	5.11	2	0.876	0.768
FALSE	High	Master Pro	Q3U962	Collagen alpha-2(V) chain [OS=Mus musculus]	0	2.679	1	2	3	1	1	1497	144.9	6.7	7.27	2	0.585	0.571
FALSE	High	Master Pro	Q921I1	Serotransferrin [OS=Mus musculus]	0	2.599	3	2	9	1	1	697	76.7	7.18	23.82	2	0.374	0.253
FALSE	High	Master Pro	Q9JHH6	Carboxypeptidase B2 [OS=Mus musculus]	0	2.595	3	2	4	2	1	422	48.8	7.97	10.36	2	0.328	0.263
FALSE	High	Master Pro	P54071	Isocitrate dehydrogenase [NADP], mitochondrial [OS=Mus musculus]	0	2.581	4	2	3	1	1	452	50.9	8.69	7.79	2	1.328	1.436
FALSE	High	Master Pro	Q99LX0	protein/nucleic acid deglycase DJ-1 [OS=Mus musculus]	0	2.562	8	2	4	2	1	189	20	6.77	12.52	2	1.45	1.606
FALSE	High	Master Pro	Q91VH6	Protein MEMO1 [OS=Mus musculus]	0	2.418	10	2	3	2	1	297	33.7	7.14	5.8	2	2.334	3.009
FALSE	High	Master Pro	Q9DBP5	UMP-CMP kinase [OS=Mus musculus]	0	2.363	10	2	2	2	1	196	22.2	5.83	4.91	2	0.389	0.377
FALSE	High	Master Pro	P14211	Calreticulin [OS=Mus musculus]	0	2.342	3	2	4	2	1	416	48	4.49	10.01	2	1.703	1.003
FALSE	High	Master Pro	P24452	Macrophage-capping protein [OS=Mus musculus]	0	2.238	4	2	3	2	1	352	39.2	7.2	8.42	2	4.952	3.189
FALSE	High	Master Pro	P02468	Laminin subunit gamma-1 [OS=Mus musculus]	0	2.036	1	2	3	2	1	1607	177.2	5.21	7.54	2	0.481	0.559

Sample	TMT reagent
Primary OEC+LPS sup	126
OEmyc790_C7+LPS sup	127
OEmyc790_C4+LPS sup	128

Checked	Protein FDI	Master	Accession	Description	Exp. q-valu	Sum PEP Sc	Coverage [	# Peptides	# PSMs	# Unique P	# Protein G	# AAs	MW [kDa]	calc. pI	Score Sequ	# Peptides	Abundance Ratio: (F1, 130) / (F1, 129)	Abundance Ratio: (F1, 131) / (F1, 129)
FALSE	High	Master Pro	Q9QXS1-1	plectin [OS=Mus musculus]	0	168.56	11	45	87	45	1	4691	533.9	5.96	306.49	45	1.227	1.431
FALSE	High	Master Pro	P58252	Elongation factor 2 [OS=Mus musculus]	0	99.744	21	16	66	16	1	858	95.3	6.83	247.29	16	2.718	3.012
FALSE	High	Master Pro	P11276	fibronectin [OS=Mus musculus]	0	97.128	11	20	50	20	1	2477	272.4	5.59	188.54	20	0.747	1.133
FALSE	High	Master Pro	P52480	Pyruvate kinase PKM [OS=Mus musculus]	0	86.418	35	14	45	2	1	531	57.8	7.47	180.9	14	2.225	1.745
FALSE	High	Master Pro	P63017	Heat shock cognate 71 kDa protein [OS=Mus musculus]	0	75.674	21	13	55	10	1	646	70.8	5.52	210.48	13	2.528	2.014
FALSE	High	Master Pro	P09411	phosphoglycerate kinase 1 [OS=Mus musculus]	0	68.779	34	13	46	13	1	417	44.5	7.9	157.04	13	4.423	4.896
FALSE	High	Master Pro	P60710	Actin, cytoplasmic 1 [OS=Mus musculus]	0	68.401	39	12	43	5	1	375	41.7	5.48	164.18	12	1.544	1.161
FALSE	High	Master Pro	Q8BTM8	Filamin-A [OS=Mus musculus]	0	68.209	8	19	44	15	1	2647	281	6.04	160.39	19	1.186	1.359
FALSE	High	Master Pro	P17182	alpha-enolase [OS=Mus musculus]	0	63.905	33	11	43	11	1	434	47.1	6.8	172.55	11	2.32	2.511
FALSE	High	Master Pro	P20152	Vimentin [OS=Mus musculus]	0	58.757	28	13	49	13	1	466	53.7	5.12	176.17	13	2.621	2.81
FALSE	High	Master Pro	P52480-2	Isoform M1 of Pyruvate kinase PKM [OS=Mus musculus]	0	58.552	29	13	38	1	1	531	57.9	7.14	136.08	13	1.092	0.948
FALSE	High	Master Pro	P10107	annexin A1 [OS=Mus musculus]	0	57.805	29	10	28	10	1	346	38.7	7.37	107.18	10	2.352	2.329
FALSE	High	Master Pro	P26041	Moesin [OS=Mus musculus]	0	56.362	28	15	40	10	1	577	67.7	6.6	131.47	15	1.893	1.637
FALSE	High	Master Pro	P57780	Alpha-actinin-4 [OS=Mus musculus]	0	48.178	14	12	35	3	1	912	104.9	5.41	113.6	12	0.834	0.863
FALSE	High	Master Pro	P05064	fructose-bisphosphate aldolase A [OS=Mus musculus]	0	48.053	29	10	30	9	1	364	39.3	8.09	104.94	10	1.843	1.574
FALSE	High	Master Pro	P11087-1	Collagen alpha-1(I) chain [OS=Mus musculus]	0	46.912	11	14	28	13	1	1453	137.9	5.85	97.19	14	0.696	0.492
FALSE	High	Master Pro	P10126	Elongation factor 1-alpha 1 [OS=Mus musculus]	0	45.662	21	9	28	9	1	462	50.1	9.01	109.97	9	1.6	1.98
FALSE	High	Master Pro	Q64727	Vinculin [OS=Mus musculus]	0	45.505	11	10	15	10	1	1066	116.6	6	54.03	10	0.493	0.603
FALSE	High	Master Pro	P01027-1	Complement C3 [OS=Mus musculus]	0	45.355	5	8	28	8	1	1663	186.4	6.73	112.15	8	0.328	0.232
FALSE	High	Master Pro	Q07235	Glia-derived nexin [OS=Mus musculus]	0	44.736	24	9	21	9	1	397	44.2	9.85	77.39	9	1.072	1.139
FALSE	High	Master Pro	P26039	Talin-1 [OS=Mus musculus]	0	43.551	6	12	23	12	1	2541	269.7	6.18	67.37	12	0.649	0.731
FALSE	High	Master Pro	Q7TPR4	Alpha-actinin-1 [OS=Mus musculus]	0	43.441	12	10	29	1	1	892	103	5.38	94.42	10	0.752	0.757
FALSE	High	Master Pro	Q8VDD5	Myosin-9 [OS=Mus musculus]	0	41.956	6	11	22	9	1	1960	226.2	5.66	73.14	11	0.944	1.328
FALSE	High	Master Pro	Q61171	Peroxiredoxin-2 [OS=Mus musculus]	0	41.525	32	6	21	6	1	198	21.8	5.41	86.85	6	2.01	2.002
FALSE	High	Master Pro	P18760	Cofilin-1 [OS=Mus musculus]	0	41.122	54	7	24	7	1	166	18.5	8.09	106.74	7	3.541	4.467
FALSE	High	Master Pro	Q80X90	Filamin-B [OS=Mus musculus]	0	39.005	4	9	21	5	1	2602	277.7	5.71	75.34	9	0.691	0.51
FALSE	High	Master Pro	Q61598	Rab GDP dissociation inhibitor beta [OS=Mus musculus]	0	38.652	25	8	18	6	1	445	50.5	6.25	68.74	8	2.459	1.689
FALSE	High	Master Pro	Q61703	Inter-alpha-trypsin inhibitor heavy chain H2 [OS=Mus musculus]	0	38.479	8	9	22	9	1	946	105.9	7.27	78.85	9	0.364	0.232
FALSE	High	Master Pro	P05213	Tubulin alpha-1B chain [OS=Mus musculus]	0	36.125	19	7	15	7	1	451	50.1	5.06	70.82	7	0.896	0.664
FALSE	High	Master Pro	P63101	14-3-3 protein zeta/delta [OS=Mus musculus]	0	35.393	38	8	23	5	1	245	27.8	4.79	85.23	8	2.05	2.084
FALSE	High	Master Pro	P62962	profilin-1 [OS=Mus musculus]	0	34.186	45	5	28	5	1	140	14.9	8.28	114.32	5	1.548	1.489
FALSE	High	Master Pro	O88569	heterogeneous nuclear ribonucleoproteins A2/B1 [OS=Mus musculus]	0	33.745	16	7	18	5	1	353	37.4	8.95	65.38	7	2.474	2.507
FALSE	High	Master Pro	Q60847	Collagen alpha-1(XII) chain [OS=Mus musculus]	0	33.473	3	10	14	10	1	3120	340	5.64	46.12	10	0.626	0.698
FALSE	High	Master Pro	P09405	Nucleolin [OS=Mus musculus]	0	32.325	14	11	28	11	1	707	76.7	4.75	88.5	11	1.778	3.878
FALSE	High	Master Pro	P15532	Nucleoside diphosphate kinase A [OS=Mus musculus]	0	32.292	53	6	26	3	1	152	17.2	7.37	90.28	6	3.703	3.418
FALSE	High	Master Pro	P62737	Actin, aortic smooth muscle [OS=Mus musculus]	0	31.81	24	8	25	1	1	377	42	5.39	77.32	8	0.91	0.587
FALSE	High	Master Pro	Q9JMH6-1	Thioredoxin reductase 1, cytoplasmic [OS=Mus musculus]	0	31.631	11	5	11	5	1	613	67	7.44	52.36	5	1.334	0.981
FALSE	High	Master Pro	Q9WVA4	Transgelin-2 [OS=Mus musculus]	0	31.513	42	8	21	8	1	199	22.4	8.24	69.09	8	1.223	1.594
FALSE	High	Master Pro	Q64433	10 kDa heat shock protein, mitochondrial [OS=Mus musculus]	0	31.398	68	8	18	8	1	102	11	8.35	67.39	8	3.75	8.955
FALSE	High	Master Pro	P27773	Protein disulfide-isomerase A3 [OS=Mus musculus]	0	30.8	19	10	19	10	1	505	56.6	6.21	62.51	10	1.89	1.286
FALSE	High	Master Pro	P06745	glucose-6-phosphate isomerase [OS=Mus musculus]	0	30.442	16	7	14	7	1	558	62.7	8.13	44.29	7	1.155	0.81
FALSE	High	Master Pro	Q01768	nucleoside diphosphate kinase b [OS=Mus musculus]	0	29.932	53	6	19	3	1	152	17.4	7.5	75.76	6	2.156	2.261
FALSE	High	Master Pro	P35441	thrombospondin-1 [OS=Mus musculus]	0	29.845	8	9	17	9	1	1170	129.6	4.96	60.03	9	0.436	0.391
FALSE	High	Master Pro	P25444	40S ribosomal protein S2 [OS=Mus musculus]	0	28.66	18	5	22	5	1	293	31.2	10.24	79.24	5	1.557	1.683
FALSE	High	Master Pro	Q05793	Basement membrane-specific heparan sulfate proteoglycan core protein [OS=Mus musculus]	0	28.565	3	9	15	9	1	3707	398	6.32	38.48	9	0.48	0.564
FALSE	High	Master Pro	Q62009	Periostin [OS=Mus musculus]	0	27.848	8	6	16	6	1	838	93.1	7.53	59.25	6	0.417	0.515
FALSE	High	Master Pro	Q9JKF1	Ras GTPase-activating-like protein IQGAP1 [OS=Mus musculus]	0	27.598	5	6	7	6	1	1657	188.6	6.48	29.32	6	0.977	0.892
FALSE	High	Master Pro	P07356	Annexin A2 [OS=Mus musculus]	0	27.585	28	9	16	9	1	339	38.7	7.69	50.66	9	1.691	1.226
FALSE	High	Master Pro	P06151	L-lactate dehydrogenase A chain [OS=Mus musculus]	0	27.541	16	5	16	5	1	332	36.5	7.74	60.26	5	1.529	2.075
FALSE	High	Master Pro	P48678-1	Prelamin-A/C [OS=Mus musculus]	0	27.457	11	8	22	8	1	665	74.2	6.98	77.17	8	1.68	1.5
FALSE	High	Master Pro	P61979-2	Isoform 2 of Heterogeneous nuclear ribonucleoprotein K [OS=Mus musculus]	0	27.04	16	5	13	5	1	464	51	5.33	53.94	5	1.741	2.143
FALSE	High	Master Pro	P17225	Polypyrimidine tract-binding protein 1 [OS=Mus musculus]	0	26.803	10	4	11	4	1	527	56.4	8.34	52.51	4	1.514	2.107
FALSE	High	Master Pro	Q61704	Inter-alpha-trypsin inhibitor heavy chain H3 [OS=Mus musculus]	0	26.569	4	4	14	4	1	889	99.3	6.05	60.83	4	0.351	0.216
FALSE	High	Master Pro	P99029	Peroxiredoxin-5, mitochondrial [OS=Mus musculus]	0	26.55	24	4	17	4	1	210	21.9	8.85	61.02	4	2.042	4.8
FALSE	High	Master Pro	Q01853	Transitional endoplasmic reticulum ATPase [OS=Mus musculus]	0	26.494	9	7	12	7	1	806	89.3	5.26	42.11	7	0.89	1.269
FALSE	High	Master Pro	Q99020	Heterogeneous nuclear ribonucleoprotein A/B [OS=Mus musculus]	0	26.267	25	6	15	5	1	285	30.8	7.91	50.92	6	2.721	1.949
FALSE	High	Master Pro	O88844	Isocitrate dehydrogenase [NADP] cytoplasmic [OS=Mus musculus]	0	26.07	21	8	14	7	1	414	46.6	7.17	50.2	8	0.819	1.562
FALSE	High	Master Pro	O08709	Peroxiredoxin-6 [OS=Mus musculus]	0	25.626	28	5	24	5	1	224	24.9	6.01	86.32	5	1.215	2.257
FALSE	High	Master Pro	P35700	peroxiredoxin-1 [OS=Mus musculus]	0	25.532	34	7	21	5	1	199	22.2	8.12	77.24	7	1.626	1.807
FALSE	High	Master Pro	P63038-1	60 kDa heat shock protein, mitochondrial [OS=Mus musculus]	0	25.225	14	6	10	6	1	573	60.9	6.18	42.24	6	1.533	2.52
FALSE	High	Master Pro	P97298	Pigment epithelium-derived factor [OS=Mus musculus]	0	25.151	15	5	10	5	1	417	46.2	6.98	44.23	5	0.254	0.215
FALSE	High	Master Pro	P14152	Malate dehydrogenase, cytoplasmic [OS=Mus musculus]	0	24.795	19	7	16	7	1	334	36.5	6.58	56.85	7	3.319	2.319
FALSE	High	Master Pro	Q9D8N0	elongation factor 1-gamma [OS=Mus musculus]	0	24.487	15	6	11	6	1	437	50	6.74	36.57	6	0.898	1.293
FALSE	High	Master Pro	Q61207	Prosaposin [OS=Mus musculus]	0	24.46	11	6	19	6	1	557	61.4	5.19	61.01	6	1.645	2.828
FALSE	High	Master Pro	Q9DBJ1	Phosphoglycerate mutase 1 [OS=Mus musculus]	0	24.19	24	4	19	4	1	254	28.8	7.18	72.08	4	2.29	2.702
FALSE	High	Master Pro	P16546	Spectrin alpha chain, non-erythrocytic 1 [OS=Mus musculus]	0	24.188	3	5	6	5	1	2472	284.4	5.33	24.36	5	0.872	0.635
FALSE	High	Master Pro	P49312-1	Heterogeneous nuclear ribonucleoprotein A1 [OS=Mus musculus]	0	24.171	13	5	15	3	1	320	34.2	9.23	53.78	5	1.545	1.597
FALSE	High	Master Pro	P62259	14-3-3 protein epsilon [OS=Mus musculus]	0	23.394	26	6	15	3	1	255	29.2	4.74	51.55	6	1.208	1.05
FALSE	High	Master Pro	P32261	Antithrombin-III [OS=Mus musculus]	0	23.178	16	9	23	9	1	465	52	6.46	68.54	9	0.315	0.196
FALSE	High	Master Pro	Q9CQV8-1	14-3-3 protein beta/alpha [OS=Mus musculus]	0	22.817	26	6	17	2	1	246	28.1	4.83	61.24	6	1.392	1.627
FALSE	High	Master Pro	P16627	Heat shock 70 kDa protein 1-like [OS=Mus musculus]	0	22.668	8	4	13	1	1	641	70.6	6.24	53.95	4	0.398	0.203
FALSE	High	Master Pro	Q60864	stress-induced-phosphoprotein 1 [OS=Mus musculus]	0	21.795	11	6	11	6	1	543	62.5	6.8	43.05	6	1.134	1.46
FALSE	High	Master Pro	P17751	Triosephosphate isomerase [OS=Mus musculus]	0	21.404	17	5	19	5	1	299	32.2	5.74	69.32	5	2.904	5.766
FALSE	High	Master Pro	Q93092	Transaldolase [OS=Mus musculus]	0	21.211	19	7	17	7	1	337	37.4	7.03	50.1	7	2.582	1.41
FALSE	High	Master Pro	Q9DCD0	6-phosphogluconate dehydrogenase, decarboxylating [OS=Mus musculus]	0	21.116	12	6	11	6	1	483	53.2	7.23	37.76	6	1.078	0.861
FALSE	High	Master Pro	P08249	Malate dehydrogenase, mitochondrial [OS=Mus musculus]	0	20.256	18	4	6	4	1	338	35.6	8.68	25.22	4	1.833	1.989
FALSE	High	Master Pro	P00493	Hypoxanthine-guanine phosphoribosyltransferase [OS=Mus musculus]	0	20.247	21	4	10	4	1	218	24.6	6.68	32.59	4	1.598	1.789
FALSE	High	Master Pro	P61982	14-3-3 protein gamma [OS=Mus musculus]	0	20.049	21	6	20	2	1	247	28.3	4.89	72.38	6	2.62	2.583
FALSE	High	Master Pro	P62082	40S ribosomal protein S7 [OS=Mus musculus]	0	20.021	30	5	11	5	1	194	22.1	10.1	39.33	5	2.636	3.166
FALSE	High	Master Pro	P29341	Polyadenylate-binding protein 1 [OS=Mus musculus]	0	19.758	6	5	9	5	1	636	70.6	9.5	30.36	5	0.778	0.846

FALSE	High	Master Pro	P20029	78 kDa glucose-regulated protein [OS=Mus musculus]	0	19.584	5	3	10	1	1	655	72.4	5.16	44.78	3	0.376	0.265
FALSE	High	Master Pro	P50396	Rab GDP dissociation inhibitor alpha [OS=Mus musculus]	0	19.466	13	5	8	3	1	447	50.5	5.08	27.29	5	2.205	1.682
FALSE	High	Master Pro	Q9Z204	Heterogeneous nuclear ribonucleoproteins C1/C2 [OS=Mus musculus]	0	19.302	15	4	8	4	1	313	34.4	5.05	35.37	4	1.513	2.478
FALSE	High	Master Pro	P13020-1	Gelsolin [OS=Mus musculus]	0	18.991	13	9	23	9	1	780	85.9	6.18	65.04	9	0.51	0.41
FALSE	High	Master Pro	Q60668-1	heterogeneous nuclear ribonucleoprotein D0 [OS=Mus musculus]	0	18.914	12	4	7	3	1	355	38.3	7.81	23.83	4	5.072	4.098
FALSE	High	Master Pro	Q61553	Fascin [OS=Mus musculus]	0	18.859	10	4	14	4	1	493	54.5	6.89	56.49	4	2.059	3.991
FALSE	High	Master Pro	P17710-1	Hexokinase-1 [OS=Mus musculus]	0	18.788	7	7	10	7	1	974	108.2	6.8	31.7	7	0.846	1.107
FALSE	High	Master Pro	Q6GQT1	Alpha-2-macroglobulin-P [OS=Mus musculus]	0	18.785	2	3	22	2	1	1474	164.2	6.61	73.42	3	0.362	0.22
FALSE	High	Master Pro	P62908	40S ribosomal protein S3 [OS=Mus musculus]	0	18.757	23	6	14	6	1	243	26.7	9.66	45.78	6	1.831	1.904
FALSE	High	Master Pro	P10649	Glutathione S-transferase Mu 1 [OS=Mus musculus]	0	18.605	23	5	16	2	1	218	26	7.94	57.61	5	2.614	4.41
FALSE	High	Master Pro	P99024	tubulin beta-5 chain [OS=Mus musculus]	0	18.548	20	7	12	7	1	444	49.6	4.89	38.22	7	0.678	0.471
FALSE	High	Master Pro	P24527	leukotriene A-4 hydrolase [OS=Mus musculus]	0	18.241	6	4	10	4	1	611	69	6.42	36.68	4	1.681	1.407
FALSE	High	Master Pro	Q04857	Collagen alpha-1(VI) chain [OS=Mus musculus]	0	17.902	5	4	11	4	1	1025	108.4	5.36	37.8	4	0.628	0.729
FALSE	High	Master Pro	P18242	Cathepsin D [OS=Mus musculus]	0	17.858	17	5	9	5	1	410	44.9	7.15	33.76	5	1.313	1.306
FALSE	High	Master Pro	Q99K51	Plastin-3 [OS=Mus musculus]	0	17.561	9	5	10	3	1	630	70.7	5.62	36.31	5	0.762	0.819
FALSE	High	Master Pro	Q9CZD3	Glycine--tRNA ligase [OS=Mus musculus]	0	17.534	8	5	12	5	1	729	81.8	6.65	33.51	5	1.972	1.291
FALSE	High	Master Pro	P68254-1	14-3-3 protein theta [OS=Mus musculus]	0	17.51	21	5	15	1	1	245	27.8	4.78	53.21	5	1.731	1.757
FALSE	High	Master Pro	Q00493	Carboxypeptidase E [OS=Mus musculus]	0	17.46	9	3	9	3	1	476	53.2	5.19	37.97	3	0.971	0.777
FALSE	High	Master Pro	P15116	Cadherin-2 [OS=Mus musculus]	0	17.422	6	4	7	4	1	906	99.7	4.78	26.23	4	0.626	0.516
FALSE	High	Master Pro	P43277	Histone H1.3 [OS=Mus musculus]	0	17.402	14	4	8	3	1	221	22.1	11.03	29.78	4	1.792	2.131
FALSE	High	Master Pro	Q91ZX7	prolow-density lipoprotein receptor-related protein 1 [OS=Mus musculus]	0	16.975	1	5	8	5	1	4545	504.4	5.36	19.79	5	0.475	0.413
FALSE	High	Master Pro	Q6P1B1	xaa-Pro aminopeptidase 1 [OS=Mus musculus]	0	16.921	8	3	6	3	1	623	69.5	5.54	23.46	3	1.101	1.158
FALSE	High	Master Pro	P17742	peptidyl-prolyl cis-trans isomerase A [OS=Mus musculus]	0	16.884	28	5	34	5	1	164	18	7.9	110.96	5	3.269	2.981
FALSE	High	Master Pro	Q9CPU0	lactoylglutathione lyase [OS=Mus musculus]	0	16.871	23	6	18	6	1	184	20.8	5.47	59.73	6	3.214	1.344
FALSE	High	Master Pro	P62827	GTP-binding nuclear protein RAN [OS=Mus musculus]	0	16.869	20	3	5	3	1	216	24.4	7.49	19.06	3	1.666	1.481
FALSE	High	Master Pro	P19324	Serpin H1 [OS=Mus musculus]	0	16.823	12	5	9	5	1	417	46.5	8.82	31.93	5	1.006	0.805
FALSE	High	Master Pro	Q8BG05	Heterogeneous nuclear ribonucleoprotein A3 [OS=Mus musculus]	0	16.653	6	3	9	1	1	379	39.6	9.01	33.45	3	1.038	0.988
FALSE	High	Master Pro	P68510	14-3-3 protein eta [OS=Mus musculus]	0	16.587	17	5	17	1	1	246	28.2	4.89	59.37	5	2.04	1.476
FALSE	High	Master Pro	P26043	radixin [OS=Mus musculus]	0	16.521	11	7	13	2	1	583	68.5	6.2	43.24	7	1.292	1.235
FALSE	High	Master Pro	P51885	Lumican [OS=Mus musculus]	0	16.356	17	5	13	5	1	338	38.2	6.43	47.21	5	0.364	0.23
FALSE	High	Master Pro	P57776-3	Isoform 3 of Elongation factor 1-delta [OS=Mus musculus]	0	16.32	4	2	7	2	1	660	72.9	6.43	29.37	2	0.782	1.261
FALSE	High	Master Pro	P39061-3	Collagen alpha-1(XVIII) chain [OS=Mus musculus]	0	16.292	3	6	15	6	1	1774	182.1	5.62	46.76	6	0.935	1.182
FALSE	High	Master Pro	P30412	peptidyl-prolyl cis-trans isomerase C [OS=Mus musculus]	0	16.284	17	3	7	3	1	212	22.8	7.5	21.67	3	0.776	0.776
FALSE	High	Master Pro	P15626	Glutathione S-transferase Mu 2 [OS=Mus musculus]	0	16.26	23	4	9	1	1	218	25.7	7.39	33.94	4	0.349	0.432
FALSE	High	Master Pro	P80315	T-complex protein 1 subunit delta [OS=Mus musculus]	0	16.246	10	3	4	3	1	539	58	8.02	15.57	3	0.663	0.455
FALSE	High	Master Pro	P14206	40S ribosomal protein SA [OS=Mus musculus]	0	16.091	17	5	6	5	1	295	32.8	4.87	22.24	5	1.252	1.061
FALSE	High	Master Pro	Q61316	Heat shock 70 kDa protein 4 [OS=Mus musculus]	0	16.089	4	3	8	3	1	841	94.1	5.24	31.23	3	1.071	1.165
FALSE	High	Master Pro	Q91VM5	RNA binding motif protein, X-linked-like-1 [OS=Mus musculus]	0	16.048	10	4	9	4	1	388	42.1	9.99	31.49	4	1.821	1.641
FALSE	High	Master Pro	Q922R8	Protein disulfide-isomerase A6 [OS=Mus musculus]	0	15.839	7	2	4	2	1	440	48.1	5.14	13.45	2	0.411	0.329
FALSE	High	Master Pro	Q60605	Myosin light polypeptide 6 [OS=Mus musculus]	0	15.68	25	3	8	3	1	151	16.9	4.65	26.86	3	1.128	1.089
FALSE	High	Master Pro	P10639	thioredoxin [OS=Mus musculus]	0	15.323	21	2	9	2	1	105	11.7	4.92	44.43	2	1.414	1.453
FALSE	High	Master Pro	P16045	Galectin-1 [OS=Mus musculus]	0	15.04	30	4	11	4	1	135	14.9	5.49	35.77	4	2.722	3.159
FALSE	High	Master Pro	Q9CR57	60S ribosomal protein L14 [OS=Mus musculus]	0	14.814	12	2	5	2	1	217	23.5	11.02	23.51	2	0.498	0.48
FALSE	High	Master Pro	Q6ZWN5	40S ribosomal protein S9 [OS=Mus musculus]	0	14.652	23	5	9	5	1	194	22.6	10.65	29.22	5	2.994	3.308
FALSE	High	Master Pro	P06801	NADP-dependent malic enzyme [OS=Mus musculus]	0	14.516	10	4	6	4	1	572	63.9	7.44	15.73	4	0.631	0.426
FALSE	High	Master Pro	P33434-1	72 kDa type IV collagenase [OS=Mus musculus]	0	14.437	9	6	8	6	1	662	74.1	5.53	24.84	6	0.664	0.708
FALSE	High	Master Pro	Q9D0F9	Phosphoglucomutase-1 [OS=Mus musculus]	0	14.399	10	5	8	5	1	562	61.4	6.57	26.94	5	0.856	0.75
FALSE	High	Master Pro	P48036	annexin A5 [OS=Mus musculus]	0	14.367	14	4	9	4	1	319	35.7	4.96	29.55	4	2.519	1.699
FALSE	High	Master Pro	P68040	Receptor of activated protein C kinase 1 [OS=Mus musculus]	0	14.207	14	5	12	5	1	317	35.1	7.69	35.75	5	2.082	2.088
FALSE	High	Master Pro	O70251	Elongation factor 1-beta [OS=Mus musculus]	0	13.931	17	4	13	4	1	225	24.7	4.69	39.29	4	1.733	2.458
FALSE	High	Master Pro	Q9JII6	alcohol dehydrogenase [NADP(+)] [OS=Mus musculus]	0	13.906	14	4	7	4	1	325	36.6	7.39	24.78	4	1.093	0.97
FALSE	High	Master Pro	P26040	Ezrin [OS=Mus musculus]	0	13.824	10	6	12	1	1	586	69.4	6.1	38.8	6	0.56	0.714
FALSE	High	Master Pro	Q3TCN2	Putative phospholipase B-like 2 [OS=Mus musculus]	0	13.818	5	3	9	3	1	594	66.2	6.13	34.86	3	1.122	1.112
FALSE	High	Master Pro	P07724	Serum albumin [OS=Mus musculus]	0	13.806	4	2	118	2	1	608	68.6	6.07	412.31	2	0.268	0.178
FALSE	High	Master Pro	P62301	40S ribosomal protein S13 [OS=Mus musculus]	0	13.77	29	4	8	4	1	151	17.2	10.54	27.15	4	1.175	1.44
FALSE	High	Master Pro	P21460	Cystatin-C [OS=Mus musculus]	0	13.737	25	4	7	4	1	140	15.5	9	24.31	4	1.27	1.561
FALSE	High	Master Pro	P62855	40S ribosomal protein S26 [OS=Mus musculus]	0	13.687	21	2	6	2	1	115	13	11	24.23	2	1.669	1.815
FALSE	High	Master Pro	P40142	Transketolase [OS=Mus musculus]	0	13.564	5	3	10	3	1	623	67.6	7.5	35.43	3	0.945	0.591
FALSE	High	Master Pro	P47754	F-actin-capping protein subunit alpha-2 [OS=Mus musculus]	0	13.559	15	3	6	2	1	286	32.9	5.85	20.59	3	1.24	1.366
FALSE	High	Master Pro	P70168	Importin subunit beta-1 [OS=Mus musculus]	0	13.449	3	2	7	2	1	876	97.1	4.78	30.55	2	0.823	0.916
FALSE	High	Master Pro	P14869	60S acidic ribosomal protein P0 [OS=Mus musculus]	0	13.334	11	3	5	3	1	317	34.2	6.25	16.44	3	0.657	0.692
FALSE	High	Master Pro	Q9R0P5	Destrin [OS=Mus musculus]	0	13.148	25	3	9	3	1	165	18.5	7.97	26.96	3	0.646	0.54
FALSE	High	Master Pro	Q9Z1N5	spliceosome RNA helicase DDX39B [OS=Mus musculus]	0	13.105	9	4	8	4	1	428	49	5.67	23.6	4	0.958	0.726
FALSE	High	Master Pro	Q99PT1	rho GDP-dissociation inhibitor 1 [OS=Mus musculus]	0	13.101	11	2	8	2	1	204	23.4	5.2	26.74	2	1.034	0.773
FALSE	High	Master Pro	P62204	Calmodulin [OS=Mus musculus]	0	13.02	27	4	7	4	1	149	16.8	4.22	24.8	4	2.809	2.663
FALSE	High	Master Pro	Q9CPV4-1	Glyoxalase domain-containing protein 4 [OS=Mus musculus]	0	12.993	12	3	4	3	1	298	33.3	5.47	16.06	3	0.702	0.789
FALSE	High	Master Pro	P09103	Protein disulfide-isomerase [OS=Mus musculus]	0	12.894	9	5	9	5	1	509	57	4.88	30.54	5	1.224	1.489
FALSE	High	Master Pro	Q91ZJ5-1	UTP--glucose-1-phosphate uridylyltransferase [OS=Mus musculus]	0	12.811	9	4	9	4	1	508	56.9	7.61	27.8	4	1.462	1.442
FALSE	High	Master Pro	Q8R2Y2-1	Cell surface glycoprotein MUC18 [OS=Mus musculus]	0	12.719	5	3	6	3	1	648	71.5	5.83	23.08	3	1.122	0.376
FALSE	High	Master Pro	Q8K4Z3	NAD(P)H-hydrate epimerase [OS=Mus musculus]	0	12.695	13	3	8	3	1	282	31	7.69	24.84	3	0.99	1.033
FALSE	High	Master Pro	P63242	Eukaryotic translation initiation factor 5A-1 [OS=Mus musculus]	0	12.453	33	4	14	4	1	154	16.8	5.24	33.44	4	1.641	1.597
FALSE	High	Master Pro	Q99KI0	Aconitate hydratase, mitochondrial [OS=Mus musculus]	0	12.34	5	4	8	4	1	780	85.4	7.93	28.5	4	1.867	2.674
FALSE	High	Master Pro	Q9Z2X1-1	Heterogeneous nuclear ribonucleoprotein F [OS=Mus musculus]	0	12.083	8	2	3	1	1	415	45.7	5.49	10.03	2	3.265	5.654
FALSE	High	Master Pro	Q920E5	Farnesyl pyrophosphate synthase [OS=Mus musculus]	0	12.059	8	2	4	2	1	353	40.6	5.66	14.02	2	0.888	1.297
FALSE	High	Master Pro	Q9CWJ9	bifunctional purine biosynthesis protein purH [OS=Mus musculus]	0	12.046	7	3	5	3	1	592	64.2	6.76	18.24	3	0.556	0.627
FALSE	High	Master Pro	P50580	proliferation-associated protein 2G4 [OS=Mus musculus]	0	11.912	8	3	7	3	1	394	43.7	6.86	26.93	3	2.511	2.117
FALSE	High	Master Pro	Q64674	spermidine synthase [OS=Mus musculus]	0	11.838	10	3	7	3	1	302	34	5.5	23.99	3	0.887	0.925
FALSE	High	Master Pro	Q8CGC7	Bifunctional glutamate/proline--tRNA ligase [OS=Mus musculus]	0	11.544	4	5	6	5	1	1512	170	7.66	12.79	5	1.318	1.679
FALSE	High	Master Pro	Q9CQ65	S-methyl-5'-thioadenosine phosphorylase [OS=Mus musculus]	0	11.511	23	4	5	4	1	283	31	7.14	11.8	4	0.638	0.615
FALSE	High	Master Pro	P61205	ADP-ribosylation factor 3 [OS=Mus musculus]	0	11.503	17	2	8	2	1	181	20.6	7.43	34.14	2	1.583	1.938
FALSE	High	Master Pro	P45376	aldose reductase [OS=Mus musculus]	0	11.226	11	4	9	4	1	316	35.7	7.18	31.34	4	1.106	0.925

FALSE	High	Master Pro	P22777	Plasminogen activator inhibitor 1 [OS=Mus musculus]	0	11.226	10	3	5	3	1	402	45.1	6.64	18	3	0.556	0.45
FALSE	High	Master Pro	Q8VEK3	Heterogeneous nuclear ribonucleoprotein U [OS=Mus musculus]	0	11.19	4	3	5	3	1	800	87.9	6.24	17	3	1.193	2.216
FALSE	High	Master Pro	Q9WUM4	coronin-1C [OS=Mus musculus]	0	11.189	7	3	5	3	1	474	53.1	7.08	17.93	3	1.182	1.022
FALSE	High	Master Pro	Q99K85	phosphoserine aminotransferase [OS=Mus musculus]	0	11.14	15	4	4	4	1	370	40.4	8.03	11.19	4	0.634	0.577
FALSE	High	Master Pro	Q9Z175	Lysyl oxidase homolog 3 [OS=Mus musculus]	0	10.979	6	4	5	4	1	754	83.7	7.01	19.05	4	0.511	0.879
FALSE	High	Master Pro	Q00612	Glucose-6-phosphate 1-dehydrogenase X [OS=Mus musculus]	0	10.86	5	2	4	2	1	515	59.2	6.49	14.96	2	1.481	0.992
FALSE	High	Master Pro	P62900	60S ribosomal protein L31 [OS=Mus musculus]	0	10.816	18	2	7	2	1	125	14.5	10.54	25.37	2	1.528	1.986
FALSE	High	Master Pro	Q7TQI3	Ubiquitin thioesterase otub1 [OS=Mus musculus]	0	10.756	12	3	6	3	1	271	31.3	4.94	22.35	3	1.108	1.888
FALSE	High	Master Pro	Q6ZQ38	cullin-associated nedd8-dissociated protein 1 [OS=Mus musculus]	0	10.753	3	3	4	3	1	1230	136.2	5.78	12.17	3	0.856	0.948
FALSE	High	Master Pro	Q68FD5	Clathrin heavy chain 1 [OS=Mus musculus]	0	10.646	3	5	8	5	1	1675	191.4	5.69	21.14	5	0.535	0.613
FALSE	High	Master Pro	Q9D1A2	cytosolic non-specific dipeptidase [OS=Mus musculus]	0	10.569	13	4	7	4	1	475	52.7	5.66	26.48	4	0.569	0.429
FALSE	High	Master Pro	Q99KC8	von Willebrand factor A domain-containing protein 5A [OS=Mus musculus]	0	10.519	4	3	7	3	1	793	87.1	6.58	26.04	3	2.451	2.228
FALSE	High	Master Pro	P54728	UV excision repair protein RAD23 homolog B [OS=Mus musculus]	0	10.414	8	4	7	4	1	416	43.5	4.83	24.51	4	1.072	1.52
FALSE	High	Master Pro	Q5XJY5	Coatomer subunit delta [OS=Mus musculus]	0	10.296	4	2	7	2	1	511	57.2	6.21	24.81	2	1.135	1.418
FALSE	High	Master Pro	P24369	peptidyl-prolyl cis-trans isomerase B [OS=Mus musculus]	0	10.239	16	4	9	4	1	216	23.7	9.55	31.27	4	2.971	2.249
FALSE	High	Master Pro	P60843	Eukaryotic initiation factor 4A-I [OS=Mus musculus]	0	10.122	7	4	5	1	1	406	46.1	5.48	15.41	4	0.736	0.59
FALSE	High	Master Pro	P99027	60S acidic ribosomal protein P2 [OS=Mus musculus]	0	9.854	27	2	4	2	1	115	11.6	4.54	11.68	2	0.813	1.072
FALSE	High	Master Pro	Q61990	Poly(rC)-binding protein 2 [OS=Mus musculus]	0	9.798	6	2	6	1	1	362	38.2	6.79	18.49	2	1.36	2.288
FALSE	High	Master Pro	P61089	ubiquitin-conjugating enzyme E2 N [OS=Mus musculus]	0	9.783	16	2	10	2	1	152	17.1	6.57	35.43	2	1.364	2.013
FALSE	High	Master Pro	P19096	Fatty acid synthase [OS=Mus musculus]	0	9.593	1	4	6	4	1	2504	272.3	6.58	18.91	4	1.268	1.21
FALSE	High	Master Pro	Q9D8E6	60S ribosomal protein L4 [OS=Mus musculus]	0	9.585	6	2	2	2	1	419	47.1	11	10.19	2	0.659	0.795
FALSE	High	Master Pro	Q61035	Histidine--tRNA ligase, cytoplasmic [OS=Mus musculus]	0	9.571	4	2	7	2	1	509	57.4	6	22.62	2	1.589	1.213
FALSE	High	Master Pro	Q99KK7	dipeptidyl peptidase 3 [OS=Mus musculus]	0	9.569	7	3	3	3	1	738	82.8	5.38	10.65	3	0.459	0.439
FALSE	High	Master Pro	Q61581	Insulin-like growth factor-binding protein 7 [OS=Mus musculus]	0	9.498	7	2	6	2	1	281	29	8.31	23.92	2	0.361	0.279
FALSE	High	Master Pro	O35737	Heterogeneous nuclear ribonucleoprotein H [OS=Mus musculus]	0	9.332	8	2	2	1	1	449	49.2	6.3	7.46	2	0.43	0.445
FALSE	High	Master Pro	P05202	Aspartate aminotransferase, mitochondrial [OS=Mus musculus]	0	9.294	7	3	7	3	1	430	47.4	9	17.06	3	0.839	0.618
FALSE	High	Master Pro	P10630-2	Isoform 2 of Eukaryotic initiation factor 4A-II [OS=Mus musculus]	0	9.235	7	4	4	1	1	408	46.5	5.48	11.24	4	1.368	1.738
FALSE	High	Master Pro	P97855	Ras GTPase-activating protein-binding protein 1 [OS=Mus musculus]	0	9.162	6	2	5	2	1	465	51.8	5.59	17.32	2	0.617	0.675
FALSE	High	Master Pro	P62983	Ubiquitin-40S ribosomal protein S27a [OS=Mus musculus]	0	9.095	22	3	7	3	1	156	17.9	9.64	27.96	3	1.915	1.986
FALSE	High	Master Pro	Q9D819	Inorganic pyrophosphatase [OS=Mus musculus]	0	9.062	9	3	7	3	1	289	32.6	5.6	23.87	3	1.299	2.162
FALSE	High	Master Pro	Q11011	puromycin-sensitive aminopeptidase [OS=Mus musculus]	0	9.056	4	4	6	4	1	920	103.3	5.9	21.17	4	1.252	1.525
FALSE	High	Master Pro	Q60854	serpin B6 [OS=Mus musculus]	0	9.048	9	2	4	2	1	378	42.6	5.74	12.46	2	1.031	0.615
FALSE	High	Master Pro	P62821	Ras-related protein Rab-1A [OS=Mus musculus]	0	9.041	13	2	5	2	1	205	22.7	6.21	19.57	2	0.654	0.71
FALSE	High	Master Pro	P46638	Ras-related protein Rab-11B [OS=Mus musculus]	0	9.024	15	3	6	3	1	218	24.5	5.94	19.06	3	0.765	0.794
FALSE	High	Master Pro	P70296	phosphatidylethanolamine-binding protein 1 [OS=Mus musculus]	0	8.967	17	3	3	3	1	187	20.8	5.4	11.23	3	1.851	2.28
FALSE	High	Master Pro	Q9CRB6	Tubulin polymerization-promoting protein family member 3 [OS=Mus musculus]	0	8.868	13	2	4	2	1	176	19	9.11	13.15	2	2.165	0.776
FALSE	High	Master Pro	P62852	40S ribosomal protein S25 [OS=Mus musculus]	0	8.532	22	3	5	3	1	125	13.7	10.11	18.92	3	1.682	1.709
FALSE	High	Master Pro	Q3UGR5-1	haloacid dehalogenase-like hydrolase domain-containing protein 2 [OS=Mus musculus]	0	8.527	8	2	4	2	1	259	28.7	6.05	16.04	2	1.252	0.814
FALSE	High	Master Pro	P14131	40S ribosomal protein S16 [OS=Mus musculus]	0	8.493	12	2	8	2	1	146	16.4	10.21	30.49	2	1.73	2.081
FALSE	High	Master Pro	Q3U1J4	DNA damage-binding protein 1 [OS=Mus musculus]	0	8.469	3	4	8	4	1	1140	126.8	5.26	24.14	4	1.21	1.078
FALSE	High	Master Pro	Q9CQ60	6-phosphogluconolactonase [OS=Mus musculus]	0	8.288	9	2	5	2	1	257	27.2	5.85	18.63	2	3.98	3.859
FALSE	High	Master Pro	Q91W90	Thioredoxin domain-containing protein 5 [OS=Mus musculus]	0	8.009	8	3	4	3	1	417	46.4	5.78	13.01	3	1.421	1.123
FALSE	High	Master Pro	Q06138	Calcium-binding protein 39 [OS=Mus musculus]	0	7.962	10	4	6	4	1	341	39.8	6.89	16.14	4	1.21	1.235
FALSE	High	Master Pro	P17918	proliferating cell nuclear antigen [OS=Mus musculus]	0	7.956	11	2	5	2	1	261	28.8	4.77	15.79	2	1.994	1.555
FALSE	High	Master Pro	Q9Z247	Peptidyl-prolyl cis-trans isomerase FKBP9 [OS=Mus musculus]	0	7.892	7	2	2	2	1	570	63	5.21	7.38	2	0.55	0.343
FALSE	High	Master Pro	P68037	Ubiquitin-conjugating enzyme E2 L3 [OS=Mus musculus]	0	7.8	16	2	4	2	1	154	17.9	8.51	8.33	2	0.871	0.781
FALSE	High	Master Pro	Q9Z1Q9	Valine--tRNA ligase [OS=Mus musculus]	0	7.799	2	3	6	3	1	1263	140.1	7.77	17.11	3	1.009	0.931
FALSE	High	Master Pro	Q69ZN7-1	Myoferlin [OS=Mus musculus]	0	7.695	1	2	2	2	1	2048	233.2	6.16	8.14	2	1.248	2.322
FALSE	High	Master Pro	O08807	Peroxiredoxin-4 [OS=Mus musculus]	0	7.598	11	3	5	1	1	274	31	7.15	17.49	3	1.722	1.776
FALSE	High	Master Pro	Q61033-1	Lamina-associated polypeptide 2, isoforms alpha/zeta [OS=Mus musculus]	0	7.57	4	2	2	2	1	693	75.1	8.05	5.93	2	0.203	0.316
FALSE	High	Master Pro	P01029	Complement C4-B [OS=Mus musculus]	0	7.52	1	3	4	3	1	1738	192.8	7.53	13.95	3	0.379	0.219
FALSE	High	Master Pro	Q9R0Y5-2	Isoform 2 of Adenylate kinase isoenzyme 1 [OS=Mus musculus]	0	7.49	12	2	3	2	1	210	23.1	5.83	8.51	2	0.733	0.674
FALSE	High	Master Pro	Q6IRU2	Tropomyosin alpha-4 chain [OS=Mus musculus]	0	7.454	10	3	6	3	1	248	28.5	4.68	18.25	3	0.679	0.699
FALSE	High	Master Pro	Q61233	Plastin-2 [OS=Mus musculus]	0	7.425	4	3	7	1	1	627	70.1	5.33	23.79	3	0.455	0.383
FALSE	High	Master Pro	Q9WU78-3	Isoform 3 of Programmed cell death 6-interacting protein [OS=Mus musculus]	0	7.314	2	2	3	2	1	874	96.7	6.52	9.98	2	0.606	0.867
FALSE	High	Master Pro	Q9D154	Leukocyte elastase inhibitor A [OS=Mus musculus]	0	7.229	7	2	2	2	1	379	42.5	6.21	7.32	2	0.493	1.625
FALSE	High	Master Pro	P37804	transgelin [OS=Mus musculus]	0	7.226	15	3	3	3	1	201	22.6	8.81	7.7	3	0.063	0.049
FALSE	High	Master Pro	Q8BFR4	N-acetylglucosamine-6-sulfatase [OS=Mus musculus]	0	7.22	6	3	4	3	1	544	61.1	8.24	8.77	3	0.81	1.042
FALSE	High	Master Pro	P07214	Sparc [OS=Mus musculus]	0	7.21	8	2	5	2	1	302	34.4	4.86	16.88	2	0.64	0.394
FALSE	High	Master Pro	P63280	SUMO-conjugating enzyme ubc9 [OS=Mus musculus]	0	7.13	14	2	3	2	1	158	18	8.66	12.26	2	7.995	5.828
FALSE	High	Master Pro	P63001	Ras-related C3 botulinum toxin substrate 1 [OS=Mus musculus]	0	7.119	12	3	3	3	1	192	21.4	8.5	11.91	3	0.819	0.772
FALSE	High	Master Pro	P23927	Alpha-crystallin B chain [OS=Mus musculus]	0	7.045	11	2	3	2	1	175	20.1	7.33	10.11	2	0.955	0.286
FALSE	High	Master Pro	Q9CQE8	UPF0568 protein C14orf166 homolog [OS=Mus musculus]	0	7.036	10	2	2	2	1	244	28.1	6.89	6.02	2	1.009	1.166
FALSE	High	Master Pro	A6X935-1	inter alpha-trypsin inhibitor, heavy chain 4 [OS=Mus musculus]	0	6.946	2	2	9	2	1	942	104.6	6.4	31.46	2	0.353	0.229
FALSE	High	Master Pro	Q8R081	Heterogeneous nuclear ribonucleoprotein L [OS=Mus musculus]	0	6.868	4	2	4	2	1	586	63.9	8.1	10.56	2	2.864	3.207
FALSE	High	Master Pro	Q61398	Procollagen C-endopeptidase enhancer 1 [OS=Mus musculus]	0	6.851	5	2	4	2	1	468	50.1	8.41	11.68	2	0.771	0.811
FALSE	High	Master Pro	P60335	Poly(RC)-binding protein 1 [OS=Mus musculus]	0	6.781	6	2	6	1	1	356	37.5	7.09	17.36	2	3.412	4.643
FALSE	High	Master Pro	P61961	Ubiquitin-fold modifier 1 [OS=Mus musculus]	0	6.766	51	2	3	2	1	85	9.1	9.31	12.5	2	0.593	0.499
FALSE	High	Master Pro	O08997	Copper transport protein ATOX1 [OS=Mus musculus]	0	6.727	32	2	6	2	1	68	7.3	6.51	20.4	2	1.727	1.823
FALSE	High	Master Pro	P62897	Cytochrome c, somatic [OS=Mus musculus]	0	6.677	18	2	7	2	1	105	11.6	9.58	25.33	2	6.587	5.559
FALSE	High	Master Pro	P63323	40S ribosomal protein S12 [OS=Mus musculus]	0	6.624	20	3	6	3	1	132	14.5	7.24	17.84	3	1.049	1.122
FALSE	High	Master Pro	P62849-1	40S ribosomal protein S24 [OS=Mus musculus]	0	6.611	26	3	3	3	1	133	15.4	10.78	8.44	3	0.807	0.795
FALSE	High	Master Pro	Q9D0I9	arginine--tRNA ligase, cytoplasmic [OS=Mus musculus]	0	6.535	5	2	2	2	1	660	75.6	7.55	8.25	2	1.263	1.262
FALSE	High	Master Pro	O08553	Dihydropyrimidinase-related protein 2 [OS=Mus musculus]	0	6.508	3	2	7	2	1	572	62.2	6.38	22.03	2	0.68	0.694
FALSE	High	Master Pro	O08638-1	Myosin-11 [OS=Mus musculus]	0	6.482	2	3	5	1	1	1972	226.9	5.45	12.47	3		
FALSE	High	Master Pro	P16858	glyceraldehyde-3-phosphate dehydrogenase [OS=Mus musculus]	0	6.331	9	2	3	2	1	333	35.8	8.25	8.7	2	1.306	1.243
FALSE	High	Master Pro	Q9Z2T6	Keratin, type II cuticular Hb5 [OS=Mus musculus]	0	6.276	4	2	3	2	1	507	55.7	6.42	7.99	2	0.258	0.424
FALSE	High	Master Pro	Q8R3Q6	coiled-coil domain-containing protein 58 [OS=Mus musculus]	0	6.224	18	2	2	2	1	144	16.7	8.16	6.04	2	0.393	0.236
FALSE	High	Master Pro	P45377	Aldose reductase-related protein 2 [OS=Mus musculus]	0	6.216	9	2	3	2	1	316	36.1	6.37	4.82	2	0.953	1.059
FALSE	High	Master Pro	P61161	Actin-related protein 2 [OS=Mus musculus]	0	6.214	8	2	3	2	1	394	44.7	6.74	6.24	2	0.403	0.256
FALSE	High	Master Pro	Q9CR16	peptidyl-prolyl cis-trans isomerase D [OS=Mus musculus]	0	6.203	5	2	4	2	1	370	40.7	7.43	15.15	2	1.809	3.461

FALSE	High	Master Pro	P02088	Hemoglobin subunit beta-1 [OS=Mus musculus]	0	6.18	13	2	9	2	1	147	15.8	7.65	27.25	2	0.329	0.253
FALSE	High	Master Pro	Q9CPY7-1	cytosol aminopeptidase [OS=Mus musculus]	0	6.163	5	3	7	3	1	519	56.1	7.72	19.81	3	1.238	1.229
FALSE	High	Master Pro	Q9Z1Q5	chloride intracellular channel protein 1 [OS=Mus musculus]	0	6.118	11	2	3	2	1	241	27	5.17	10.34	2	1.171	1.039
FALSE	High	Master Pro	P47199	Quinone oxidoreductase [OS=Mus musculus]	0	6.103	8	2	3	2	1	331	35.2	8.07	11.15	2	1.347	1.41
FALSE	High	Master Pro	Q02053	Ubiquitin-like modifier-activating enzyme 1 [OS=Mus musculus]	0	6.1	3	2	2	2	1	1058	117.7	5.66	7.77	2	0.43	0.285
FALSE	High	Master Pro	O88207	Collagen alpha-1(V) chain [OS=Mus musculus]	0	6.038	2	2	5	2	1	1838	183.6	4.98	17.42	2	1.383	1.543
FALSE	High	Master Pro	O88342	WD repeat-containing protein 1 [OS=Mus musculus]	0	6.036	4	3	7	3	1	606	66.4	6.6	22.73	3	1.927	1.858
FALSE	High	Master Pro	Q8R1F1	Niban-like protein 1 [OS=Mus musculus]	0	6.028	3	2	3	2	1	749	84.8	5.94	8.06	2	1.287	0.981
FALSE	High	Master Pro	P62264	40S ribosomal protein S14 [OS=Mus musculus]	0	5.995	14	2	3	2	1	151	16.3	10.05	11.37	2	1.85	1.815
FALSE	High	Master Pro	Q9CZ30-1	obg-like ATPase 1 [OS=Mus musculus]	0	5.98	7	2	2	2	1	396	44.7	7.81	6.85	2	0.61	0.541
FALSE	High	Master Pro	Q03958	Prefoldin subunit 6 [OS=Mus musculus]	0	5.974	17	2	3	2	1	127	14.4	8.88	9.59	2	0.972	1.372
FALSE	High	Master Pro	P26369	Splicing factor U2AF 65 kDa subunit [OS=Mus musculus]	0	5.961	4	2	4	2	1	475	53.5	9.09	14.78	2	2.411	2.942
FALSE	High	Master Pro	P97371	Proteasome activator complex subunit 1 [OS=Mus musculus]	0	5.938	8	2	3	2	1	249	28.7	5.97	10.2	2	0.572	2.182
FALSE	High	Master Pro	Q64437	Alcohol dehydrogenase class 4 mu/sigma chain [OS=Mus musculus]	0	5.851	8	2	4	2	1	374	39.9	7.85	13	2	7.339	11.192
FALSE	High	Master Pro	Q9CWS0	N(G),N(G)-dimethylarginine dimethylaminohydrolase 1 [OS=Mus musculus]	0	5.848	6	2	3	2	1	285	31.4	5.97	11.03	2	0.431	0.328
FALSE	High	Master Pro	Q8CIE6	coatomer subunit alpha [OS=Mus musculus]	0	5.812	2	2	3	2	1	1224	138.3	7.65	12.04	2	1.176	1.458
FALSE	High	Master Pro	Q921M3-1	Splicing factor 3B subunit 3 [OS=Mus musculus]	0	5.773	2	2	2	2	1	1217	135.5	5.26	5.56	2	0.528	0.439
FALSE	High	Master Pro	P97351	40S ribosomal protein S3a [OS=Mus musculus]	0	5.703	9	3	8	3	1	264	29.9	9.73	23.16	3	1.183	1.146
FALSE	High	Master Pro	P47738	Aldehyde dehydrogenase, mitochondrial [OS=Mus musculus]	0	5.643	4	2	3	2	1	519	56.5	7.62	9.63	2	0.951	1.875
FALSE	High	Master Pro	Q99KJ8	dynactin subunit 2 [OS=Mus musculus]	0	5.634	8	2	2	2	1	402	44.1	5.26	7.39	2	0.671	0.528
FALSE	High	Master Pro	Q8VIJ6	splicing factor, proline- and glutamine-rich [OS=Mus musculus]	0	5.552	4	3	3	3	1	699	75.4	9.44	9.35	3	1.291	1.095
FALSE	High	Master Pro	Q9JM76	Actin-related protein 2/3 complex subunit 3 [OS=Mus musculus]	0	5.524	13	2	4	2	1	178	20.5	8.59	9.7	2	0.806	0.716
FALSE	High	Master Pro	Q8BVI4	dihydropteridine reductase [OS=Mus musculus]	0	5.51	7	2	3	2	1	241	25.6	7.81	8.85	2	1.392	1.974
FALSE	High	Master Pro	Q05186	Reticulocalbin-1 [OS=Mus musculus]	0	5.494	6	2	2	2	1	325	38.1	4.84	5.93	2	0.403	0.284
FALSE	High	Master Pro	P05201	Aspartate aminotransferase, cytoplasmic [OS=Mus musculus]	0	5.486	6	3	5	3	1	413	46.2	7.14	11.76	3	0.681	0.626
FALSE	High	Master Pro	P09671	Superoxide dismutase [Mn], mitochondrial [OS=Mus musculus]	0	5.448	10	2	3	2	1	222	24.6	8.62	9.29	2	0.923	0.842
FALSE	High	Master Pro	P42208	septin-2 [OS=Mus musculus]	0	5.404	6	2	2	2	1	361	41.5	6.55	5.51	2	0.609	0.585
FALSE	High	Master Pro	P31938	Dual specificity mitogen-activated protein kinase kinase 1 [OS=Mus musculus]	0	5.36	6	2	2	2	1	393	43.4	6.7	5.94	2	0.74	0.409
FALSE	High	Master Pro	O35887	Calumenin [OS=Mus musculus]	0	5.351	8	2	3	2	1	315	37	4.67	8.15	2	1.251	0.97
FALSE	High	Master Pro	P42932	T-complex protein 1 subunit theta [OS=Mus musculus]	0	5.332	3	2	4	2	1	548	59.5	5.62	9.65	2	0.495	0.373
FALSE	High	Master Pro	P11499	Heat shock protein HSP 90-beta [OS=Mus musculus]	0	5.307	4	3	3	2	1	724	83.2	5.03	8.92	3	0.993	1.174
FALSE	High	Master Pro	Q91Y97	fructose-bisphosphate aldolase B [OS=Mus musculus]	0	5.282	5	2	5	1	1	364	39.5	8.27	14.43	2	0.236	0.168
FALSE	High	Master Pro	P47753	F-actin-capping protein subunit alpha-1 [OS=Mus musculus]	0	5.197	9	2	4	1	1	286	32.9	5.55	14.49	2	0.843	0.866
FALSE	High	Master Pro	P21107	Tropomyosin alpha-3 chain [OS=Mus musculus]	0	5.146	6	2	3	2	1	285	33	4.72	9.99	2	0.811	1.479
FALSE	High	Master Pro	P32067	Lupus La protein homolog [OS=Mus musculus]	0	4.95	5	2	2	2	1	415	47.7	9.77	7.66	2	2.433	2.444
FALSE	High	Master Pro	P07091	Protein S100-A4 [OS=Mus musculus]	0	4.943	16	2	7	2	1	101	11.7	5.31	22.41	2	2.264	3.54
FALSE	High	Master Pro	Q08879	Fibulin-1 [OS=Mus musculus]	0	4.941	3	2	3	2	1	705	78	5.16	11.06	2	0.277	0.233
FALSE	High	Master Pro	Q9Z2W0	Aspartyl aminopeptidase [OS=Mus musculus]	0	4.937	4	2	3	2	1	473	52.2	7.25	10.29	2	0.8	1.151
FALSE	High	Master Pro	Q9DAR7	M7GpppX diphosphatase [OS=Mus musculus]	0	4.873	11	2	3	2	1	338	39	6.48	8	2	0.638	0.518
FALSE	High	Master Pro	P54822	adenylosuccinate lyase [OS=Mus musculus]	0	4.838	4	2	4	2	1	484	54.8	7.27	10.43	2	1.041	1.103
FALSE	High	Master Pro	Q11136	xaa-Pro dipeptidase [OS=Mus musculus]	0	4.828	3	2	3	2	1	493	55	5.78	5.95	2	0.728	0.485
FALSE	High	Master Pro	O55142	60S ribosomal protein L35a [OS=Mus musculus]	0	4.82	21	3	5	3	1	110	12.5	10.89	12.11	3	1.146	1.041
FALSE	High	Master Pro	Q62465	Synaptic vesicle membrane protein VAT-1 homolog [OS=Mus musculus]	0	4.804	4	2	4	2	1	406	43.1	6.37	13.27	2	0.991	0.495
FALSE	High	Master Pro	P14069	protein S100-A6 [OS=Mus musculus]	0	4.78	37	2	2	2	1	89	10	5.48	6.5	2	1.619	2.681
FALSE	High	Master Pro	Q61838	Pregnancy zone protein [OS=Mus musculus]	0	4.778	1	2	5	1	1	1495	165.7	6.68	14.14	2	0.361	0.243
FALSE	High	Master Pro	P50247	Adenosylhomocysteinase [OS=Mus musculus]	0	4.702	4	2	2	2	1	432	47.7	6.54	5.72	2	1.134	1.064
FALSE	High	Master Pro	Q9CQI3	glia maturation factor beta [OS=Mus musculus]	0	4.696	11	2	4	2	1	142	16.7	5.16	13.19	2	0.781	0.688
FALSE	High	Master Pro	P56399	Ubiquitin carboxyl-terminal hydrolase 5 [OS=Mus musculus]	0	4.628	3	2	4	2	1	858	95.8	5.01	9.79	2	0.537	0.514
FALSE	High	Master Pro	Q9CQM5	Thioredoxin domain-containing protein 17 [OS=Mus musculus]	0	4.483	15	2	5	2	1	123	14	4.77	17.41	2	3.139	3.088
FALSE	High	Master Pro	Q91WQ3	Tyrosine--tRNA ligase, cytoplasmic [OS=Mus musculus]	0	4.448	3	2	2	2	1	528	59.1	7.01	4.88	2	0.789	0.67
FALSE	High	Master Pro	Q8BFS6-1	Serine/threonine-protein phosphatase CPPED1 [OS=Mus musculus]	0	4.405	8	2	3	2	1	312	35.2	5.34	9.26	2	1.288	1.195
FALSE	High	Master Pro	Q9CXW3	Calcyclin-binding protein [OS=Mus musculus]	0	4.389	7	2	3	2	1	229	26.5	7.87	10.06	2	3.41	9.381
FALSE	High	Master Pro	P08071	Lactotransferrin [OS=Mus musculus]	0	4.378	3	2	3	1	1	707	77.8	8.53	9.98	2	0.409	0.306
FALSE	High	Master Pro	P07901	Heat shock protein HSP 90-alpha [OS=Mus musculus]	0	4.32	2	2	3	1	1	733	84.7	5.01	8.48	2	1.371	1.656
FALSE	High	Master Pro	Q6NZB0	DnaJ homolog subfamily C member 8 [OS=Mus musculus]	0	4.275	7	2	2	2	1	253	29.8	9.06	3	2	0.668	0.409
FALSE	High	Master Pro	P01942	Hemoglobin subunit alpha [OS=Mus musculus]	0	4.184	6	2	5	2	1	142	15.1	8.22	14.58	2	0.317	0.242
FALSE	High	Master Pro	P62245	40S ribosomal protein S15a [OS=Mus musculus]	0	4.152	13	2	4	2	1	130	14.8	10.13	10.56	2	2.93	2.895
FALSE	High	Master Pro	P17426	AP-2 complex subunit alpha-1 [OS=Mus musculus]	0	4.13	3	2	3	2	1	977	107.6	7.03	8.39	2	0.794	0.708
FALSE	High	Master Pro	Q9Z1X4-3	Isoform 3 of Interleukin enhancer-binding factor 3 [OS=Mus musculus]	0	4.129	3	2	2	2	1	911	97.7	8.95	3.68	2	0.89	0.876
FALSE	High	Master Pro	Q76MZ3	serine/threonine-protein phosphatase 2A 65 kDa regulatory subunit A alpha isoform [OS=Mus musculus]	0	4.12	4	2	3	2	1	589	65.3	5.11	9.16	2	1.134	0.909
FALSE	High	Master Pro	P43276	Histone H1.5 [OS=Mus musculus]	0	4.098	9	2	5	1	1	223	22.6	10.92	15.33	2	1.362	1.441
FALSE	High	Master Pro	Q8BML9	glutamine--tRNA ligase [OS=Mus musculus]	0	4.034	3	2	4	2	1	775	87.6	7.31	10.28	2	0.818	0.856
FALSE	High	Master Pro	Q3UEB3-1	poly(U)-binding-splicing factor PUF60 [OS=Mus musculus]	0	4.011	3	2	3	2	1	564	60.2	5.29	8.93	2	0.728	0.841
FALSE	High	Master Pro	P50608	Fibromodulin [OS=Mus musculus]	0	4.001	6	2	4	2	1	376	43	6.04	10.3	2	0.413	0.322
FALSE	High	Master Pro	Q9CZX8	40S ribosomal protein S19 [OS=Mus musculus]	0	3.987	13	2	4	2	1	145	16.1	10.4	10.04	2	4.773	6.091
FALSE	High	Master Pro	P47941	Crk-like protein [OS=Mus musculus]	0	3.928	7	2	2	2	1	303	33.8	6.74	5.61	2	0.681	0.608
FALSE	High	Master Pro	P59999	Actin-related protein 2/3 complex subunit 4 [OS=Mus musculus]	0	3.926	13	2	3	2	1	168	19.7	8.43	8.66	2	1.202	1.281
FALSE	High	Master Pro	P14824	annexin A6 [OS=Mus musculus]	0	3.83	3	2	2	2	1	673	75.8	5.5	5.81	2	0.487	0.369
FALSE	High	Master Pro	Q9WV32	Actin-related protein 2/3 complex subunit 1B [OS=Mus musculus]	0	3.611	5	2	2	2	1	372	41	8.35	6.22	2	1.268	1.265
FALSE	High	Master Pro	Q9JII5	DAZ-associated protein 1 [OS=Mus musculus]	0	3.576	8	2	2	2	1	406	43.2	8.56	2.07	2	0.413	0.347
FALSE	High	Master Pro	P70349	Histidine triad nucleotide-binding protein 1 [OS=Mus musculus]	0	3.554	27	2	2	2	1	126	13.8	6.87	2.26	2	1.029	0.746
FALSE	High	Master Pro	Q8C1A5	thimet oligopeptidase [OS=Mus musculus]	0	3.359	2	2	4	2	1	687	78	6.06	11.25	2	1.394	1.72
FALSE	High	Master Pro	Q91WJ8-2	Isoform 2 of Far upstream element-binding protein 1 [OS=Mus musculus]	0	3.356	2	2	5	1	1	672	70.8	7.69	16.77	2	2.141	2.122
FALSE	High	Master Pro	P80318	T-complex protein 1 subunit gamma [OS=Mus musculus]	0	3.334	3	2	3	2	1	545	60.6	6.7	8.04	2	0.763	0.612
FALSE	High	Master Pro	Q9CQC6	Basic leucine zipper and W2 domain-containing protein 1 [OS=Mus musculus]	0	3.263	3	2	2	2	1	419	48	5.92	6.12	2	1.863	2.484
FALSE	High	Master Pro	P62751	60S ribosomal protein L23a [OS=Mus musculus]	0	3.243	10	2	5	2	1	156	17.7	10.45	13.08	2	0.931	1.24
FALSE	High	Master Pro	P84104-1	Serine/arginine-rich splicing factor 3 [OS=Mus musculus]	0	3.225	14	2	3	1	1	164	19.3	11.65	5.11	2	5.696	1.903
FALSE	High	Master Pro	Q60972	Histone-binding protein RBBP4 [OS=Mus musculus]	0	3.076	4	2	3	2	1	425	47.6	4.89	8.79	2	1.727	1.477
FALSE	High	Master Pro	Q9EQH3	Vacuolar protein sorting-associated protein 35 [OS=Mus musculus]	0	3.073	3	2	3	2	1	796	91.7	5.44	4.9	2	1.482	1.226
FALSE	High	Master Pro	Q3U0V1	Far upstream element-binding protein 2 [OS=Mus musculus]	0	3.027	3	2	5	1	1	748	76.7	7.33	15.81	2	0.76	1.096
FALSE	High	Master Pro	Q9CPW4	Actin-related protein 2/3 complex subunit 5 [OS=Mus musculus]	0	2.966	13	2	3	2	1	151	16.3	5.67	6.39	2	1.067	1.118

FALSE	High	Master Pro	P63005-1	Platelet-activating factor acetylhydrolase IB subunit alpha [OS=Mus musculus]	0	2.924	3	2	4	2	1	410	46.6	7.37	11.2	2	1.811	1.34
FALSE	High	Master Pro	P35979	60S ribosomal protein L12 [OS=Mus musculus]	0	2.886	10	2	5	2	1	165	17.8	9.42	13.54	2	1.233	1.113
FALSE	High	Master Pro	Q8VCT3	aminopeptidase B [OS=Mus musculus]	0	2.847	2	2	4	2	1	650	72.4	5.35	9.59	2	0.593	1.236
FALSE	High	Master Pro	Q8BL97-1	serine/arginine-rich splicing factor 7 [OS=Mus musculus]	0	2.767	9	2	3	1	1	267	30.8	11.9	4.16	2	3.212	1.283
FALSE	High	Master Pro	P63163	small nuclear ribonucleoprotein-associated protein N [OS=Mus musculus]	0	2.765	6	2	2	2	1	240	24.6	11.19	5.7	2	4.804	3.38
FALSE	High	Master Pro	Q91VW3	SH3 domain-binding glutamic acid-rich-like protein 3 [OS=Mus musculus]	0	2.717	18	2	4	2	1	93	10.5	5.14	9.44	2	1.593	2.146
FALSE	High	Master Pro	Q8CJG0	Protein argonaute-2 [OS=Mus musculus]	0	2.703	3	2	2	2	1	860	97.2	9.19	5.11	2	0.88	0.869
FALSE	High	Master Pro	Q3U962	Collagen alpha-2(V) chain [OS=Mus musculus]	0	2.679	1	2	3	1	1	1497	144.9	6.7	7.27	2	0.502	0.425
FALSE	High	Master Pro	Q921I1	Serotransferrin [OS=Mus musculus]	0	2.599	3	2	9	1	1	697	76.7	7.18	23.82	2	0.417	0.236
FALSE	High	Master Pro	Q9JHH6	Carboxypeptidase B2 [OS=Mus musculus]	0	2.595	3	2	4	2	1	422	48.8	7.97	10.36	2	0.383	0.238
FALSE	High	Master Pro	P54071	Isocitrate dehydrogenase [NADP], mitochondrial [OS=Mus musculus]	0	2.581	4	2	3	1	1	452	50.9	8.69	7.79	2	1.222	1.084
FALSE	High	Master Pro	Q99LX0	protein/nucleic acid deglycase DJ-1 [OS=Mus musculus]	0	2.562	8	2	4	2	1	189	20	6.77	12.52	2	1.721	1.686
FALSE	High	Master Pro	Q91VH6	Protein MEMO1 [OS=Mus musculus]	0	2.418	10	2	3	2	1	297	33.7	7.14	5.8	2	2.85	3.844
FALSE	High	Master Pro	Q9DBP5	UMP-CMP kinase [OS=Mus musculus]	0	2.363	10	2	2	2	1	196	22.2	5.83	4.91	2	0.496	0.349
FALSE	High	Master Pro	P14211	Calreticulin [OS=Mus musculus]	0	2.342	3	2	4	2	1	416	48	4.49	10.01	2	1.018	0.762
FALSE	High	Master Pro	P24452	Macrophage-capping protein [OS=Mus musculus]	0	2.238	4	2	3	2	1	352	39.2	7.2	8.42	2	7.503	5.594
FALSE	High	Master Pro	P02468	Laminin subunit gamma-1 [OS=Mus musculus]	0	2.036	1	2	3	2	1	1607	177.2	5.21	7.54	2	0.414	0.505

Sample	TMT reagent
Primary OEC+ 5nMA1 sup	129
OEmyc790_C7+ 5nMA1 sup	130
OEmyc790_C4+ 5nMA1 sup	131